Enhancing mechanical properties of CEB (compressed earth blocks) with natural fibres

Laurence Paquet

Academic year

2019-2020

Master thesis submitted under the supervision of

Prof. Dr. Ir. Bertrand François

In order to be awarded the Master's Degree in

Master of Science in Architectural Engineering

Acknowledgements

I would first like to thank Professor Bertrand François who followed me during this master thesis, for according me his time and sharing his precious advice during this whole year. I am also grateful to Nicolas Canu and Fabiano Pucci for helping me out with the experimental tests, and for being of such great support.

Then I would like to express my gratitude to Julie Piérard and her colleagues Benjamin and Christophe, the team that welcomed me at the CSTC-WTCB and helped me with the fabrication of Compressed Earth Blocks.

I also wanted to warmly thank my family and friends, without whom these study years would not have been the same. I am especially grateful to Baptiste for his unconditional support during the past academic years.

Finally, I wanted to dedicate this work to Jean Paquet, who always believed in me.

Table of contents

List of tables

List of Figures

Abstract

This study focuses on reinforcing Compressed Earth Blocks with straw in order to enhance their mechanical properties. The main research frame of this work is to (i) find the optimal straw ratio to incorporate into CEBs to improve their mechanical characteristics by means of experimental tests; and to (ii) find out how the results obtained in the experimental part will be translated in a structural point of view, and to which ecological extends. This investigation was carried out essentially because of CEB's promising future deals in the construction sector compared to other construction materials. Implementing natural fibres in CEBs could enhance their mechanical behaviour, and thus contribute to their attractiveness within the actual material reign. The experimental part of this work was performed methodically to identify which parameters played a role for mechanical properties of reinforced CEBs, mainly regarding density, compression and tensile strengths, and Young modulus. It was demonstrated that the behaviour of straw reinforced CEBs depended on quite a number of parameters. Parameters such as the compaction mode of the samples (static or dynamic); the use of an adapted fabrication procedure for straw reinforced CEBs; the nature and ratio of the straw incorporated in CEBs; the water content of the samples and their time of cure. The outcomes of this experimental part were then used to evaluate the potential of CEBs through a structural and energy-wise approach. A structural dimensioning phase allowed to estimate how high one could possibly build with CEB and straw-CEB masonry. It was then found that CEB structures had a significantly lower embodied energy than traditional masonry structures. Besides that, it could be observed that the transport parameter represented an important weight in the embodied energy of CEBs, but that this parameter could be optimised. Finally, it was proven that the recycling possibilities of CEBs would imply lower environmental impacts than the end-of-life scenarios of conventional materials, like fired brick masonry.

Key words: Compressed earth blocks, Natural fibre reinforcement, Mechanical properties, Structural potential, Environmental impacts.

1. Problem statement

Materiality in architecture is what gives the physical identity of a building in its cultural and environmental context. It is the result of a complex process of choices related to physical properties, contextual and financial data, and to architectural and environmental criteria.

The implementation of materials in buildings now comes along with the challenge of answering to the world-wide environmental stakes. This challenge concerns every sector, especially construction which is nowadays responsible for more than 40% of the global energy consumption, and for over one third of the greenhouse gas emission in the world (Data and Statistics, 2020). Apart from the architectural design choices directly affecting the energy demand in buildings, this high energy consumption level is due to the utilisation of materials having an important embodied energy (Elizondo, Guerrero, & Mendoza, 2011). The embodied energy of a material or product includes the total amount of energy consumed during its lifetime.

Embodied energy = Harvesting + Manufacture + Transport + Construction

Higher is this embodied energy, more energy demanding is the material, and the more it contributes to the level of energy consumption in the construction sector (Khan, 2017-2018).

With a continuously increasing demand in the construction sector, today's challenge in architecture and construction is to find strategies to build in a more sustainable way. Amongst other approaches, like the rehabilitation of existing buildings, the upcycling of materials, … (National Institute of Building, 2020), this can be achieved by a more cautious selection of the materials involved in a project, and thus by reducing the project's total embodied energy (Hoyet, 2013).

This is not that easy in the current post-industrial period. There is an almost counter-productive duality between sustainable development and the growing supply in new high-tech materials. In fact, while there's a growing interest to rediscover the benefits of the ancient techniques of earth building since a few decades (Morel, Mesbah, Oggero, & Walker, 2000), it is unfortunately not in total agreement with current modern construction industries, where innovation in technology and economical rentability are deeply anchored. Using eco-friendly materials such as earth, often go hand in hand with a more vernacular type of architecture, which is not always welcome in the actual modern humanity. Moreover, despite the fact that earth buildings have the potential to drastically reduce environmental issues for the future generations, it yet takes some courage for current construction contractors to support what appears as a step back in innovation (Hall, Lindsay, & Krayenhoff, 2012). And even though certain materials are irreplaceable, like steel for strength or aluminium for durability, the thirst of high-energy materials and the general disinterest of people towards alternative construction techniques make this challenge quite perilous.

It is so that earthen constructions, along with thoughtful designing and a clever marketing, have the potential to overcome some of the most serious environmental issues. They are and remain one of the most interesting choices in terms of low-energy design and material sustainability in the building domain. Indeed earth, this simple and humble material, can reduce the functional building energy down to a (nearly) zero carbon emission building, and substantially cut down its embodied energy, without compromising indoor quality, nor the style and desirability of such architectures. Obviously, with its structural potential and qualities such as thermal and hygric mass, long-life durability, improved acoustics, superior seismic stability and fire resistance, a well-designed earthen construction is more sustainable than any current modern building.

But, on the other hand, the non-existence of any international standards or Eurocodes makes the knowledge spreading of earth as a construction technique very complicated. Only a few countries dispose of guidelines about earthen constructions (see section *State-of-the-art* on Compressed Earth Blocks).

2. Introduction

A historical reference on the utilisation of earth

Since more than 10.000 years, ever since the first cities, earth remains one of the most used construction materials in the world. With wood, earth is the famous sedentary house material that appeared during the Neolithic Age. Earthen constructions are present all around the world and constitute more than one third of the global population's housing (Houben & Guillaud, 2006). The different techniques used to construct such earth buildings are all determined in function of their specific locations and the quality of the available materials of the area. In certain regions like Morocco or Yemen, some cities were entirely built in earth. In Europe during the Middle Age, half-timbered houses were the result of the association of cob with timber. Rammed earth became particularly well-known and widely used around the French Revolution thanks to the architect François Cointeraux (Baridon, Garric, & Richaud, 2016).

Figure 1: Utilisation of earth in architecture (CRATerre, 2020)

From the 20's, scientific studies concerning earth stabilisation began to develop and grew considerably between the 40' and 60's (Hoyet, 2013). However, the post-war years where dominated by concrete technology developments, which offered a very quick way to build (Devos, 2018-2019). Earth construction then disappeared from current practice. When concerns about climate change and environmental issues started to widen seriously among the scientific community (around the 70's - 80's (Khan, 2017-2018)), people rediscovered the beneficial aspects of earth and entities like CRATerre, a French association and research laboratory located in the National Superior School of

Architecture of Grenoble dealing with earth construction, were created. In fact, earth construction is undergoing an important interest revival, essentially because of its sustainable properties that answer to the current environmental issues (Hoyet, 2013).

Contemporary earthen buildings have proven themselves validating this revival and supporting designers to investigate the opportunities of such pieces of work. In fact, designers and craftsmen such as Martin Rauch (Kapfinger & Sauer, 2015) encourage the interest in earthen architecture through their contemporary designs, and make this yet old, but particularly appealing building material gain a wider audience.

Figure 2: House Rauch (Lehm ton Erde, 2008)

Figure 3: House Rauch interior (Lehm ton Erde, 2008)

For example, among various other projects, the House Rausch (Figure 2 and 3), which is the result of a cooperation between Roger Boltzhouser and Martin Rauch, became a world-wide inspiration in the earthen construction sector and more generally in sustainable architecture since its construction in 2008.

Earth construction methods

More than a hundred construction techniques have been reported through History. A classification of these methods could lead to the identification of twelve fundamentally different methods, all classified into three larger groups: monolithic constructions, brickwork constructions and mixed structure constructions. More details on these three mentioned groups can be found in Annex A.

Benefits of earth utilisation in construction

Physical properties

The target compressive strength for earth material used as a structural element is 2 MPa. This value can be improved by adding stabilisers like cement or by implementing fibres into the soil mixture. In those cases, the compressive strength can reach values up to more than 15 MPa (Houben & Guillaud, 2006; Hall, Lindsay, & Krayenhoff, 2012). The tensile strength of earth is only going from 0,5 to 1 MPa, which is why it is most of the time preferred as a pure compression element.

The thermal conductivity of compressed earth varies from 0,81 and 0,93 W/mK. Adobe has a thermal conductivity going from 0,46 and 0,81 W/mK, depending on its ratio of straw. These values reveal that earth is not a good insulation material. On the other hand, it has excellent thermal inertia qualities. Earth has the capacity to regulate a building's temperature by stocking and re-emitting heat in function of the space's temperature thanks to its thermal mass (Taylor & Luther, 2004). Moreover, earth has hygrothermic properties that provides a notable indoor comfort. Its capacity to absorb

ambient humidity and to restore it when indoor air is too dry enhance the quality of an indoor space (Hoyet, 2013).

Environmental impacts

Earth is an endless resource, indefinitely recyclable. A ruined earthen dwelling becomes either a new material mine for new constructions or is either reintroduced in the transformation process of the earth crust. This important quality goes together with circular economy principles, proposing a regenerative (instead of degenerative) flow of resources. These ethic environmental concepts are also known as “cradle-to-cradle” design models, or “C2C”. They have the perspective to promote responsible resource consummation in a way that these resources do not end up as downcycled products or waste (Khan, 2017-2018). In rural localities, earth is usually collected directly on the construction site or in its close vicinity, which does not affect the local ecosystems and significantly reduce the energy consumption for the transport. When this is not possible, for example in the case of industrial productions, earth is harvested in quarries. The environmental impact of quarries has then to be taken into account.

Low embodied energy

In terms of embodied energy, earth represents one of the most energy friendly materials available in the construction world (Table 1). The energy consumption related to earth production corresponds to the energy needed for the running of extraction machines, for transportation, for the soil mixing process and for its compaction. Different scenarios can be defined for the material transportation. In fact, earth is by nature a local resource. The most common practice is thus to move the needed equipment on site (press machines for compressed blocks, pneumatic dampers for rammed earth walls, etc). That way, the transportation of the materials is minimised. However, fabrication plants are sometimes preferred with respect to proximity for some specific industrial needs, which then require a regular transfer of materials to the construction site (Houben & Guillaud, 2006).

	Material	Embodied energy [kWh/m³]
Metals	Steel	60000
	Copper	140000
	Zinc	180000
	Aluminium	190000
Pipes	sandstone tubes	3200
	fibre cement tubes	4000
	PVC tubes	27000
	Steel tubes	60000
Structural walls	Cellular concrete	200
	Hollow sand lime bricks	350
	Fired clay bricks (beehive)	450
	Concrete	500
	Cladding sand-lime bricks	500
	Perforated fired clay bricks	700
	Cement bricks	700
	Plein fired clay bricks	1200
	Reinforced concrete	1850
	Earthen brick (raw clay)	**120**

Table 1: Embodied energy of construction materials (L'énergie grise des matériaux de construction, 2016)

Using earth as a construction material is a sustainable answer to the current ecological concerns in the construction sector. It is a widely accessible natural material providing numerous qualities in terms of physical properties and indoor comfort. Earth has only very few transformations to undergo when it is implemented in a construction project and is indefinitely recyclable.

Fibres in earth constructions

Natural fibres are also part of these eco-friendly materials resources. Often derived from agricultural waste and thus being biodegradable, they are widely available and do not required any heavy transformation before being introduced in a construction process (Danso, Martinson, Ali, & Williams, 2015).

Stabilising soil with fibres is not something new. Through History, mankind has always used fibres, especially straw, to reinforce earth constructions. Straw is indeed considered as a structure reinforcement in the same way as gravel is. Natural fibre reinforcement is an interesting stabilisation method because it can be applied to a whole set of earth construction methods. In fact, artisanal adobe bricks are very often reinforced with straw, but fibres have also been implemented for daubed earth, straw-clay, cob, compressed earth blocks and rammed earth. They are usually implemented with clayey soils presenting a high shrinkage coefficient (Houben & Guillaud, 2006). The main role of fibres reported through time are to:

- avoid shrinking cracks by spreading tension constrains due to clay shrinkage, and thus to improve compression strength.
- accelerate the drying time of the materials by offering a water drainage in the soil's matrix.
- make the material lighter in order to obtain better thermal insulation properties. This can be reached with high fibre ratios.
- improve the tensile strength of the material.
- improving the durability of the material against wearing (wetting-drying cycles) and erosion

Natural fibres represent a sustainable alternative to other stabilisation techniques such as cement stabilisation (Danso, Martinson, Ali, & Williams, 2015), which induces the hydration of the soil mixture, an irreversible chemical reaction (Gmira, 2013). In fact, at the end of their life, natural fibre reinforced earth will decompose naturally with time and will return to earth, while this is not the case for binder stabilised earth.

The fibres included in the soil are preserved without deterioration only if the earthen element is kept dry. If the element undergoes a too long humid phase, there is a chance that the reinforcing fibres will decompose under putrefaction. But on the other hand, wet-dry cycles will not contribute to this rotting as long as a proper drying is assured. Several analyses made on old adobes from pharaonic Egypt can prove that statement (Houben & Guillaud, 2006).

A promising future for compressed earth blocks

For a long time, earth blocks were fabricated by compressing soil in moulds with little pestles or with heavy mould lids. This procedure has been mechanised during the Industrial Period and today the fabrication of earth blocks is highly varied and can be obtained with a large range of pressing machines. Constructing in earth is known as being time consuming and physically hard for the workmanship. That is why CEBs are one of the favourite earth construction methods. With their standardisation possibilities and industrial production, CEB have a renewed interest among today's construction world, especially vis a vis the classical terracotta masonry brick (Mansour, Jelidi, Cherif, & Jabrallah, 2015). In fact, it's a natural resource produced at low costs, where the fabrication

process has the advantage of being super flexible: from small manual installations to large automated productions, the rate of CEBs produced in a day varies from 300 (Cinva-Ram press) to 20.000 blocks (Hans Sumpf plant in Fresno, California) (Houben & Guillaud, 2006). Moreover, the production of CEBs does not require a trained workforce. That way, locally harvested materials are produced with local workforces, which contributes actively to sustainable construction strategies (Hoyet, 2013).

In terms of mechanical properties, the compression strength of CEBs depends on a whole range of parameters, especially on the compression stress applied during manufacture, and on the presence or not of a hydraulic stabiliser (cement, lime, …) or other reinforcement elements like fibres.

Objectives

It is so that while being one of the oldest building materials in the world, earth is also the less tackled subject among the scientific community. Nevertheless, this subject has gained interest again and scientific studies have drastically increased since the past few decades (Morel, Mesbah, Oggero, & Walker, 2000; Pacheco-Torgal & Jalali, 2011). Currently, the CEB construction method has the biggest development perspectives (Mansour, Jelidi, Cherif, & Jabrallah, 2015).

The aim of this study will be to investigate mechanical properties of CEBs reinforced with natural fibres (straw), essentially because of its promising future deals in the construction sector compared to other earth construction methods. Implementing natural fibres in such CEBs could enhance the mechanical behaviour of CEB, and thus contribute to its attractiveness within the actual material reign. The potential of CEBs will then be tackled through a structural and energy-wise approach, in order to estimate how high one could possibly build with CEB masonry, and to which ecological extends.

The following questions were formulated to present the research frame of this study.

- What is the optimal straw ratio to incorporate in CEBs in order to enhance their mechanical properties?
- How are these results translated from a structural and energy wise point of view?

Research method

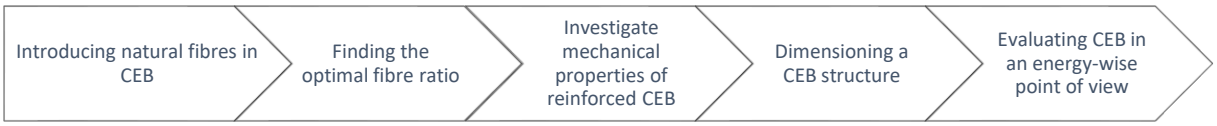

The experiments required to work on this paper could all be performed in the laboratory of Geomechanics, except for the confection of the CEBs, for which a manual pressing machine was needed. Such a machine was available at the CSTC – WTCB (FR: *Centre scientifique et technique de la construction* - NL: *Wetenschappelijk en Technisch Centrum voor het Bouwbedrijf*) in Limelette, Belgium.

One of the objectives of this study was to find out the optimal straw ratio to reinforce CEBs, requiring a high accessibility of the sample moulds. As the access to a pressing machine was quite limited, it was decided to split the experimental research in two parts: finding the optimal straw ratio on one hand and testing the mechanical properties of straw-reinforced CEBs with the optimal straw on the other hand.

The first part could be completely done at the lab, while using the testing procedures applicable for soil studies. Dynamically compacted cylindrical samples (with a diameter of 36mm and a height of 70mm) will thus be created and tested according to the unconfined compression test (François, 2017-2018).

The second part focuses on the testing procedures to perform on CEBs. Once the optimal straw ratio was determined, the confection of the CEB could be prepared in advance and realised in two half days at the CSTC-WTCB. All testing of the CEBs could then be completed in the lab.

The blocks were thus tested for some of the main physical and mechanical properties, namely density, water content, compressive strength, Young modulus and three-point flexural strength, in order to cover a similar range of data as found in literature (see *State-of-the-art*). For the first experimental part, up to 6 samples were tested for each series. For the second part, three samples were tested for each series, and were randomly chosen among a large stock of samples (104 samples were produced while 48 samples were needed).

The results obtained during the experimental part were then applied in a structural dimensioning, in order to understand the structural potential of CEBs and straw reinforced CEBs from a larger scale point of view. This structural step was compared to the case of traditional fired brick masonry to have a comparable situation to refer to.

The environmental advantages of CEB were then evaluated energy-wisely with the determination of its embodied energy. The calculations of the embodied energy of CEBs, straw reinforced CEBs and traditional masonry were based on the results obtained in the structural dimensioning part. In addition to that, the benefits of earth as a construction material were discussed through a cradle-to-gate analysis, focusing on the transport parameter; and finally, the recycling possibilities of CEBs were analysed.

3. State-of-the-art on Compressed Earth Blocks

Earth building standards and norms

Nowadays, reference norms and standards are necessary in order to fit to very strict technical inspections. Earth as a construction material has gained interest during the last decades due to its positive ecological characteristics and its favourable impact in sustainable architecture. This "new" consciousness induced the number of standards of earthen buildings to rise in this same period, but compared to other construction materials, this number remains quite little. Moreover, there is no commonly accepted terminology for such building systems, which is essential in the process of establishing normative documents for modern earthen constructions (Houben & Guillaud, 2006).

Likewise, the methods proposed to determine the material's properties and design values are not internationally recognised. In fact, the current testing procedures are developed for soil mechanics or concrete, which do not consider intrinsic properties of earth as a building material. Moreover, their suitability for earth testing's tor still needs to be verified (Silveira, Varum, & Costa, 2013). Even though certain published regional, national or local recommendations are of a first help for small earth buildings, they are not enough for larger-scale project. Taking earth testing procedures to the same level as other more conventional materials could widen their scope and attractiveness in the building sector (Sharma, Marwaha, & Vinayak, 2016).

Testing methods for compression strength on CEBs

All the existing procedures that exist to test compressed earth blocks, provided by national standards/ guidelines (Rilem (France), India, Peru, Brazil, Cuba, etc) can be classified into the four following methods, as shown on Figure 4:

- RILEM method: this testing method was adopted by the RILEM group in 1997 (Olivier, Mesbah, Gharbi, & Morel, 1997). It consists in a compression test performed on two superposed half-blocks joints with an earthen mortar. The half blocks are obtained thanks to a splitting by three-points bending test.
- Half block method: This second method consists in testing only one-half block (Pkla, 2002).
- Cylindrical test: This method, essentially used in Morocco, proposes to test cylindrical samples with the same densities than the CEBs used on construction site (Hakimi, Yamani, & Ouissi, 1996).
- Direct block test: The last testing method found in literature is to test a CEB as it is, without any anti-platen effect system. The final strength value is then multiplied by a slenderness coefficient, to counter the platen confinement effects (Aubert, Fabbri, Morel, & Maillard, 2013).

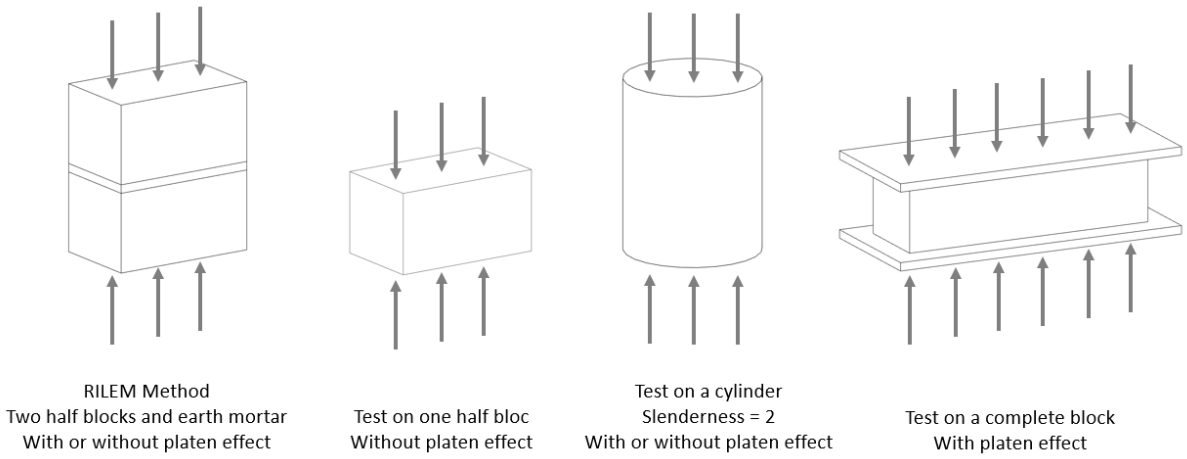

Figure 4: Compression test methods

Figure 5 represents the principle of the first testing method (RILEM). This method suggests using a Teflon plate and a neoprene joint between the contact surfaces of the sample and the press machine to be as unconfined as possible in order to counter platen confinement effects. The advantage with this first method, is that the slenderness is doubled compared to the entire block, which will automatically induce less platen confinement effects. Moreover, when the RILEM method is used with an efficient anti-platen constraint system, the results are less linked to the geometry of the CEBs when compared with the direct block test, but they are more representative of a masonry strength than of a pure block strength (Morel, Pkla, & Walker, 2007).

Another advantage of this method is that the tensile strength of the CEBs can be determined during the preliminary splitting test of the block in two half blocks. It has been shown that even though this test is not perfect and does not give the exact CEB compression strength (Hakimi, Yamani, & Ouissi, 1996), it is still a reliable test to reproduce a CEB masonry behaviour (Pkla, 2002).

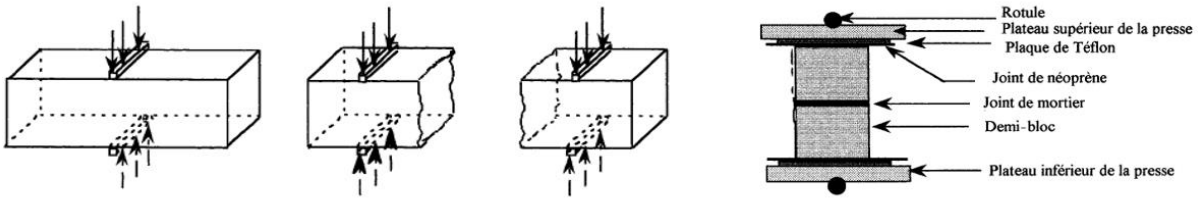

Figure 5: RILEM testing procedure (Olivier, Mesbah, Gharbi, & Morel, 1997)

On the other hand, other references prefer opting for the direct block test and propose to counter the platen constraints afterwards, by applying a correction factor on the final confined strength value, like the standards of New Zealand and Australia (Standards New Zealand, 1998) (Morel, Pkla, & Walker, Compressive strength testing of compressed earth blocks, 2007). This methodology is not perfect neither. There are still some discussions about the correlation between both methods especially because the confined blocks testing results currently do not fit unconfined block testing results. In fact, when a correction factor is applied afterwards, the geometry of the blocks sometimes still induces large disparities in the results, which are questioning the applicability of the correction factors (namely “Krefeld’s” and “Heathcore and Jankulovski’s” correction factors). These studies suggest that the relation between geometry and compression strength should be investigated further for CEBs.

The role of fibres

As said before in the introduction, adding fibres in a soil mixture is beneficial in a whole set of domains, especially on a mechanical point of view, but also in terms of physical properties and durability of the material (Danso, Martinson, Ali, & Williams, 2015). In fact, it has been reported that fibres are in direct relation with thermal conductivity (Cardinale, Arleo, Bernardo, & Feo, 2017), water adsorption, density, shrinkage (in the case of cob) (Hamard, Cazacliu, Razakamanantsoa, & Morel, 2016), durability (Aymerich, Fenu, & Meloni, 2011), etc. These domains are all detailed in the following paragraphs.

Compression strength

In most of the cases, the compression strength was enhanced with the addition of fibres. The reasons to explain this improvement are mainly that the fibres provide a better adherence in the mixture matrix, reduce the apparition of cracks thanks to their good tensile properties. This binding effect of the fibers induces also, by consequence, an improvement of the compressive strength (Laborel-Préneron, Aubert, Magniont, Tribout, & Bertron, 2016; Millogo, Aubert, Hamard, & Morel, 2015). Nevertheless, this improvement in compression strength was different from study to study. A lot of other parameters made that the added fibres had other effects on the sample's strength (Laborel-Préneron, Aubert, Magniont, Tribout, & Bertron, 2016). Parameters such as the nature, the ratio and the length of the fibres, as well as their combination with a certain type of grain-size distribution, show specific compression strength evolutions (Aymerich, Fenu, & Meloni, 2011; Danso, Martinson, Ali, & Williams, 2015). Cement or lime stabilisation of the sample has also an impact on the magnitude of fibre reinforcement (Laborel-Préneron, Aubert, Magniont, Tribout, & Bertron, 2016).

On another hand, in a very few numbers of cases, the compression strength decreased when the samples were reinforced. This was the case for a cotton reinforcement, where the compression strength went down due to a too large porosity (Algin & Turgut, 2007). The same happened for a sheep wool reinforcement where a greater amount of water had to be included in the mixture to obtain a good workability (Cardinale, Arleo, Bernardo, & Feo, 2017). A study also showed some reduced compression strength results for a wood aggregate reinforcement where the adhesion between the aggregates and the clay was really poor (Bouguerra, Ledhem, de Barquin, Dheilly, & Que'neudec, 1998).

Tensile strength

In most of the cases, the tensile strength of reinforced blocks increased due to the addition of natural fibres in the soil mixture. In fact, this increase of the tensile strength could go up to 38% when compared to unreinforced blocks. This can be explained by an improved adhesion in the sample matrix between the fibres and the soil particles (Danso, Martinson, Ali, & Williams, 2015). In the meantime, the addition of fibres also enhanced the ductility of reinforced soil blocks, which could take more elastic energy in, and thus retard failure (Laborel-Préneron, Aubert, Magniont, Tribout, & Bertron, 2016).

Thermal conductivity

When blocks are reinforced with natural fibres, the thermal conductivity tends to decrease, sometimes from 0,24 W/mK for unreinforced blocks to 0,008 W/mK for fibre-reinforced blocks in some cases (Al Rim, Ledhem, Douzane, Dheilly, & Que'neudec, 1999). This can be explained through the decrease in density and the rise in porosity of reinforced blocks. Some studies also link the decrease of the thermal conductivity with the nature of the fibres added in the soil mixture and their length (Laborel-Préneron, Aubert, Magniont, Tribout, & Bertron, 2016).

Density & Water absorption shrinkage

A decrease in density could be observed in all studies related to natural fibre-reinforced earthen blocks. In fact, as the density of the fibres (500 – 810 kg/m³) are much lower than the density of non-reinforced CEBs (between 1700 and 2200 kg/m³), one could easily expect the density of fibre-reinforced blocks to drop. In most of the cases, a reduction in density of up to 10% for fibre-reinforced blocks could be observed (Houben & Guillaud, 2006).

On the other hand, an increase of the water absorption was observed for the fibre-reinforced blocks, along with the increase of fibres incorporated in the soil mixture. This is probably caused by the high absorbance of cellulose contained in natural fibres, which allows water to penetrate easier into the block (Laborel-Préneron, Aubert, Magniont, Tribout, & Bertron, 2016).

The shrinkage of blocks could be limited for blocks reinforced with a proper amount of fibres. In fact, shrinkage tensions due to the block drying can be balanced thanks to the good tensile strength of fibres, which then can avoid most of the shrinkage cracks (Houben & Guillaud, 2006).

Durability

The incorporation of fibres in CEB induces a reduction of wearing (resistance to wetting and drying cycles) from 20% up to 50% compared to pure soil blocks, depending on the type of soil used and the nature and ratio of the reinforcing fibres. It has been exposed that after certain ratio of fibre content, around 0,5% weight-ratio, this behaviour tented to stabilise, without presenting any further reduction for larger fibre ratios (Danso, Martinson, Ali, & Williams, 2015).

The same behaviour could be observed for the erosion testing, with an erosion decrease from 44% up to 70% compared to pure soil blocks, again depending on the type of soil and the nature and ratio of the included fibres (Danso, Martinson, Ali, & Williams, 2015; Bui, Morel, Reddy, & Ghayad, 2009).

This means that fibre-reinforced blocks are more resistant than non-reinforced blocks to external parameters like wind, rain, sunny weather as well as human activities (Houben & Guillaud, 2006).

Optimum ratio of fibres

A lot of different results can be found in literature about fibre contents in earth blocks (adobe, CEB) as well as a few studies on rammed earth and cob techniques. The range of fibre content in adobe goes from 0,2 to 3,8 % depending on the type of fibres. The same dependence has been reported for CEB, where the fibre ratio values are a lot more dispersed and can go up to 22%. Figure 6 is showing these dispersed data.

Soils						Plant aggregates or fibers		
w_L (%)	w_P (%)	PI (%)	Clay (%)	Silts (%)	Sand (%)	Type	Length (cm)	Content (wt%)
28	17	11	7	58	35	Wool	1, 2 or 3	2–3
			Lateritic			Millet		0–12.2
			Lateritic			Millet		0–12.2
57	23	33				Barley straw	1–6	0–3.5
33	15	18						
32	18	14						
40	22	18						
33	21	12	19			Hemp	0.5–3.5	15–22
35	24	11	11	–	–	Palm		0–1.5

Figure 6: Characteristics of soil and plant aggregates or fibres used in CEB (Laborel-Préneron, Aubert, Magniont, Tribout, & Bertron, 2016)

Legend:
w_L = liquid limit
w_P = plastic limit
PI= plasticity index

For rammed earth, only two scientific studies were found where the authors compared the mechanical performances of RE with cob, but they were not relevant from the straw ratio point of

view. In fact, the first one didn't mention the results obtained for the straw-reinforced rammed earth walls (Bui, Morel, Reddy, & Ghayad, 2009), and the second one didn't specify the proportions of straw in the mixture of rammed earth (Miccoli, Müller, & Fontana, 2014). Nevertheless, the second of these two studies also specified that the straw weight ratio to create cob samples was of 1,3 to 2%. In terms of volume ratio, this study mentions that they incorporated a straw ratio of 20 to 30 kg/m³ of fresh cob, alongside with another study dealing cob (Laurent, 1986), which corresponds to the French recommendation, CRATerre.

A whole set of fibres can be introduced in earth samples. Among all the studies dealing with fibre-reinforced earth that were found, the reinforcement fibres were generally always chosen with respect to the availability of fibres and in function of the location of the study. The most encountered fibres were sheep wool, hemp, cereal straw, wood aggregates, and different kinds of leaf fibres.

The determination of the optimal ratio to incorporate in a soil mixture is generally done by comparing mechanical properties of sample having several fibre ratios. As said before, it has been reported that up to a certain amount of fibres in the soil mixture, the mechanical properties of the reinforced earth samples were increased thanks to the good cohesion into the matrix between fibres and soil. Over a certain ratio of fibres, situated between 0.25 and 0.5 % (Danso, Martinson, Ali, & Williams, 2015), mechanical properties began to decrease because of the too large amount of fibres present in the samples. In fact, fibres where getting to close to each other, which caused the soil matrix to weaken and the porosity of the samples to increase considerably. It was found that the optimal ratio of fibres where the same for compression and tension strengths (Danso, Martinson, Ali, & Williams, 2015). However, the strict correlation between the compressive strength and tensile strength of a block is still in discussion, because it shows too disperse results in function of the soil nature, the type of fibre used, and whether the samples were stabilised or not (Cardinale, Arleo, Bernardo, & Feo, 2017), or reinforced or not (Walker, 2004; Venkatarama Reddy & Jagadish, 1995; Danso, Martinson, Ali, & Williams, 2015).

In any case, it is not possible to propose generic results for the optimal fibre ratio to incorporate in earth samples because to many parameters are involved in such studies (nature of the fibre, fibre ratio, soil composition, testing procedure,…).

Optimal water ratio: the difference between static and dynamic compaction

Incorporating a proper water content in a soil mixture is essential to reach a superior dry density. It will allow the most suited lubrification of the soil mixture, which will ensure an optimal rearrangement of the soil particles.

In Geotechnics, the Proctor testing method has been developed to find the optimal water content of a given soil mixture. The Proctor testing method is a standardised dynamic compaction procedure determining the relation between the dry density of a soil in function of its water content. This relation allows to obtain the maximal dry density for the type of soil tested (François, 2017-2018).

The fabrication of CEBs on the other hand is performed through static compaction, but also requires the knowledge of the optimum water content of the soil mixture. At first, the Proctor test sounded suitable to find the optimum water content of CEBs, but recent studies revealed that this geotechnical method is not representative of the mechanical behaviour of CEBs, and that there seems to be no relation between the Proctor compaction energy and the static compression load.

In fact, since scientific studies about earthen constructions began to extend again around the early 90's (Morel, Mesbah, Oggero, & Walker, 2000; Pacheco-Torgal & Jalali, 2011), a lot of discussions were made around the Proctor compaction test and its suitability for CEB studies. There is indeed an essential difference between both test procedures: the compaction method. By opposition to the Proctor test, which is dynamic, the CEBs are statically compressed. Experimentation results revealed that this optimum didn't fit for statically compacted samples, like shown on Figure 7 (Mesbah, Morel, & Olivier, 1999) (all literature found about this subject share similar graphical results).

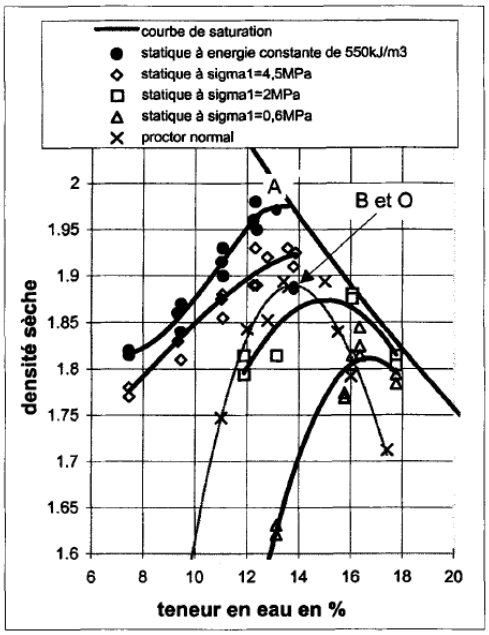

Figure 7: Water content optimisation (Mesbah, Morel, & Olivier, 1999)

According to these results, one can see that the optimum water content for statically compacted samples depends on the compaction stress, and that a different water content is needed to reach the same dry density whether samples are dynamically compacted or statically compacted.

To stress even more this disparity between proctor compaction and static compaction, other authors studied these compaction methods by comparing several soil mixtures compacted both ways, while being consciously prepared with the optimum proctor water content (Pkla, 2002). The results can be seen on Figure 8. The compression strength of these samples highly depends on the type of soil used, and the strong relation between compression strength and dry density (Olivier & Mesbah, 1986) could not be verified when such comparisons are made. The outcome of these results is clearly that no link can be found between dynamic and static compaction (Pkla, 2002).

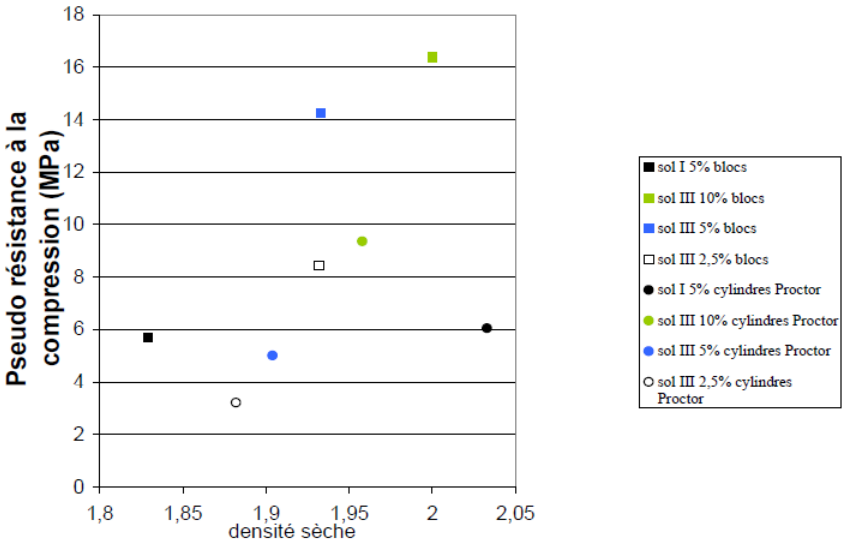

Figure 8: Comparison between Proctor and static samples (Pkla, 2002)

Moreover, because of this huge disparity, a static compaction testing procedure was studied to find an equivalence between the water ratio, the dry density and the static compaction stress. So that instead of testing a brick, one could use cylindrical samples as for the usual geotechnical testing while being exactly representative of statically compacted blocks (Mesbah, Morel, & Olivier, 1999; Walker, 2004).

The previous observations could imply that any study found in literature dealing with CEBs that does not take this Proctor/Static difference into account can't be 100% reliable (Pkla, 2002). In fact, samples made with the Proctor compaction will be too heterogeneous in terms of density, while statically compacted samples made with the optimal Proctor water content will contain too much water. In both cases, the samples will not be representative of the reality.

Cure

Most of the studies recommend curing the samples even if non stabilised earth samples do not need a hydration period like the stabilised ones. This is to make sure that the sample have reached a stable weight, and that the testing conditions are representative of a real situation. In fact, the water content present in the blocks after their manufacture has an important effect on their compression strength (Aymerich, Fenu, & Meloni, 2011; Aubert, Fabbri, Morel, & Maillard, 2013; Pkla, 2002). A recent review also insists on the positive effects of a good after-treatment of stabilised CEBs. It has been proved that stabilised CEB cured in "bad" conditions (30°C and <50% R.H.) were 35% less strong than the ones cured in good conditions (30°C and >90% R.H.) (Vyncke, Kupers, & Denies, 2017).

4. Materials

Type of soil

As many authors already reported it, the soil type for earth construction is one of the most important parameters to obtain a satisfying product.

The soil used for this study is top-layer silty soil from the stone quarry situated in Marche-les-Dames, Belgium. In this paper, this soil is referred to as "MLD", short for "Limon de Marche-les-Dames". As the soil of this study is the same as the one that Alexandre Robert used in his thesis (Robert, Non-stabilized rammed earth constructions: Material characteristics and Application to Urban Co-Housing in Brussels, 2013), the characteristics of this specific soil will be based on his results. Figure 9 and Figure 10 resume the soil identification of MLD.

Soil	MLD
Origin	Marche-Les-Dames, Belgium
Shrinkage limit	17.4%
Plastic limit	22%
Liquid limit	33.44%
Plasticity Index (Ip)	13.24
Clay proportion I	13%
Silt proportion II	58%
ABEM classification	Silt / Silty Clay

Figure 9: Identification of MLD soil (Robert, 2013)

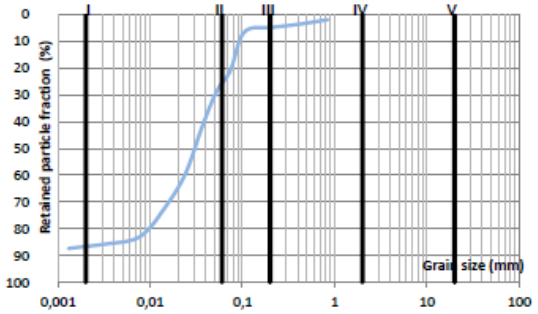

Figure 10: Grain-size distribution of MLD soil (Robert, 2013)

It has been proven that soils performed better when they contained a significant proportion of clay, namely that they included between 14% and 30% of clay (Pkla, 2002; Danso, Martinson, Ali, & Williams, 2015). This is in opposition to the norm recommendations CRATerre which recommends the following grain size distribution, while containing an average of 15% of clay particles (Houben & Guillaud, 2006).

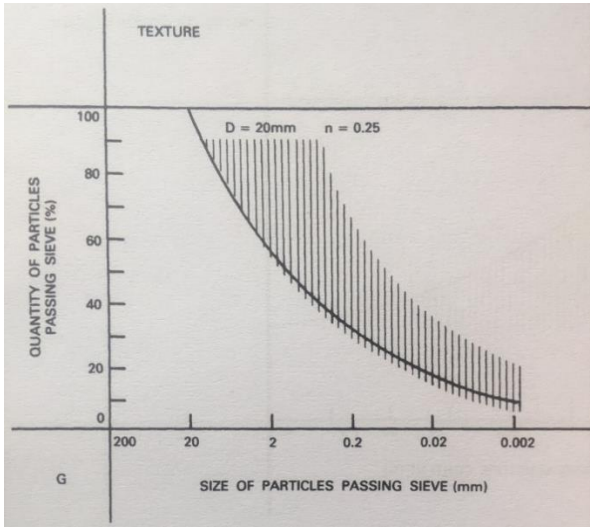

Figure 11: Ideal interval of grain-size distribution (Houben & Guillaud, 2006)

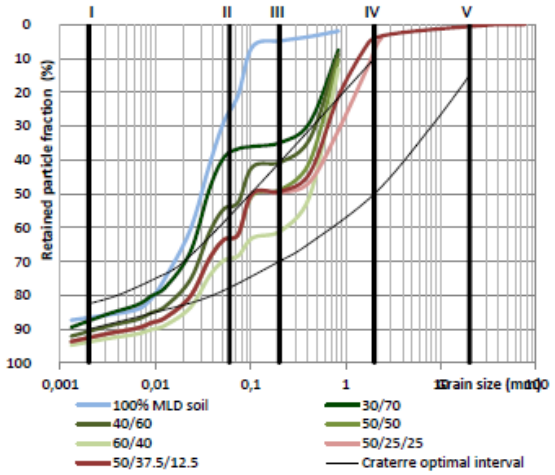

Figure 6 : Grain-size optimisation of MLD soil with sand and gravel

Figure 12: Grain-size optimisation of MLD (Robert, 2013)

The study of the nature of the soil and its suitability to be used as construction element was part of the scope of Alexandre Robert's master thesis. He optimised the soil structure by modifying the grain-size distribution of MLD in order to fit the optimal interval proposed by CRATerre (Figure 11 and Figure 12). He concluded that this MLD soil performed better when it was not optimised according to the grain size distribution recommended by CRATerre. In fact, the 100% MLD reached a compressive strength of 3,8 MPa while the modified MLD only reached 2,4 MPa (Robert, 2013). This may be explained by the fact that this grain size distribution is also applicable for the confection of stabilised earth blocks (Houben & Guillaud, 2006), and thus not optimised for the confection of unstabilised soil.

For this thesis, the conclusions of Alexandre will be taken into account and the experiments will be done with unmodified and unstabilised MLD. This choice is also in line with the wish to have a minimum of transformation between the extraction of the soil and the construction phase.

Fibre type: why straw?

Among a large series of possible natural fibres to use as reinforcement in CEB, the choice for this study was to opt for straw as natural reinforcement, more particularly wheat straw.

Although various other types of natural fibres have proved to have good mechanical properties when incorporated in soil (see section *State-of-the-art* on Compressed Earth Blocks), the choice of fibres to use for this study is based on the availability of natural fibres in a close vicinity. Literature as shown that mechanical and physical properties highly depend on the type of soil and on the nature of the fibres. These parameters are in direct relation with the location where experimental studies and construction projects took place. In fact, the availability of certain soil types and particular natural fibres will vary from regions to regions. Moreover, it was also decided for this study to opt for a waste material rather than for food products (oil plants, hay, oat, barley, wheat,…) or for raw materials used in textile industry (sheep wool, cotton,…).

In Belgium, wheat production represents more than 60% of the cereal agricultural sector (StatBel, Belgium in figures, 2019) and is harvested once a year (the winter wheat straw being the most common one). Wheat seeds are then used to produce floor, while straw is recycled for cattle litter (by opposition to oat or barley straw that are used for cattle food). These few reasons constituted the selection criteria for the choice of fibres to incorporate in the soil mixture and directed it towards the utilisation of wheat straw.

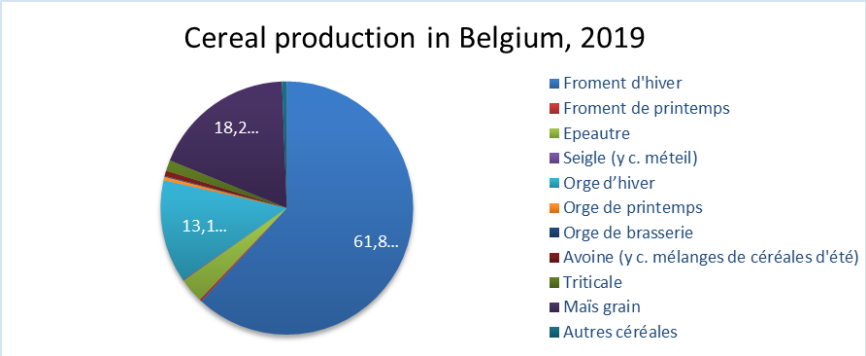

Figure 13: Cereal production in Belgium in 2019 (StatBel, Belgium in figures, 2019)

5. Experimental tests

The outcomes of the first experimental part will be the optimal straw ratio to reinforce compressed earth blocks on a primary basis, and on a secondary basis, the recommended procedure to follow to obtain the most homogeneous samples. To do so, the procedure for non-reinforced samples will be followed as a starting point. In a second time, this procedure will be modified according to the changes that the new reinforcement elements induce and according to the possibilities of the available testing equipment.

The outcomes of the second experimental part will be the recommended procedures to follow in order to test the mechanical properties of CEB samples on a primary basis. On a secondary basis, the cure benefits and the influence of water content on CEBs will be exposed.

Part 1: Optimal straw ratio

1. Preliminary steps

1.1. Water content

As this first part of the study focuses on the finding of the optimal straw ratio while using the recommendations for soil testing, the cylindrical samples (diameter = 36mm; height = 70mm) will be made according to these same recommendations. The samples will thus be dynamically compacted, which is why the water content used for this first experimental part will be chosen according to the optimal Proctor test. For this soil, the optimum Proctor water content is of 15%, as shown on Figure 14.

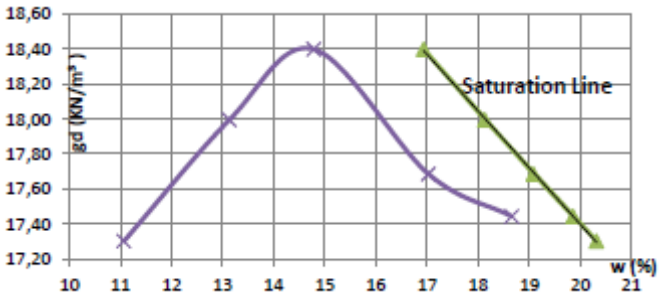

Figure 14: Proctor curve for MLD (Robert, 2013)

1.2. Soil preparation

The soil was stored in the big delivery bag and could not be used directly to prepare the soil mixture. In fact, before being able to put the soil mixture in the mould, the soil first needed to undergo several steps in order to be homogeneous and dry. First, the soil had to be crushed and sieved with the mesh number 6 to remove any particles larger than 3,36 mm. After that, the soil needed to pass through the mechanical cutter to obtain the most fine-grained soil possible. Finally, thin layers of cut soil could be disposed on plates in a hot room in order to allow the soil to dry correctly. After 24 hours, the soil could be considered completely dry and was ready to be prepared in a mixture.

1.3. Straw preparation

Types of straw

Two types of straw were used in the optimisation part. The first one comes from a typical straw bag sold in a pet shop. The second one was ordered from an equestrian centre which had access to industrially chopped straw.

A great disparity could be observed for the first type of straw. The lengths of the straw wisps could vary from 1cm to more than 30cm. Most of the wisps were still complete, meaning that they were hollow and that knots were often present. Sometimes hay was found in the bag, as well as ears of wheat. The nature of this first type of straw can thus be qualified as highly heterogeneous (Figure 15).

The second type of straw presented a less dispersed appearance, with straw wisps having a maximal length of approximately 10cm. Only few of the wisps were still complete, resulting in a much more homogeneous straw type (Figure 16).

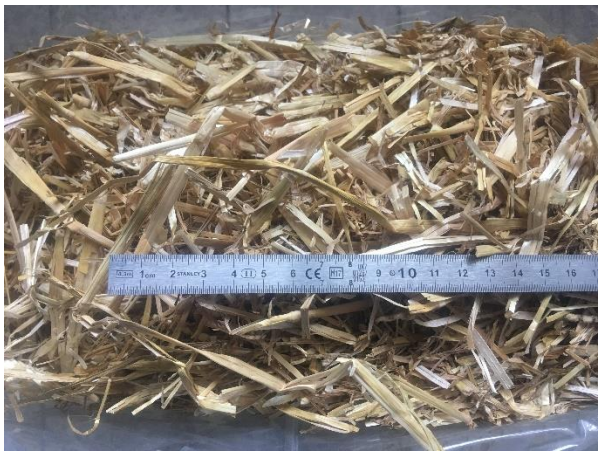

Figure 15: Type of straw 1 (Personal picture)

Figure 16: Type of straw 2 (Personal picture)

Saturation process of straw

Two manners to add natural fibres in a soil mixture were identified in literature:

- Mixing the dry materials together and add water in a second time (Danso, Martinson, Ali, & Williams, 2015; Aymerich, Fenu, & Meloni, 2011; Cardinale, Arleo, Bernardo, & Feo, 2017).

- Mixing the dry soil with the saturated natural fibres and add water in a second time (Catalan, Hegyi, Dico, & Mircea, 2015; Danso, Martinson, Ali, & Williams, 2015).

To know which one of them was the most suited, the saturation behaviour of straw was first analysed to predict the water diffusion into a reinforced sample. In fact, straw is known to be highly absorbent (more than 100% of its dry mass), which could become a problem for the diffusion of water between the soil particles, having a porosity of approximately 40%.

After a saturation testing (see next section *Saturation of straw*), we concluded that straw was not saturated after one hour, as recommended by Catalan, Hegyi, Dico, & Mircea, 2015, but after one day. In fact, one hour after the immersion of straw into a bucket of water, the straw was still floating at the water surface. After waiting 23 hours extra, all wisps of straw were completely immersed, staying at the bottom of the water bucket.

To avoid any capillary force in the sample caused by the slower saturation process of straw, the mixing procedure will follow the second option mentioned before, namely mixing dry soil with saturated straw and water. Saturating straw beforehand will also allow a better cohesion with the soil and the fibres because it will limit water absorption during manufacturing. This is often preferable since an important water absorption could induce a large variation of the dimensions of the fibres, which goes hand in hand with lower binding with the soil matrix (Laborel-Préneron, Aubert, Magniont, Tribout, & Bertron, 2016).

This mixture procedure will allow to compare samples reinforced with different kinds of straw in a more objective way, as the saturation parameter will already be fixed. In fact, both types of straw had a different water content at saturation (see section

Preparation of the soil mixture), which could induce a different behaviour of water diffusion in the silty clay soil.

Preparation and saturation of straw

Before incorporating the straw to the earth mixture, several steps needed to be followed to have an optimum mixture. The straw bales contained a non-negligible amount of dust, which could interfere with the determination of the straw water content at saturation. A cleaning phase and elimination of small particles should thus take place in any case, even if the straw package stipulates that the straw has been dedusted. In fact, the straw dust represented over 3% of the mass of straw. In addition to the possible water content interfering, these small particles could have a negative impact on the soil matrix cohesion, as it happened with wood shavings reinforcement (Laborel-Préneron, Aubert, Magniont, Tribout, & Bertron, 2016). Eliminating straw dust and other impurities is thus an essential phase in the straw preparation process.

Moreover, even if the second type of straw used for this study was already chopped, the wisps of straw in both cases were still too long with respect to the samples to test. Better results were obtained with a multidirectional distribution of the fibres into the samples, and to allow that, it has been recommended (Houben & Guillaud, 2006; Laborel-Préneron, Aubert, Magniont, Tribout, & Bertron, 2016) to limit the maximal length of fibres to the smallest dimensions of the sample. As the samples used in this first experimental part are cylinders with a 3,6 cm diameter and a height of 7 cm, the straw wisps were cut every 3 cm.

The straw saturation and its preparation for further incorporation into a soil mixture are summarised through the following steps:

1. Pass small amounts of straw through the sieve number 8 (2,362mm opening). The dust and most of any other impurities will pass through the sieve. Thin wisps of straw (up to 1 cm) will also pass vertically through the mesh.
2. Rinse three time at least, until the rinsing water is clear.
3. Cut the straw to reduce the maximal length to approximately 3 cm.
4. Immerge the straw in a water bucket and cover it with the sieve so that none of the straw is floating at the surface of the water.
5. Wait at least 24h hours to be sure that the straw is completely soaked. One can verify that the straw is saturated by removing the sieve and checking if the straw stays at the bottom of the bucket.
6. Once the straw is completely saturated, remove the water of the bucket.
7. Shake the straw dry to remove the additional water. Repeat this step three times.
8. Let the straw rest in the bucket for a moment (15min) to let the extra water drop downwards.
9. Repeat steps 6 and 7.
10. Now that most of the extra water has been removed, the straw is ready to be incorporated into the earth mixture.

Figure 17: Rinsing phase (Personal picture)

Figure 18: Opaque cleaning water (Personal picture)

Figure 19: Immersion phase (Personal picture)

Figure 20: Soaked straw (Personal picture)

1.4. Preparation of the soil mixture

When the soil is completely dry and the straw saturated, the preparation of the mixture can start. To know exactly which proportion of water to incorporate in the mixture, the water content of the saturated straw needed to be found. This can be done when step 10 has been reached. For this study, the first type of straw had a water content at saturation of 121%, and the second type of straw had one of 580%. These results confirmed that the type of straw could also induce disparities in terms of physical properties aside from the differences observed about their general appearance (see section *Types of straw*). The amount of water to add in the mixture can be found with the following equation:

$$x = x_{wt} - x_{straw}$$

With: $x_{straw} = \frac{x_{straw,sat}}{1+w_{straw}}$

Where: $x = additionnal\ mass\ of\ water\ to\ incorporate\ in\ the\ mixture\ (for\ water: 1g = 1ml)$

$x_{wt} = total\ mass\ of\ water\ of\ the\ mixture$

$x_{straw} = mass\ of\ water\ of\ the\ saturated\ straw$

$x_{straw,sat} = mass\ of\ saturated\ straw$

$w_{straw} = water\ content\ of\ straw\ at\ saturation$

It has to be noted that the order of incorporation in the mixture is important. In fact, when the dry soil is introduced after the saturated straw, the formation of wet soil clusters occurred around the straw wisps (Figure 21Figure 22). This resulted in a very heterogeneous water repartition in the mixture and required to separate the agglomerated clusters one by one to create a more homogeneous mixture. Introducing the straw after the preparation of the earth-water mixture allows to avoid this cluster formation around the straw wisps (Figure 23 Figure 24). Once the mixture has been prepared, it should rest during 24 hours in a hermetically closed bag placed in a chilled humid room to allow the homogenisation of the water in the mixture.

Figure 21: Soil after straw introduction (Personal picture)

Figure 22: Heterogeneous mixture (Personal picture)

Figure 23: Straw after soil introduction (Personal picture)

Figure 24: Homogeneous mixture (Personal picture)

2. Sample production

2.1. Steps of the production procedure

When the preparation of the mixture is done, the sample production can begin with the cylindrical mould of 76mm height with a 36mm diameter. It is important to differentiate the moulding of the non-reinforced samples from the reinforced samples. In fact, when no straw is added in the mixture, soil can just be poured into the cylindrical mould, while if straw is introduced in the mixture, the soil particles and straw wisps will not flow out at the same time. Due to their difference in density and geometry[1], the soil particles will pour out first, leaving the straw for the end. This will result in heterogeneous samples having a majority of soil on one extremity of the sample and a majority of straw on the other extremity.

To avoid this situation, it is important to fill the mould in several spoonful of earth-straw mixture, equivalent in terms of straw quantity. The spoonful will require some help to pass through the funnel. To do so, it is recommended to use a stick and push the mixture through it instead of shaking it. Indeed, the up and down movements will create the Brazilian nut effect, meaning that the small particles of the mixture (i.e. the soil) will go down, and that the largest particles (i.e. the straw) will come up, resulting again in non-homogeneous repartition of the mixture in the mould.

To ensure a good repartition of the straw in the mould, it is important to slightly compress each spoonful of mixture and to roughen the flattened surface to guarantee cohesion with the next spoonful. Once the complete mixture is filled into the mould and that the upper cover of the mould is pushed into it, the lower cover has to be hammered into the mould but only by half, in order to hammer the second half on the side of the upper cover. This supplementary step is necessary because otherwise the samples presented differences in their appearance (grainy on one side and smooth on the other side, see Figure 25Figure 26) and in their compression failure scheme (according to the orientation of the sample in the compression machine). Moreover, samples hammered only on one side presented a water content disparity at their edges. Even if this disparity could be due to the more or less irregular straw distribution in the sample, the fact that they are hammered equally on both edges makes them more homogeneous. This observation could also be verified when a sample is cut in half lengthwise.

[1] Granular flow

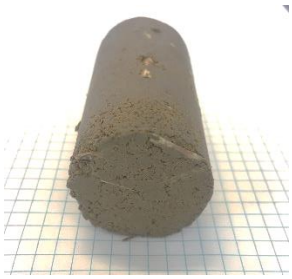

Figure 25: Granular side (Personal picture)

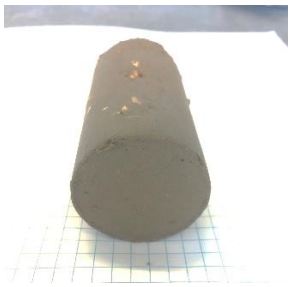

Figure 26: Smooth side (Personal picture)

Figure 27: Smooth side 1 (Personal picture)

Figure 28: Smooth side 2 (Personal picture)

One could note the importance of this procedure when the test results of two series of straw reinforced samples were compared, where the only modified parameter between both series of samples was the way straw had been introduced into the mould, namely series "P" and "Q" (see results further, in section *Samples Q)*.

Note: As the straw incorporated into the mixture is saturated, the straw ratios were defined as saturated values to stress the fact that the proportions of straw to add to the mixture highly depends on their absorbance (see section *Type of straw II*).

3. Compressive strength

3.1. Testing procedure

The testing procedure follows the unconfined compression test as described in the course of Soil Mechanics (François, 2017-2018). The unconfined compression test is performed as a triaxial test, except that the confining pressure is equal to zero. This rapid test allows to obtain the approximate values of the compressive strength of the soil samples, failing under shear stress. This one-dimensional loading will also provide the Young-modulus E of the samples tested. The recommended speed of the mechanical press is of 0.06666mm/min. The force sensor used for these cylindrical samples is 500kg sensor.

Figure 29: Unconfined compression test apparatus - (Personal picture)

Figure 30: Sample to compress (Personal picture)

Figure 31: Sample failure (Personal picture)

For these tests, the compression strength was calculated with the following formula, taking into account the Poisson effect occurring during compression with the corrected area (A_C):

$$\sigma = \frac{F}{A_c}$$

Where: $F = maximal\ force\ applied\ by\ the\ piston$

$$A_C = A_0(1 - \varepsilon_a)$$

$$\varepsilon_a = \frac{\Delta H}{H_0}$$

The Young modulus was calculated according to the steepest slope of the axial compression stress – strain curve, in an interval of 0,2% around a centred point of this slope.

3.2. Summary of the tested samples

The samples were tested following the timeline here-below. A first phase was focused on improving of the production process, using the first type of straw. When the second type of straw was available, a second phase was centred around finding the optimal straw ratio of reinforced samples.

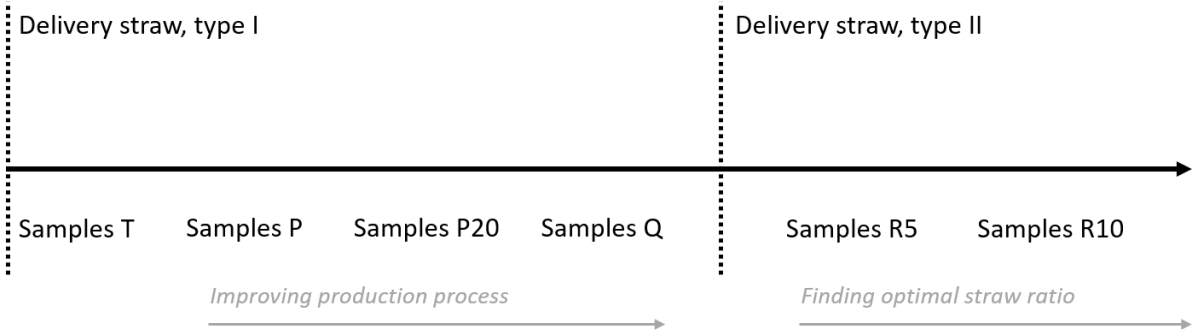

Table 2 summarises the main properties of the samples tested during this first experimental part.

	Samples T	Samples P	Samples P20	Samples Q	Samples R	Samples R10
Water content	15	15	15	15	15	15
Presence of straw	No	Yes	Yes	Yes	Yes	Yes
Type of straw	None	I	I	I	II	II
Saturated straw ratio	0	5	20	5	5	10
Dry straw ratio	0	2,3	9	2,3	0,74	1,5
Density	1697	1652	/	1728	1735	1610

Table 2: Summary of the cylindrical samples tested

3.3. Type of straw I

The two first series of tests performed were the series T and P. The T samples were made out of a 100% soil mixture, while the P samples were made out of a mixture containing the first type of straw. At first, no particular procedure was followed to introduce the straw. As already stated previously,

the water content used for this first experimental part is of 15%, according to the optimum Proctor test.

Two saturated straw ratios were defined to delimit an interval of possible straw reinforcement, namely 5% and 20%. The samples containing 20% of straw (Samples P20) presented large deformations after the demoulding process, such as expansion and bending, and were therefore not tested. Figure 32 and Figure 33 show these deformations. Figure 34 and Figure 35 give an idea of the amount of straw present in a mixture reinforced at 5% of saturated straw and at 20% of saturated straw.

Figure 32: Sample P, 20% straw: Deformation 1 (Personal picture)

Figure 33: Sample P, 20% straw: Deformation 2 (Personal picture)

Figure 34: Mixture earth-straw 5% (Personal picture)

Figure 35: Mixture earth-straw 20% (Personal picture)

Samples T and P

The results of this first series of tests are reported on Figure 36.

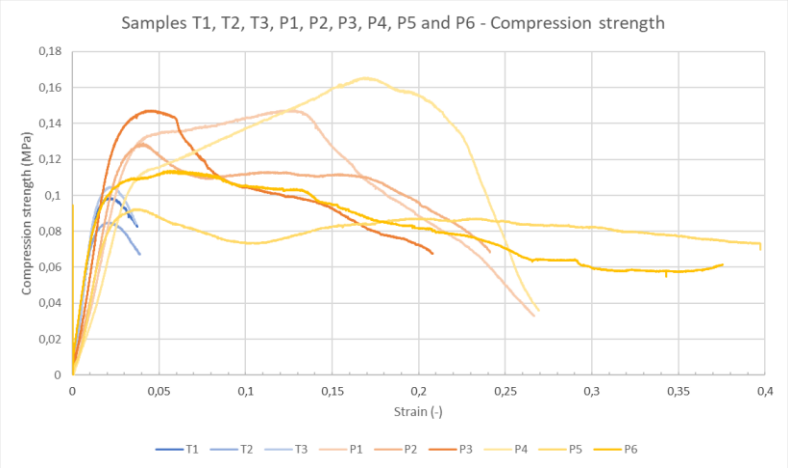

Figure 36: Samples T and P - Compression strength

As it can be seen on this graph, the compression curves of the reinforced samples presented a large disparity between the first compression slopes as well as between the plateau's following that slope. This large disparity is essentially due to the heterogeneity of the samples. In fact, the random repartition of the straw in the mould and the nature of the straw itself represented a great deal in the compression behaviour of the samples. The main information retrieved from these tests are resumes in the table here-below.

	Force Max (kg)	W (%)	ρ_{dry} (kg/m³)	Compr. Str. (MPa)	E-modulus (MPa)
T1	10.31	15.90	1700	0.098	6,64
T2	8.84	16.70	1695	0.085	10,31
T3	10.99	16.10	1695	0.105	8,52
T	**10.05**	**16.23**	**1697**	**0.096**	**8,49**
P1	17.25	17.10	1657	0.147	4,66
P2	13.78	17.46	1635	0.129	5,41
P3	15.84	17.11	1650	0.147	6,80
P4	20.48	17.93	1623	0.165	3,96
P5	12.45	15.25	1688	**barrelling** 0.074	5,36
P6	12.52	16.35	1656	0.112	7,02
P	**15.39**	**16.87**	**1652**	**0.140**	**5,54**

Table 3: Results samples T and samples P

As shown in Table 3, the results obtained for this first comparison revealed an improvement by 1,46 of the compression strength for the reinforced samples P, with σ_T = 0,096 MPa versus σ_P = 0,140 MPa. On the other hand, the Young modulus of the reinforced samples decreased by 1,53, with E_T = 8,5 MPa versus E_P = 5,5 MPa. This decrease could be explained by the compressibility of the fibres, which induced a higher elasticity of the samples P, characterised by a less sharp first compression slope which can be observed on the previous graph. This first series of tests was particularly useful to ameliorate the preparation procedure to create more homogeneous future samples.

Samples Q

The third series of samples (samples Q) was made with the same mixture as for samples P but following the improved moulding procedure of the samples (see section *Steps of the production procedure*). Figure 37 presents the results obtained for the samples Q.

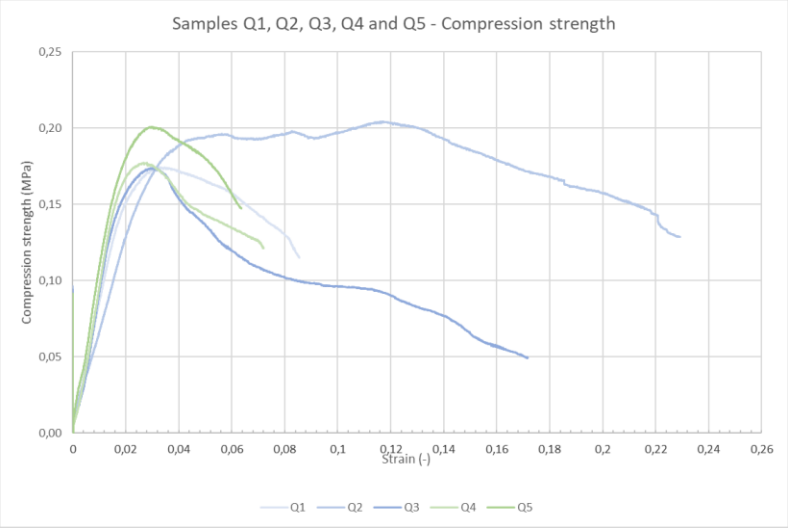

Figure 37: Samples Q - Compression strength

When compared to the first results of the samples P, these results show a less dispersed compression slope with quite similar maximal compression loads. Nevertheless, the behaviour of these samples after this first compression slope is still as dispersed as for the samples P. This disparity is probably only due to the nature of the straw used for these series because it disappears for the samples created with the second type of straw (see further, in section *Samples R*).

	Force Max (kg)	W (%)	ρ_{dry} (kg/m³)	Compr. str. (MPa)	E-modulus (MPa)
Q1	18.50	16.15	1735	0,174	8,54
Q2	23.73	17.46	1704	0,204	6,64
Q3	18.41	15.41	1741	0,174	11,30
Q4	18.77	16.05	1735	0,177	10,74
Q5	21.26	16.21	1725	0,201	11,27
Q	**20,13**	**16,26**	**1728**	**0,186**	**9,70**

Table 4: Results samples Q

As shown in Table 4, besides of providing a less dispersed behaviour of the first compression phase of the samples, this improved sample production procedure allowed to enhance the compression strength of samples Q by 1,33 compared to the samples P (σ_P = 0,140 MPa versus σ_Q = 0,186 MPa). An improvement of their Young modulus could also be observed, with an increase by 1,75 compared to samples P (E_Q = 9,70 MPa versus E_P = 5,54 MPa), and by 1,14 compared to samples T (E_Q = 9,70 MPa versus E_T = 8,49 MPa). These positive effects on compression strength and Young modulus could both be a consequence of the samples moulding procedure, allowing an homogenisation of the reinforced samples and a general increase of dry density of the samples ($\rho_{dry,Q}$ = 1728 kg/m³ > $\rho_{dry,T}$ = 1697 kg/m³ > $\rho_{dry,P}$ = 1652 kg/m³).

3.4. Type of straw II

As both types of straw presented a different water content at saturation, 121% for the first type of straw and 580% for the second type of straw, a conversion had to be made to deal with this difference in water content at saturation. A compromise needed to be made between the dry amount of straw to add and its absorbance, hence the water content present in the soil before the incorporation of straw. The following reasoning shows that the optimal straw ratio is not only a matter of finding the ideal dry amount of straw to incorporate in a mixture.

In fact, a first conversion was made in function of the dry proportion of straw in the mixture. According to the dry ratio of straw present in the samples P and Q (made with a 5% saturated straw ratio of type I), the reinforced samples made with the second type of straw should be of 20% saturated straw. Indeed, the dry proportion of straw incorporated in samples P and Q is of 0,023 which would correspond to a hypothetical dry proportion of straw II of 0,029, as shown in Table 5.

But due to the high absorbance of the second type of straw, incorporating a 20% ratio of this saturated straw could not be possible. In fact, this would imply whether to add a negative amount of water to the mixture, which is impossible, whether to end with a higher water content of the mixture than required (17,1% instead of 15,0%). So, the conversion was made in function of the amount of water mixed with the dry soil before the incorporation of the saturated straw, representing the "pseudo initial water content" of the mixture.

	Samples reinforced with straw I Absorbance: 121%		Samples reinforced with straw II Absorbance: 580%	
Saturated straw ratio (%)	dry straw ratio (%)	Initial water content (%)	dry straw ratio (%)	Initial water content (%)
5	2,3	12,26	0,74	10,74
10	4,5	9,52	1,50	6,47
20	9,0	4,05	2,90	(negative)

Table 5: Saturated straw ratios of reinforced samples

In a first time, this reasoning lead to create a mixture including 5% of saturated straw of type II (samples R). In fact, the initial water content of samples reinforced with 5% of the first type of straw was of 12,26%, while it was of 10,74% in the case of 5% of the second type of straw and of 6,47% in the case of 10% of the second type of straw. In a second time, it was also decided to make the mixture containing a 10% of saturated straw ratio of type II (samples R10), in order to compare the behaviour of both 5% and 10% reinforcement made with the second type of straw and to opt for the best ratio according to their respective results. This compromise between the dry amount of straw and its absorbance could thus be expressed by means of using a *saturated straw ratio* instead of a *dry straw ratio*.

Samples R

As a reminder, this series of tests was performed with samples having a 15% water content, reinforced with the second type of straw (which was not yet available for the previous series P and Q). The results of this fourth series are reported on Figure 38.

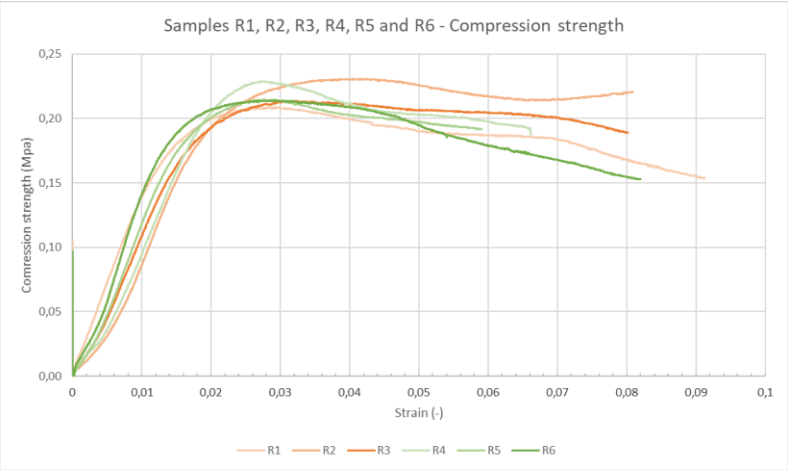

Figure 38: Samples R5 - Compression strength

The results obtained for this series shows that the nature of straw used to reinforce the samples plays an important role in the compression behaviour of these samples. In fact, as already stated in the section *Types of straw*, the second type of straw used in this study presented a less strong heterogeneity in terms of appearance and quality, which directly impacted the results of the compression tests. In fact, it can be seen on Figure 38 that the compression slopes and resistance loss phases are quite similar among this series of samples. The numerical results resumed in Table 6 also show a satisfying regularity within the six samples.

	Force Max (kg)	W (%)	ρ_{dry} (kg/m³)	Compr. Str. (MPa)	E-modulus (MPa)
R1	22.02	14.65	1735	0,209	13,99
R2	24.82	15.06	1726	0,230	13,47
R3	22.57	15.38	1723	0,213	12,42
R4	24.16	15.43	1728	0,229	12,79
R5	22.73	14.92	1740	0,214	14,38
R6	22.64	14.51	1758	0.214	17,21
R	**23,16**	**14,99**	**1735**	**0,218**	**14,05**

Table 6: Results samples R

Samples R10

This fifth series of samples was also made with the second type of straw, but the ratio for these samples was chosen at 10% instead of 5%, in order to verify if doubling the straw ratio was interesting. Figure 39 and Table 7 resume the results of this fifth series of samples.

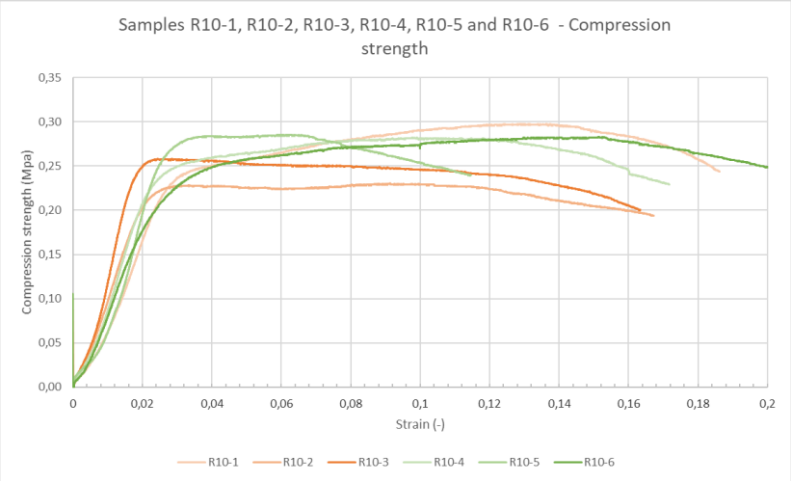

Figure 39: Samples R10 - Compression strength

The results obtained after testing these samples were in the same line as the samples R in terms of regularity and homogeneity of their compression behaviour. The average compression load accepted by these samples was much higher than for the samples R (F_R = 23,16 kg versus F_{R10} = 31,41 kg), resulting in a bigger compression strength as well (σ_R = 0,22 MPa versus σ_{R10} = 0,27 MPa). On the other hand, the Young modulus of the samples R10 remained constant compared to the values obtained for Samples R (E_R = 14,0 MPa versus E_{R10} = 13,9 GPa). This very small decrease of the Young modulus is due to the fact that the samples R10 present a more elastic behaviour than samples R, since they contain a doubled amount of straw with respect to samples R, and that the compressibility of straw induces a more elastic behaviour of the reinforced samples.

	Force Max (kg)	W (%)	ρ_{dry} (kg/m³)	Compr. Str. (MPa)	E-modulus (MPa)
R10-1	35.51	15.10	1576	0.297	11,22
R10-2	26.32	14.25	1593	0.227	12,38
R10-3	28.27	13.34	1644	0.245	18,64
R10-4	32.69	13.04	1642	0.281	13,52
R10-5	31.40	13.63	1610	0.286	16,31
R10-6	34.25	14.19	1594	0.283	11,23
R10	**31.41**	**13.93**	**1610**	**0.270**	**13,88**

Table 7: Results samples R10

4. Conclusions

After this first experimental part, two main observations could be noted. First, an adapted fabrication procedure for reinforced samples is mandatory to reach samples as uniform as possible. In fact, a good distribution of the straw wisps in the sample's matrix is necessary to ensure cohesion. Secondly, the nature of the straw incorporated into a soil mixture plays an important role for the compression strength of the samples. Indeed, samples reinforced with the second type of straw were more homogeneous samples than the ones reinforced with the first type of straw, and presented notable regularity in their compression behaviour, by opposition to the samples reinforced with the first type of straw.

Part 2: Compressed earth blocks

1. Sample production

Before the production phase of the samples could begin, the same preparation steps as for the first experimental part had to be applied to the soil and to the straw. A particular attention needed to be paid to the rinsing part, which had to take place more than three times. As the straw quantities required for this experimental part are much higher than for the first part, resulting in a larger amount of dust to eliminate.

In fact, the quantity of mixture to prepare was of 60 kg instead of 1kg. Most of the straw dust and impurities could be eliminated with the sieving of smaller quantities of straw. Nevertheless, the rinsing step of this procedure could not be omitted because it allowed to eliminate the last remaining straw dust particles, which could skew the straw water content at saturation. As it can be seen on Figure 40, the third rinsing water was brown and quite opaque. More than three rinsing's were thus required to clean the straw properly. The straw could be assumed clean when the rinsing water was clear. After the saturation of the straw, the mixtures could be prepared by 2 kg ranges, to facilitate the mixing process and to guaranty a mixture as homogeneous as possible.

Figure 40: Third rinsing water (Personal picture)

Figure 41: Clean saturation water (Personal picture)

Figure 42: 2kg mixture (Personal picture)

Figure 43: Homogeneous mixture (Personal picture)

After 24 hours of rest in hermetically closed bags placed in a chilled humid room to allow water to diffuse homogeneously, the mixtures could be taken to the CSTC-WTCB to be pressed into CEBs. The CSTC-WTCB lab disposed of a manual press allowing two CEBs to be pressed at the same time. The dimensions of the moulds were the followings: 40x40x160 mm^3. The ideal dimensions for the confection of CEBs would have been around the 295x140x90 to reproduce the geometry of a CEB at best (Morel, Pkla, & Walker, 2007). Between both moulds available (cement mould: 40x40x160 and concrete mould: 10x10x300), we opted for the cement mould to stay closer to the samples dimensions of the first experimental part (cylinders with a 3,60 cm diameter and a 7,00 cm height).

The quantity of 1100 g was fixed for the pressing of non-reinforced CEB pairs. This mass was determined during a previous visit at the CSTC-WTCB by trial and error, so that the force needed to compress the mixture would be as high as possible, and still manually feasible. The same method was applied for the compression of the straw mixtures, for which a quantity of 1000g was deducted.

The densities obtained with static compaction were higher than the densities of the dynamically compacted cylindrical samples (resp. for unreinforced samples: 2055 kg/m^3 > 1700 kg/m^3; resp. for reinforced samples: 1675 kg/m^3 > 1610 kg/m^3).

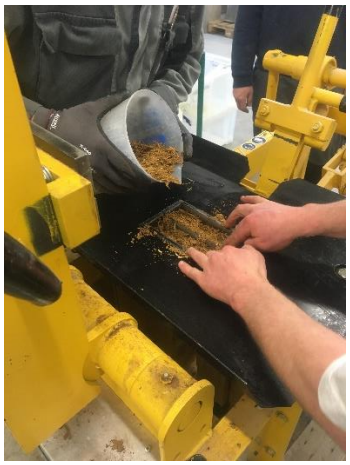

Figure 44: CEB moulds filling (Personal picture)

Figure 45: CEB compaction (Personal picture)

Figure 46: Hermatical stacking of CEBs (Personal picture)

To proceed to the fabrication of CEBs, the right amount of mixture was put into the pair of moulds, after being cleaned and greased (Figure 44). The compaction could then take place thanks to a lever arm system activated by two people (Figure 45). The compaction force highly depended on the workforce of the workers because all the compaction process was manual. After compaction, the pairs of CEBs were hermetically wrapped and stored to be transported back to the ULB lab (Figure 46).

2. Water content

As this second experimental part focuses on the CEB testing, the water content of the samples should be adapted accordingly. In fact, CEBs are statically compacted and should therefore not be created with the optimum Proctor water content, as it has been stated in the State-of-the-art.

In order to compare the effects of water content of the mechanical properties of CEBs, both dynamic and static optimum water contents will be used to create the CEBs. The series created with a 15% water content, namely the dynamic optimum, will be called “Samples E” and the series created with a 11% water content, namely the theoretical static optimum, as deduced here-below, will be called “Samples C”. This theoretical static water content of 11% was determined according to the following theoretical reasoning.

First, the difference in dry density in this study between dynamically compacted cylinders and statically compacted blocks, both made with the optimal Proctor water content (15%), appeared to be quite important, being of 1700 kg/m³ for the cylinders and of 2055 kg/m³ for the blocks. This could be explained by the higher compaction energy provided by the pressing machine during the static compaction of the blocks.

Moreover, according to A. Robert’s thesis, the maximum compression strength was reached for samples having an 8% water content, and a 2050kg/m³ dry density. These results were also found by increasing the compaction energy. It was then assumed that it was possible to reach a higher compressive strength with lower water contents for the statically compressed blocks.

So, taking into account the behaviour of the static water content curves proposed by Mesbah, Morel, & Olivier, 1999, a theoretical static curve could be determined (Figure 47), stipulating that for a reduced water content and a larger compaction energy, one could obtain a higher compression

strength. The maximum of this theoretical curve being situated at a water content around 11%. Therefore, this value was chosen to test this hypothesis.

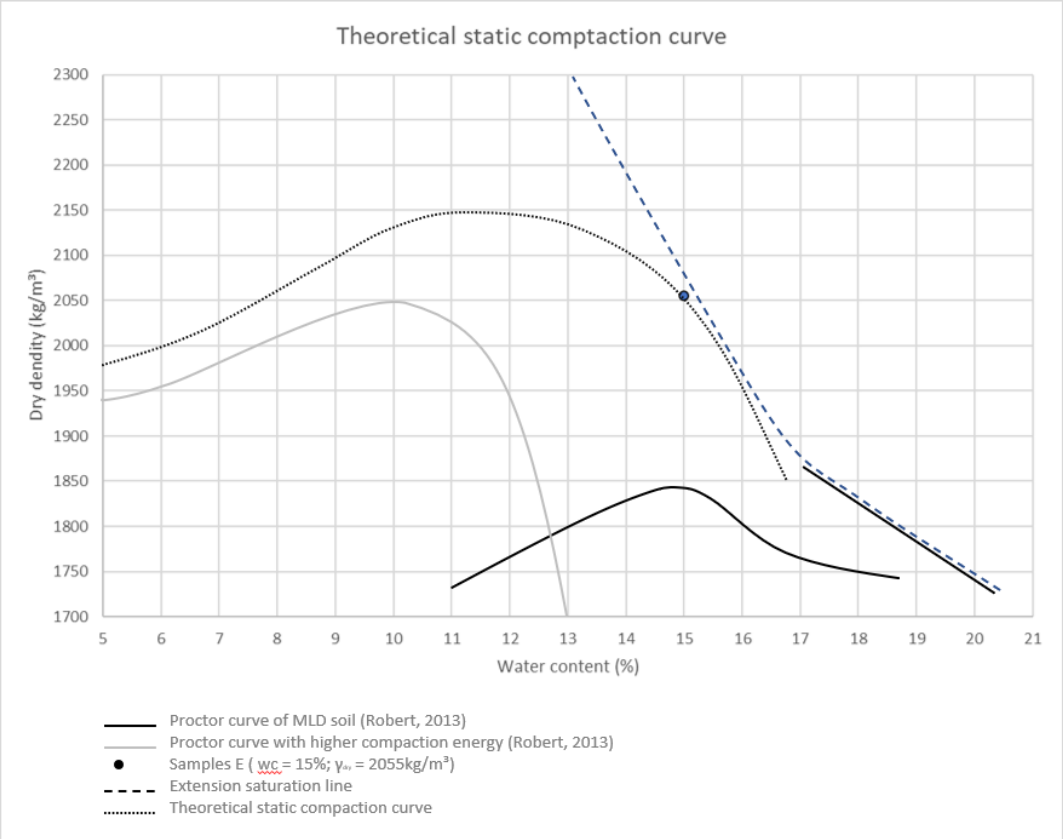

Figure 47: Theoretical static compaction curve

3. Cure

It was advised through literature to cure samples before testing them to obtain their real compression strength. This cure needs to reproduce the closest conditions of the samples with respect to their future application. For this study, the samples were tested in interior conditions, and were thus cured in an isothermal room at 22°C and at a relative humidity of +-45%.

Table 8 summarises the main properties of the samples tested during this second experimental part. In order to analyse the effect of cure of the samples, each series of samples was tested at day 0, day 7, day 14 and day 28.

	Samples E	Samples EP	Samples C	Samples CP
Compaction	Static	Static	Static	Static
Water content (%)	15	15	11	11
Presence of straw	No	Yes	No	Yes
Type of straw	None	II	None	II
Saturated straw ratio (%)	0	10	0	10
Dry straw ratio (%)	0	2,3	9	2,3
Density (kg/m³)	2055	1675	1949	1712

Table 8: Main properties of samples E, EP, C, CP

4. Tensile strength and compressive strengths method

Among all compression testing methods to apply on CEBs existing in literature, the most suited for this study is the procedure proposed by the RILEM group (see section State-of-the-art on Compressed Earth Blocks). As a reminder, this method proposes to test an assembling of two half blocks put one on the top of the other. This method can be summarised into these three steps: the first one consists in performing a three-point flexural test to break the CEB in two half blocks, from which the tensile strength can be deduced. The second part consists in assembling these two half blocks on top of each other with mortar. The third and last part is to test the assemblage in simple compression.

This procedure needed to be adapted to the constrains of this study, namely the dimensions of the samples, the equipment available, etc. The three following paragraphs are detailing this adapted procedure and how these changes have been managed in our lab.

4.1. Three-point flexural test

The procedure followed to perform the three-point flexural test on the CEB was done according to the EN 1015-11 European standard for mortar testing. A 3D model has been created to satisfy these recommendations (Figure 48 and Figure 49).

Figure 48: Three-point flexural test apparatus (Personal picture)

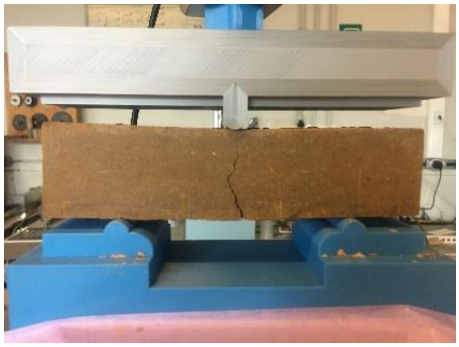

Figure 49: Failure under flexion (Personal picture)

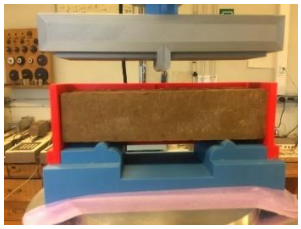

Figure 50

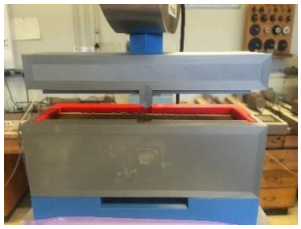

Figure 51

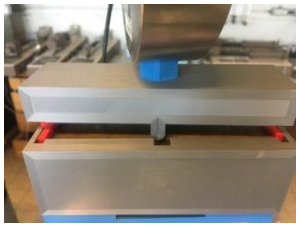

Figure 52

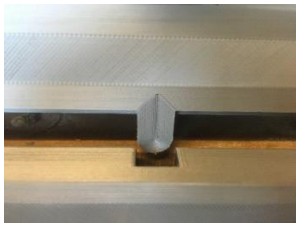

Figure 53

Figures 45,46,47 and 48: Adjusting mould for the sample's placement

In order to centre the CEBs correctly, the 3D model was composed of a mould that could help adjusting the press position so that the vertical force and the reaction on the contact surface were aligned (Figure 50,Figure 51,Figure 52 andFigure 53). The recommended speed of compression for this flexion test is of 0,002 mm/s.

Figure 54: Failure under shear stress (Personal picture)

Figure 55: Failure initiation gap (Personal picture)

Figure 56: Failure under flexural stress (Personal picture)

For the case of reinforced samples, the failure did not occur under tension but under shearing (Figure 54). To avoid this situation, it was decided to initiate the failure plane under flexion by sawing a 1,5mm gap in the middle of the bottom area of the reinforced samples (Figure 55 andFigure 56). The tensile strength calculations were adapted according to the smaller inertia of the reinforced samples.

$$\sigma_F = \frac{3FL}{2bd^2}$$

With $\sigma_F = tensile\ strength$
$F = maximal\ load\ during\ 3\ point\ flexural\ test$
$L = length\ of\ the\ sample$
$b = horizontal\ depth\ of\ the\ sample$
$d = vertical\ depth\ of\ the\ sample\ (40mm - 1{,}5mm\ gap)$

4.2. Assembling of the two half blocks

Once the three-point flexural test is finished, both half blocks are superposed on each other and joint together with an earth mortar. For this study, the water content of the mortar was based on the work of Pkla, 2002, where a water content of 25% was chosen for a similar soil composition. The thickness of the mortar layer was chosen according to the proportions of traditional masonry. The most widely used bricks in Belgium have dimensions of 290x140x140 cm³ and are superposed with a 1cm thick layer of mortar. To respect this mortar-brick ratio of 0,071 (thickness mortar / height brick = 1/14 = 0,071)

$$t_s = \frac{t_m}{h_{brick}} . h_s = \frac{1}{14} . 4cm = 0{,}29cm \cong 3mm$$

With: $t_s = thickness\ of\ the\ layer\ mortar\ for\ the\ samples$
$t_m = thickness\ of\ the\ layer\ mortar\ of\ masonry$
$h_{brick} = height\ of\ a\ traditional\ brick$
$h_s = height\ of\ the\ samples$

As the comparison of the results obtained for CEB needed to be as relevant as possible, this “hand-made” step had to be easily reproductible for all samples. In order to do so, several techniques were tried to reach this reproducibility.

The first trials were performed with two 3mm-thick wooden wedges. The wedges had to be placed along the longitudinal edges of the first half block, and the amount of mortar to insert in top of this first half block could then be approximated. The resulting assembly was not straight, and both blocks were difficult to align. A second trial was tested with a 3D printed mould that could allow a better alignment of the two half blocks. The problem of this mould was that the excess mortar could not be removed easily, which induced that a 3mm-thick layer of mortar could not be guaranteed. Then, a third 3D printed mould was created to allow a better general manipulation. After a few trials, the model could be optimised in order to remove the assembled half blocks in an easier way (see Annex B). This last 3D printed mould offered the possibility to have a neat and reproductible procedure to assemble the half blocks on each other. The following steps as well as Figure 57 summarise the method to obtain the block assembly.

- Place a half block in the lower part of the mould and humidify the top area of this half block.
- Take a certain amount of mortar and knead it on a clean impermeable surface.
- Lightly humidify the upper surface of the first half block to then spread the mortar on it. This is necessary to enhance the adherence between the two different states of matter.
- Spread the mortar until the space is homogeneously well-filled.
- Use a humidified clean spatula to remove the surplus of mortar.
- Insert the round knife in the vertical notch at the back of the mould.
- Install the upper part of the mould on the lower one.
- Slightly humidify the second half block before inserting it in in the mould.
- Compress the set of blocks manually once they are correctly aligned on one another.
- Remove the upper part of the mould and slowly shift the set of blocks out of the lower part with the knife.
- Leave the set drying for 24h into the ambient air.

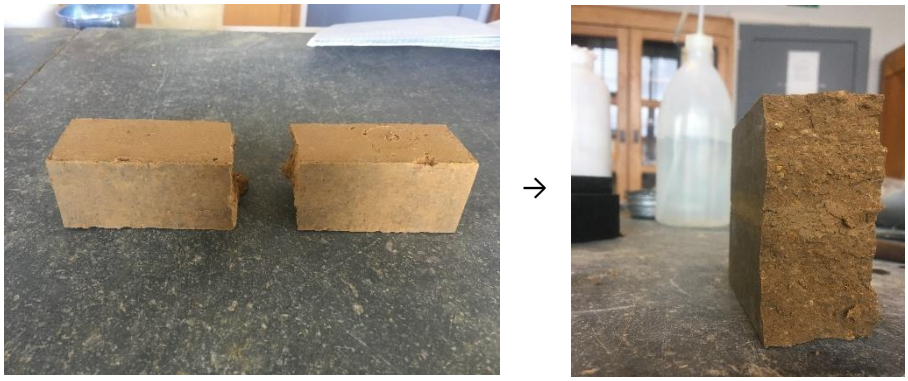

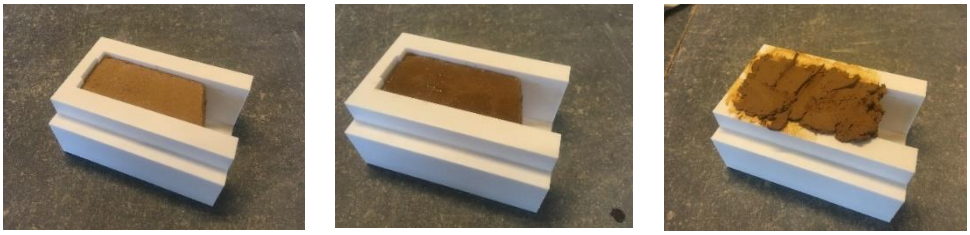

Step 1 Step 2 Step 3

Step 4 Step 5 Step 6

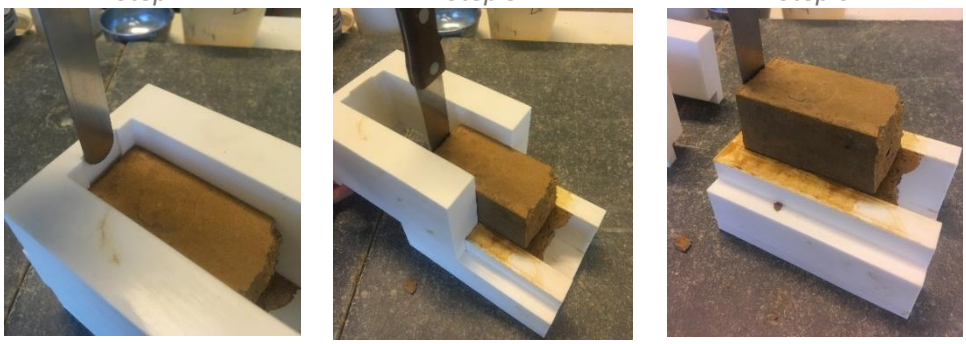

Step 7 Step 8 Step 9

Step 10 Step 11 Step 12

Figure 57: Assembling method for half blocks

4.3. Simple compression procedure

The recommended speed of compression for this test is of 0,02 mm/s. In order to minimize the platen effects that could occur during compression between both top and bottom contact surfaces of the half blocks assembling and the plates of the testing machine, a grease film was applied on the steel plates before each compression test (Figure 59). The force sensor used for these samples is a 5000kg sensor.

Figure 58: Compression test apparatus (Personal picture)

Figure 59: Greased contact surfaces (Personal picture)

After a few first trials, two additional adaptations needed to be done, aside from the change of speed and the anti-platen effect system. In fact, all the blocks needed to be levelled by a smooth scraping because their contact surfaces were not flat. Without that levelling, the real contact surfaces during the compression tests were much smaller than the predicted ones, like it can be seen on Figure 60, where the real contact surface is only half of the predicted ones.

Figure 60: Non-levelled sample (Personal picture)

Figure 61: Wrongly levelled sample (Personal picture)

Figure 62: Right levelled sample (Personal picture)

The results of the compression strength could then be underestimated because of this unevenness. In fact, the following formula would involve incorrect values for F as well as for A.

$$\sigma_c = \frac{F_{max}}{A'}$$

This irregularity would cause the block to fail under a smaller load, given that a smaller contact area than predicted had to support this force. As the force would then be unevenly distributed on the block, the failure pattern could also not be considered as relevant comparing element. Even if the reduction of both parameters could come to a similar result of compression strength, this assumption could not suit an objective comparison method in any case. A particular attention should thus be paid to the scraping, because wrongly scraped samples would be of no help (Figure 61).

Moreover, the half blocks presented rather unequal contact areas after the three-point flexural test. This uneven division of the samples also contributed to the underestimation of the compression strength, for the same reasons as mentioned before. Some of the most recurrent patterns occurring for unreinforced samples as well as for reinforced samples are shown on Figure 63,Figure 64,Figure 65 andFigure 66.

Figure 63: Regular contact area (Personal picture)

Figure 64: Irregular contact area (Personal picture)

Figure 65: Regular contact area (Personal picture)

Figure 66: Irregular contact area (Personal picture)

For the calculations of the compressive strength, the contact surface were considered to be half of the base area of each sample (around 80x40 mm²), even though it is not exactly correct. As this value is an overestimation of the real surface on which the compression force is acting, the real compression strength will be devalued in function of the flexion failure of each block. This conservative assumption will then constitute a first security factor already comprised in the devaluated resistance value (see section *Structural dimensioning*). In any case, this recommended procedure by the group RILEM also foresees the same disparities, because a perfect splitting is unlikely to happen.

5 Experimental outcomes and analysis

5.1. Water content

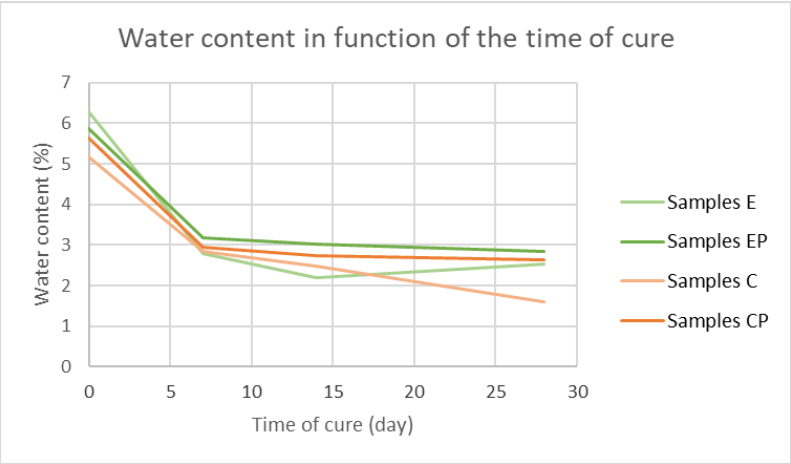

Figure 67: Water content in function of the time of cure

The evolution of the water content of the **unreinforced samples** reveals an important decrease from day 0 to day 7, but this decrease is sharper for the samples having an initial water content of 15%, than for the sample of 11%. In fact, a decrease of a factor 2,25 for Samples E can be observed between day 0 and day 7 ($W_{E,0}$ / $W_{E,7}$ = 6,28%/2,79% = 2,25), compared to a factor 1,82 decrease for Samples C ($W_{C,0}$ / $W_{C,7}$ = 5,17%/2,84% = 1,82). After this first decreasing phase, a second smoother decreasing phase takes place up to day 28 for the samples C ($W_{C,14}$ = 2,49%; $W_{C,28}$ = 1,61%). The small increase noticeable for samples E ($W_{E,14}$ = 2,19%; $W_{E,28}$ = 2,53%) was considered due to a change of humidity in the lab, because such an increase in water content is unlikely to happen.

The evolution of the water content of the **reinforced samples** is exceptionally regular, with a strong decrease of the water content from day 0 to day 7: a reduction factor of 1,85 for samples EP ($W_{EP,0}$ = 5,87%; $W_{EP,7}$ = 3,18%) and of 1,91 for samples CP ($W_{CP,0}$ = 5,63%; $W_{CP,7}$ = 2,95%). This is followed by a slight decreasing phase down to day 28, being of a factor 1,12 for samples EP and CP ($W_{EP,7}$ / $W_{EP,28}$ = 3,18% / 2,84% = 1,12 and $W_{CP,7}$ / $W_{CP,28}$ = 2,95% / 2,64% = 1,12).

Two main observations can be deducted from this analysis:

- The overall tendency of the water content evolution presents a rather high similarity between the four cases.
- Reinforced samples end up having a lower decrease of their water content compared to the unreinforced samples ($W_{EP,28}$ = 2,84 % and $W_{CP,28}$ = 2,64 % versus $W_{E,28}$ = 2,53 % and $W_{C,28}$ = 1,61 %).

5.2. Compression strength

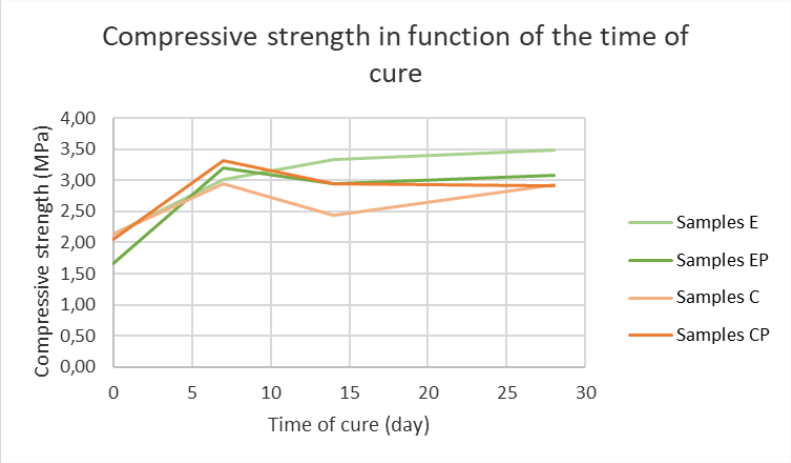

Figure 68: Compressive strength in function of the time of cure

Unreinforced samples undergo an identic first increasing phase of compression strength up to day 7, but drift apart after this first phase. In fact, the compression strength of samples E continuously increases up to a plateau on one hand ($\sigma_{E,14}$ = 3,33 MPa; $\sigma_{E,28}$ = 3,49 MPa), while the compression strength of samples C drops at day 14 and improves again up to day 28 ($\sigma_{C,14}$ = 2,44 MPa; $\sigma_{C,28}$ = 2,93 MPa).

➔ The evolution of their compression strength follows different general tendencies after a similar first increasing phase. In fact, the compressive strength evolution of samples E increases up to day 14 and tends to follow a constant from day 14 onwards, while the evolution of samples C presented a maximum at day 7, followed by a slight drop at day 14, and revealing a second increasing phase onwards.

Reinforced samples undergo a rapid increase in compression strength until day 7, with values higher than the unreinforced samples ($\sigma_{EP,7}$ = 3,19 MPa and $\sigma_{CP,7}$ = 3,32 MPa versus $\sigma_{E,7}$ = 3,01 MPa and $\sigma_{C,7}$ = 2,95 MPa). Their compression strength then slightly drops at day 14 ($\sigma_{EP,14}$ = 2,95 MPa and $\sigma_{CP,14}$ = 2,95 MPa) and stays more or less constant up to day 28 ($\sigma_{EP,28}$ = 3,07MPa and $\sigma_{CP,28}$ = 2,91 MPa).

➔ The evolution of their compression strength follows a similar general tendency, with a maximum at day 7 and a smooth drop at day 14, followed by a stabilisation phase. Even though their initial water content is different, their evolution curves reveals only small differences in values, especially at day 0.

Apart from the previous behaviour differences about the evolution the samples compression strength, two main observations can be noticed:

- Samples made with an initial water content of 15% end up having a better compressive strength than the samples made with an initial water content of 11% ($\sigma_{E,28}$ = 3,49 MPa and $\sigma_{EP,28}$ = 3,08 MPa versus $\sigma_{C,28}$ = 2,93 MPa and $\sigma_{CP,28}$ = 2,91 MPa). This was probably due to the fact that the samples made with 15% water content ended up having a larger dry density than the samples made with 11% water content ($\gamma_{dry,E}$ = 2055 kg/m³ versus $\gamma_{dry,C}$ = 1949 kg/m³; $\gamma_{dry,EP}$ = 1675 kg/m³ versus $\gamma_{dry,C}$ = 1712 kg/m³).
- Reinforced samples indicate an overall better compressive strength than unreinforced samples during the first eight days of cure, with $\sigma_{EP,0}$ = 1,67 MPa; $\sigma_{EP,7}$ = 3,19 MPa and $\sigma_{CP,0}$ = 2,05 MPa; $\sigma_{CP,7}$ = 3,32 MPa versus $\sigma_{E,0}$ = 1,67 MPa; $\sigma_{E,7}$ = 3,19 MPa and $\sigma_{C,0}$ = 2,13 MPa; $\sigma_{C,7}$ =

2,95 MPa. But with time, the unreinforced samples reported a better compressive strength ($\sigma_{E,28}$ = 3,49 MPa; $\sigma_{C,28}$ = 2,93 MPa versus $\sigma_{EP,28}$ = 3,07 MPa; $\sigma_{CP,28}$ = 2,91 MPa).

This larger compression strength of the reinforced samples during the first seven days could be explained by the increased friction between the straw wisps and the soil particles. Moreover, the fibres included in the soil mixture prevented the cracks to spread because they created "bridges" across the cracks, which also contributed to an increase of the compression strength (Danso, Martinson, Ali, & Williams, 2015).

On the other hand, their drop in compression strength after the first seven day was possibly due to the shrinkage of the fibres causes by the drying process. In fact, fibres were reduce in volume because of their loss of water during cure, which implied the strong bond between fibres and soil to lose in magnitude. This ended up in less strong samples from day 14 onwards, causing the compression strength to decrease.

5.3. E-modulus

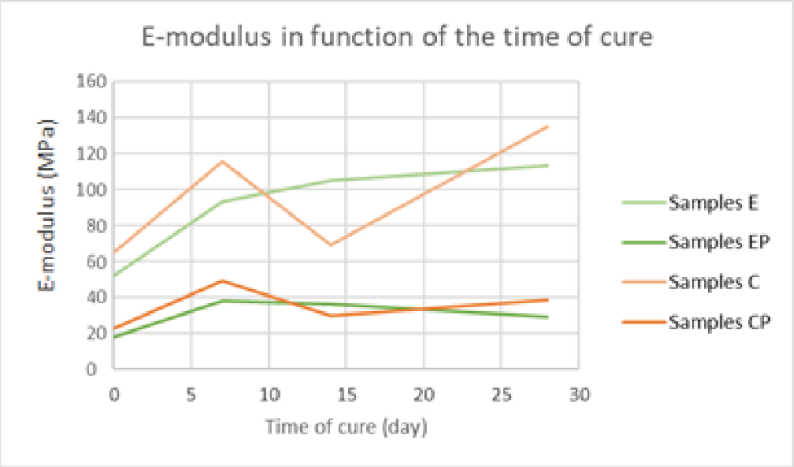

Figure 69: E-modulus in function of the time of cure

In terms of numerical values, the evolution curves of the Young modulus could be categorised in function of whether the samples are reinforced or not. In fact, unreinforced samples have a Young modulus up to 3,5 times higher than the Young modulus of reinforced samples ($E_{C,28}$ / $E_{CP,28}$ = 0,135 / 0,039 = 3,46). This was essentially to the fact that the fibres induce a more elastic behaviour of the samples. On the other hand, in terms of behaviour, the evolution curves of the Young modulus showed great similarities between samples having the same initial water content.

The evolutions of the Young modulus of samples having a **15% initial water content** followed an increase until day 7, which tended to stabilise up to day 28, with a slight increase for unreinforced samples on one hand ($E_{E,14}$ = 0,105 GPa; $E_{E,28}$ = 0,113 GPa), and a slight decrease for samples EP on the other hand ($E_{EP,14}$ = 0,036 GPa; $E_{EP,28}$ = 0,029 GPa).

The evolutions of the Young modulus of samples having a **11% initial water content** also followed an increase up to day 7 ($E_{C,0}$ = 0,065 GPa; $E_{C,7}$ = 0,115 GPa and $E_{CP,0}$ = 0,023 GPa; $E_{CP,7}$ = 0,049 GPa), but after this first improving phase, they did undergo an important decrease, nearly down to the values recorded at day 0 ($E_{C,14}$ = 0,069 GPa and $E_{CP,14}$ = 0,030 GPa). This drop was then followed by a second increase phase up to day 28, which passed the peak of day 7 in the case of unreinforced samples ($E_{C,7}$ = 0,115 GPa; $E_{C,28}$ = 0,135 GPa), in opposition to the reinforced samples, for which this second increase does not reaches the first peak of day 7 ($E_{CP,7}$ = 0,049 GPa; $E_{CP,28}$ = 0,039 GPa).

Two main observations could be deducted from this analysis:

- Although having a different evolution process, samples made with an initial water content of 11% ended up having a better Young modulus than the samples made with an initial water content of 15% ($E_{C,28}$ = 3,49 GPa and $E_{CP,28}$ = 3,08 GPa versus $E_{E,28}$ = 2,93 GPa and $E_{EP,28}$ = 2,91 GPa).T
- The evolution of the Young modulus for unreinforced samples reported an improvement from day 7 to day 28 ($E_{E,7}$ = 0,105 GPa; $E_{E,28}$ = 0,113 GPa and $E_{C,7}$ = 0,115 GPa; $E_{C,28}$ = 0,135 GPa), while for the reinforced samples this value decreases from day 7 to day 28 ($E_{EP,14}$ = 0,036 GPa; $E_{EP,28}$ = 0,029 GPa and $E_{CP,14}$ = 0,030 GPa; $E_{CP,28}$ = 0,039 GPa), meaning that the Young modulus for reinforced samples at day 7 is a maximum. As for the compression strength, this behaviour of the reinforced samples could be explained by the strong bond between straw and soil when the samples were still "wet", i.e. during the first week of cure. After that, the effect of water loss and shrinkage of the straw wisps caused the matrix of the samples to weaken, because of the lack of cohesion between straw and soil.

5.4. Tensile strength

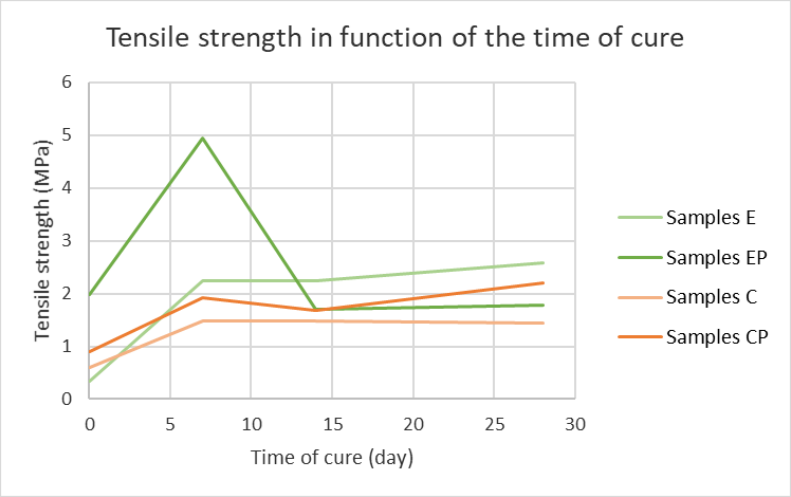

Figure 70: Tensile strength in function of the time of cure

The evolution of the tensile strength of the samples having a **15% initial water content** had an important first increasing slope where values increase of a factor 6,79 for unreinforced samples ($\sigma,flex_{E,7}$ / $\sigma,flex_{E,0}$ = 2,24/0,33 = 6,79) and of a 2,50 factor for reinforced samples ($\sigma,flex_{EP,7}$ / $\sigma,flex_{EP,0}$ = 4,93/1,97 = 2,50). After this first phase, the tensile strength of reinforced samples dropped abruptly to a value lower than the one at day 0 ($\sigma,flex_{EP,14}$ = 1,70 MPa versus $\sigma,flex_{EP,0}$ = 1,97 MPa), and stayed constant up to day 28 ($\sigma,flex_{EP,28}$ = 1,78 MPa). This drop even went lower than the values of samples E ($\sigma,flex_{EP,14}$ = 1,70 MPa; $\sigma,flex_{EP,28}$ = 1,78 MPA versus $\sigma,flex_{E,14}$ = 2,23 MPa; $\sigma,flex_{E,28}$ = 2,59 MPa). It has to be noted that some experimental inaccuracies could have caused this. No more similarities could be noticed between both series of samples from day 7 onwards. In fact, by opposition to the reinforced samples, the unreinforced samples did undergo a rather constant phase from day 7 up to day 28, with values slightly increasing ($\sigma,flex_{E,14}$ = 2,23 MPa; $\sigma,flex_{E,28}$ = 2,59 MPa), after the first strong improvement phase.

The evolution of tensile strength of the samples having a **11% initial water content** presented both a quite regular tendency, with a similar first increase between day 0 and day 7 ($\sigma,flex_{C,0}$ = 0,59 MPa; $\sigma,flex_{C,7}$ = 1,47 MPA versus $\sigma,flex_{CP,0}$ = 0,89 MPa; $\sigma,flex_{CP,7}$ = 1,92 MPa), followed by a stabilisation phase from day 7 onwards, constant for unreinforced samples ($\sigma,flex_{C,14}$ = 1,47 MPa; $\sigma,flex_{C,28}$ = 1,43

MPA), but which revealed a slight improvement for reinforced samples ($\sigma,flex_{CP,14}$ = 1,68 MPa; $\sigma,flex_{CP,28}$ = 2,21 MPA). This series of samples exposed that reinforced samples had an overall better tensile strength: 1,55 times higher than the unreinforced ones ($\sigma,flex_{CP,28}$ / $\sigma,flex_{C,28}$ = 2,21 MPa / 1,43 MPa = 1,545).

Two main observations could be noticed from this analysis:

- Reinforced samples presented better values compared to unreinforced samples for the series made with a 11% initial water ratio, while the contrary occurred for the series made with a 15% initial water ratio ($\sigma,flex_{C,28}$ = 1,43 MPa; $\sigma,flex_{CP,28}$ = 2,21 MPA versus $\sigma,flex_{E,28}$ = 2,59 MPa; $\sigma,flex_{EP,28}$ = 1,78 MPa).
- Unreinforced samples having an initial water content of 15% ended up with a larger tensile strength than unreinforced samples having an initial water content of 11% ($\sigma,flex_{E,28}$ = 2,59 MPa versus $\sigma,flex_{C,28}$ = 1,43 MPa).

5.5. Density

As expected, reinforced samples revealed to have a lower dry density than the unreinforced samples when densities were compared according to the present of straw. In fact, samples E had a dry density of 2055kg/m³ while reinforced samples EP had a dry density of 1675 kg/m³; and samples C ended up having a dry density of 1949 kg/m³ while reinforced samples CP had a dry density of 1712kg/m³.

Water content	Samples		γ_{dry} [kg/m³]
W = 15%	E	simple	2055
	EP	reinforced	1675
W = 11%	C	simple	1949
	CP	reinforced	1712

Table 9: Density of the tested samples according to their water content

This statement could be explained by the application of a different optimal water content, namely the optimal Proctor water content and the theoretical static water content. In fact, as shown in Table 9, when densities were compared according to their water content, either defined by dynamic compaction or by static compaction, a duality between reinforced samples and unreinforced samples could be noticed. The dry density of the unreinforced samples made with the dynamic optimum water content (15%) ended up having a larger dry density than the reinforced samples made with the static water content (11%). This could not be observed in the case of reinforced samples, for which the dry density happened to be higher for samples made with 11%.

This comparison allowed to state that the theoretical static curve deducted previously should be adapted and corrected in function of these results. Ideally, several water contents should be tested in order to verify the real static curve of MLD soil, in the case of unreinforced samples, as well as in the case of reinforced samples. Nevertheless, the importance of differentiating the optimal water content for dynamically compacted and for statically compacted samples is thus confirmed.

Moreover, this comparison allowed to state that the optimum static water content is probably not the same for reinforced samples than for unreinforced samples. In fact, for samples EP, an addition of 10% of saturated straw induced a decrease of 20% of the dry density of the samples, while for samples CP, the same saturated straw addition of 10% only induced a decrease of 12% of the dry density of the samples.

5.6. Failure plan

As shown on Figure 71,Figure 72,Figure 73 andFigure 74, the samples failed under shear stress (+- 45° failure plane). It could be noticed that the presence of a mortar layer did not cause any disturbance with respect to this failure plane. In fact, no crushing of the layer of mortar or discontinuities could be observed, neither for unreinforced samples as for reinforced samples.

The unreinforced samples presented a double failure plan, while the reinforced samples exposed a single failure plane. It could be observed that none of the samples failed with respect to a particular inclination due to an irregularity of the straw wisps disposition. Moreover, it has also to be noted that none of the tested samples showed a barrelling effect, which would signify that the samples are too compressible, and thus contain too much straw.

Figure 71: Unreinforced sample's failure planes 1

Figure 72: Unreinforced sample's failure plane 2

Figure 73: Reinforced sample's failure plane 1

Figure 74: Reinforced sample's failure plane 2

5.7. Experimental inaccuracies

The results obtained in this second experimental part showed a bit more disparities than for the samples tested in the first experimental part. This difference in reproducibility between the dynamically compacted samples tested in the first experimental part (cylindrical samples) and the statically compacted samples tested in this experimental part (CEBs) could be explained through the following points:

- A larger number of manipulations was performed on CEB before they were tested in compression.
- The production methodology used to fabricate the reinforced cylindrical samples could not be applied for CEBs.

In fact, CEBs did undergo a three-point flexural test, which produced by essence a disparity of the half block (a perfect cut is unfortunately impossible). After that, they were assembled with earth mortar (requiring a partial wetting of the samples) and went through a differential drying during 24h (the samples had a different water content than the earth mortar). And finally, before being test in compression, their top and bottom contact surfaces were smoothened, because of some inaccuracies caused by the moulding/compaction process.

Moreover, the meticulous moulding procedure to fabricate homogeneous reinforced cylindrical samples (presented in the first experimental part of this study) was not appropriate to produce a large amount of CEBs, because this would not be representative of the mass productions of CEBs. Straw-CEBs were thus moulded as if they were unreinforced CEBs in order to mimic a real CEB fabrication situation. This induced the results to be a bit less regular for reinforced CEBs than for

unreinforced CEBs (graphs in Annex C). An industrial way to create more homogeneous samples should probably be studied to decrease too large disparities, in order to propose the most reliable data possible.

5. Conclusions

Cure

The loss of water that the samples did undergo is in direct correlation with their improvement in compression strength. That is why it was essential to put them in cure in conditions close to their future application, to obtain relevant values of their compression strength.

Density

The dry density of the samples also influenced their compression strength, especially when compared to the samples T tested in the first experimental part. This difference was probably due to the compacting method. In fact, the samples compacted dynamically by hand had a lower dry density and compression strength than the samples compacted statically.

Nevertheless, this link could not be observed for reinforced samples: the compression strength was higher for the less dense samples. It could also be concluded that the theoretical static compaction curve deducted in this study should be corrected and verified experimentally for future experiments. Nevertheless, this first approximation of the static optimum water content showed the relevance of water content in the case of reinforced samples.

Compression strength

The use of straw reinforcement revealed to be improving the compressive strength of the samples but only during the first week of cure. After that, the compressive strengths ended up being higher for non-reinforced samples. This was probably due to the drying process of the fibres, which had an important absorbance, and did thus undergo a larger shrinkage through the curing process. This shrinkage resulted in a volumetric reduction of the straw fibres, which caused the adhesion between straw and soil particles to decrease. This again confirms the importance of cure. At first, the optimal straw ratio assumed to be found for “wet” samples, but due to the nature of the second type of straw (high absorbance!), the possibility of losing cohesion over time was neglected.

Young modulus

Due to their higher ductility, the reinforced samples presented lower values of their Young modulus than for unreinforced samples. Samples made with an initial water content of 11% presented better Young moduli than the ones made with an initial water content of 15%.

Tensile strength

The use of straw reinforcement induced an improvement of the tensile strength of samples having an initial water content of 11%, by opposition to the samples having an initial water content of 15% (optimal Proctor). This was probably related to a better cohesion between straw and soil in the matrix of the samples made with a 11% water.

Production procedure

The production procedure revealed to be of a great importance in the first experimental part. That is why it can be assumed that the disparities in the results obtained in the second part could be avoided if an adapted procedure was established to get a better homogenisation of the samples.

6. Structural dimensioning and Life Cycle assessment

Problem statement

Energy impact and structural potential are strongly linked to one another for construction materials. In fact, the energy impact of a certain material will depend on the amount of the material needed for a certain structural purpose. Therefore, comparing construction materials energy-wise with respect to a volumetric amount is not enough, neither accurate, for a complete understanding. One can truly estimate the energy-wise impacts of a material and compare them to other materials when this material is implemented in a structure, i.e. when the structure is dimensioned according to the properties of this material.

Evaluating energy and environmental concerns is one of the aims of LCA. LCA, short for Life Cycle Assessment, is a worldwide accepted method used as an important decision tool to help reaching sustainable building practices (Khasreen, Banfill, & Menzies, 2009). In the construction sector, an LCA study can thus not take place without a preliminary structural dimensioning stage. Therefore, as earth constructions are known to be low energy demanding constructions (Morel, Mesbah, Oggero, & Walker, 2000), performing an LCA on CEBs on basis of a pilot structural dimensioning would help appreciate the benefits of CEBs in the construction sector in a more accurate and quantitative way.

Objectives and methodology

This section will focus on the possibility to create structural walls made of CEB in a building on one hand, and to evaluate its attractiveness thanks to a targeted LCA study on the other hand. In order to have a qualitative reference, the CEB dimensioning outputs will be compared to the results obtained if the structure was made of traditional masonry. A discussion between both CEB and traditional masonry LCA will also take place to reveal the potential of CEB. This section will thus be divided in two parts, a structural part and an LCA part:

- In a first time, the structural dimensioning part will take place to know how high it is possible to construct in CEB. To do so, the results obtained in the previous section regarding compression strength will be implemented in a construction scale situation. In fact, this first part will consist in defining a structure to dimension, determining the ULS loads of this structure and dimensioning it. These steps will be applied both for a CEB structure and for a traditional masonry structure.
- In a second time, an LCA study will be performed regarding embodied energy, and different transport scenarios that could occur during the construction phase of a CEB building. The results of the dimensioning part will be used to define the amount of earth required to build this structure, and by extension its embodied energy.

Part I: Structural dimensioning

The dimensioning methodology followed the masonry Eurocode (EC6), its ANB (Belgian National Annex) and the NBN EN 772-1. The steps of Annex D summarise the procedure to follow to dimension a structural masonry wall.

In this structural dimensioning part, the structure to dimension and the calculation assumptions and boundaries will first be defined. After that, the material characteristics needed to perform this dimensioning will be exposed; the soliciting normal forces Nsd and resisting normal forces Nrd will be calculated and compared to one another. In fact, in the end, the soliciting actions (Nsd) need to the be smaller than the bearing capacity (Nrd) of the structure, according to the following ULS (Ultimate Limit State) control inequation:

$$N_{sd} \leq N_{rd}$$

1. Structure to dimension

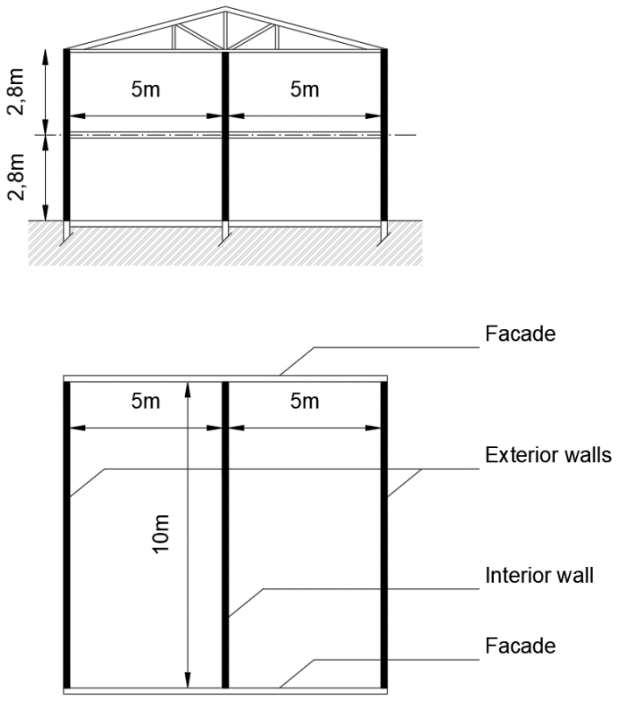

Figure 75: Plan of the structure to dimension

To limit the complexity of the dimensioning, the following residential structure was considered for this study, shown on Figure 75. The structure is composed of three 10-meter long structural walls spaced out of 5 meters, carrying the floors from side to side. As the facades have no structural purpose per se, the structural dimensioning only focuses on the three mentioned walls.

To be in line with the natural materiality of this structure, the floors and roof structure is made of timber. The floor composition is layered with a compression screed, an insulating layer, and a timber finishing. The roof covering is made of schist tales, while the interior is finished with wooden plates.

For the sake of simplicity, none of the functional openings in the structural walls, such as doors and windows, were taken into account. Such openings would induce some dimensioning calculations that are not included in the scope of this study, which focuses purely on the bearing capacity of CEBs. Nevertheless, dimensioning's like window and door lintels, etc, should be considered in a real lifetime situation. As CEBs, neither traditional masonry, are particularly resistant to traction, steel rebars inserted in mortars beds and steel lintel elements are the most commonly used solutions to solve large openings when the natural vault effect of masonry can't be reached (Matriche, 2020).

The following points define additional structural data and assumptions required to perform the dimensioning calculations.

- The walls of this building are considered supported on both horizontal sides and vertical sides.

- Angular displacements are not possible on top and bottom of the walls.
- The eccentricity due to wind loads will be considered equal to 5mm in the middle of the wall and equal to 0mm on top and bottom of the wall.
- The eccentricity due to vertical loads (Mi / Ni) is equal to 23,33 mm in the middle of the wall (e= h/12 = 2,8/12 = 0,23m) and equal to 11,67mm on top and bottom of the wall (e= h/24 = 2,8/24 = 0,11m) (see annex B).
- The security factor γ_M applied is of 2,5 (see Annex D).

2. CEB data

2.1. Dimensions

For this study, the dimensions of the CEB were chosen according to the *Brickette*©, produced by BC Materials, namely 9x29,5x14 cm³ (Figure 76), which corresponds to standard dimensions of CEB units (Morel, Pkla, & Walker, 2007).

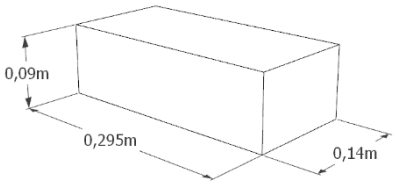

Figure 76: Standard dimensions of CEB

2.2. Mechanical characteristics

The compression strength of the blocks is determined thanks to the experimentations results performed in the experimental section of this study (see Experimental outcomes and analysis). Table 10 summarises the mean values of compression strength obtained for each case. The dry density values were rounded up to have an extra safety margin in the calculations.

Water content	Samples		γ_{dry} [kg/m³]	σ_k [N/mm²]	σ_k / γ_{dry}
W = 15%	E	simple	(2055) 2100	3,49	1,66 10^{-3}
	EP	reinforced	(1675) 1700	3,08	1,81 10^{-3}
W = 11%	C	simple	(1949) 2000	2,93	1,46 10^{-3}
	CP	reinforced	(1712) 1750	2,91	1,66 10^{-3}

Table 10: Dry density and Compression strength of the tested samples
γ_{dry} = dry density; σ_k = characteristic compression strength of the samples

Like already concluded, the most resistant samples in this study are the unreinforced ones, realised with a 15% water content. Nevertheless, the dimensioning calculations were performed for both unreinforced and reinforced samples, in order to offer a complete range of comparable data. Moreover, the ratio "density/compression strength" of reinforced CEBs was higher than for simple CEBs, which could be beneficial in the sense that a less resistant material could still sustain a lighter structure. Therefore, as the samples made with 15% water content presented an overall better range of mechanical characteristics than the samples made with 11% water content, the structural dimensioning only considered the properties of samples E and samples EP.

As the models tested were following the RILEM procedure, the compression strength obtained did not represent the compression strength of the blocks (f_{bk}), but the compression strength of the masonry (f_k). The calculations for the CEB walls could thus directly start from there. So, for samples with a water content of 15%, the characteristic compression strength value of the non-reinforced samples was of 3,49 N/mm² and the characteristic compression strength value of the reinforced samples was of 3,08 N/mm².

2.3. *Security factor*

Besides the security factor related to the control of masonry (γ_M) reducing the design bearing capacity (Nrd) of a 2,5 factor, no other reduction factor has been analytically applied to the compressive strength of CEBs for these calculations because no factor specific to CEBs could be found in literature. Nevertheless, some extra security was indirectly applied on CEBs. In fact, three elements encountered along the entire study could constitute an additional implicit devaluation factor. These are the following:

- The devaluation of the compressive strength due to the overestimated contact areas of the tested samples.
- The devaluation of the compressive strength due to experimental inaccuracies related to geometry disparities of the samples.
- The security taken with respect to the density of the CEBs, in Table 10.

3. Traditional masonry data

3.1. *Dimensions*

The most current brick dimensions were chosen to offer the most relevant comparison possible, namely bricks of 14x19x29 cm³ (Matriche, 2020), as shown on Figure 77.

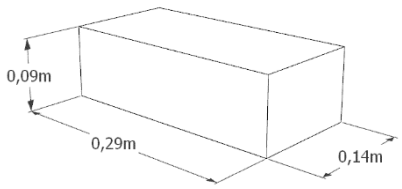

Figure 77: Usual dimensions of fired bricks

3.2. *Mechanical characteristics*

The most usual brick compression strength is of 10N/mm². For such a brick compression strength, one usually opts for a mortar compression strength of 8N/mm². The masonry group of those bricks was assumed to be part of group 2b (Annex D).

4. Determination of the ELU loads

The ultimate limit state loads are determined according to the EC0. The total ULS load was found by adding the permanent loads to the variable loads of each storey, while taking into account the corresponding safety factors, according to the following equation:

$$\Sigma\,(\gamma_g . G_k) + \Sigma\,(\gamma_q . Q_k)$$

Where $\gamma_g = 1{,}35$
$G_k = permanent\ loads$
$\gamma_q = 1{,}5$
$Q_k = variable\ loads$

The following data summarises the different load cases of this structure, respectively the roof loads, the floor loads, and the four different wall loads occurring for this study.

- Roof

Permanent loads on the roof included the schist tiles, the timber carpentry, the insulation, and the wooden finishing's, which ended up in a total of 1,5 kN/m². Variables loads on the roof included the climatic conditions of wind and snow, considered to be of 1,0 kN/m². The total load on the roof was thus equal to 3,525 kN/m²:

$$\Sigma\,(\gamma_g.G_k) + \Sigma\,(\gamma_q.Q_k) = \ 1{,}35\,.\,1{,}5 + 1{,}5\,.\,1{,}0 = \ 3{,}525\ kN/m^2$$

- Floor:

Permanent loads on the floor included the timber beams and wooden floor finishing's, together being of 1,5 kN/m². The variable loads were corresponding to the residential activities, being of 2,0 kN/m². The total load for each floor was thus equal to 5,025 kN/m²:

$$\Sigma\,(\gamma_g.G_k) + \Sigma\,(\gamma_q.Q_k) = \ 1{,}35\,.\,1{,}5 + 1{,}5\,.\,2{,}0 = 5{,}025\ kN/m^2$$

- Walls

The permanent loads of the walls were depending on their thickness, their height, and their dry density (CEBs or fired bricks). The variable loads were equal to zero because climatic conditions such as wind actions are considered in the load eccentricity of the walls, needed for the calculations of the resisting loads Nrd (see list of assumptions in Section 1: *Structure to dimension*). The total load of the walls was calculated according to the following formula:

$$\gamma_g.G_k = \ 1{,}35.t_w.h_w.\rho_m$$

Where $t_w = \ thickness\ of\ the\ wall$
$h_w = heigth\ of\ the\ wall$
$\rho_m = dry\ density\ of\ the\ wall$

The thickness of the walls depends on the piling method used. For CEB and brick masonry piled up in stretching course (Figure 78Figure 79), the thickness of the wall was of 14cm, while it was of 29,5cm for CEB and 29cm for bricks in the case of a stretching and heading alternation.

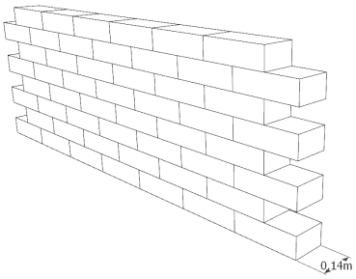

Figure 78: Stretching course

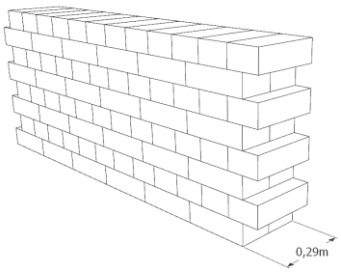

Figure 79: stretching and heading course

The height of each wall has been defined equal to 2,8m per storey (see Figure 75). The density of the walls depended on the material used. CEB walls and straw reinforced CEB walls have a density of 2100 kg/m³ and 1700 kg/m³ respectively (these values were obtained during the experimental part), while the traditional brick masonry have a density of approximately 1800 kg/m³. For this study, six different walls could occur, with the following load cases:

CEB: $t_w = \ 14cm \ \rightarrow 1{,}35\,.\,0{,}14\,.\,21\,.\,2{,}8 = 11{,}113\ kN/m$
$t_w = \ 29{,}5cm \ \rightarrow 1{,}35\,.\,0{,}295\,.\,21\,.\,2{,}8 = 23{,}417\ kN/m$

Straw-CEB: $t_w = \ 14cm \ \rightarrow 1{,}35\,.\,0{,}14\,.\,17\,.\,2{,}8 = 8{,}996\ kN/m$
$t_w = \ 29{,}5cm \ \rightarrow 1{,}35\,.\,0{,}295\,.\,17\,.\,2{,}8 = 18{,}957\ kN/m$

Brick: $t_w = \ 14cm \ \rightarrow 1{,}35\,.\,0{,}14\,.\,18\,.\,2{,}8 = 9{,}526\ kN/m$
$t_w = \ 29cm \ \rightarrow 1{,}35\,.\,0{,}29\,.\,18\,.\,2{,}8 = 19{,}732\ kN/m$

These three load contributions (roof, floors and walls) needed to be added to one another in function of the number of floors of the structure. After this combination was done for each case (details in Annex DE), they represented the soliciting compression values Nsd of the structures.

5. Results

2-storey building			Exterior walls		Interior walls	
	Thickness wall [cm]		Nsd [MPa]	Nrd [MPa]	Nsd [MPa]	Nrd [MPa]
	CEB	14,0	56,16	85,99	64,98	130,94
		29,5	68,47	253,50	102,40	299,59
	Straw-CEB	14,0	51,29	75,89	77,05	115,56
		29,5	61,89	223,52	95,83	264,58
	Fired bricks	14,0	52,99	113,84	86,93	181,60
		29,0	63,19	341,18	97,13	404,03
3-storey building			Exterior walls		Interior walls	
	Thickness wall [cm]		Nsd [MPa]	Nrd [MPa]	Nsd [MPa]	Nrd [MPa]
	CEB	14,0	68,73	85,99	126,34	130,94
		29,5	92,14	253,50	138,64	299,59
	Straw-CEB	14,0	73,49	75,89	119,99	115,56
		29,5	83,45	223,52	129,95	264,58
	Fired bricks	14,0	75,08	113,84	121,58	181,60
		29,0	93,13	341,18	131,78	404,03
4-storey building			Exterior walls		Interior walls	
	Thickness wall [cm]		Nsd [MPa]	Nrd [MPa]	Nsd [MPa]	Nrd [MPa]
	CEB	14,0	103,51	85,99	162,58	130,94
		29,5	115,82	253,50	174,88	299,59
	Straw-CEB	14,0	95,05	75,89	154,11	115,56
		29,5	105,01	223,52	174,03	264,58
	Fired bricks	14,0	97,17	113,84	156,23	181,60
		29,0	107,37	341,18	166,43	404,03
5-storey building			Exterior walls		Interior walls	
	Thickness wall [cm]		Nsd [MPa]	Nrd [MPa]	Nsd [MPa]	Nrd [MPa]
	CEB	14,0	127,19	85,99	198,81	130,94
		29,5	151,85	253,50	223,42	299,59
	Straw-CEB	14,0	116,61	75,89	188,23	115,56
		29,5	136,53	223,52	218,11	264,58
	Fired bricks	14,0	119,25	113,84	190,88	181,60
		29,0	129,46	341,18	201,09	404,03
6-storey building			Exterior walls		Interior walls	
	Thickness wall [cm]		Nsd [MPa]	Nrd [MPa]	Nsd [MPa]	Nrd [MPa]
	CEB	14,0	150,86	85,99	235,05	130,94
		29,5	187,77	253,50	271,96	299,59
	Straw-CEB	14,0	138,16	75,89	222,35	115,56
		29,5	168,05	223,52	262,19	264,58
	Fired bricks	14,0	141,34	113,84	225,53	181,60
		29,0	161,75	341,18	245,94	404,03
7-storey building			Exterior walls		Interior walls	
	Thickness wall [cm]		Nsd [MPa]	Nrd [MPa]	Nsd [MPa]	Nrd [MPa]
	CEB	14,0	174,54	85,99	271,29	130,94
		29,5	223,76	253,50	320,51	299,59
	Straw-CEB	14,0	159,72	75,89	256,47	115,56
		29,5	199,57	223,52	306,28	264,58
	Fired bricks	14,0	163,43	113,84	260,18	181,60
		29,0	194,05	341,18	290,80	404,03

Table 11: Structural dimensioning summary

As the final purpose of this first part was to know how high one could build in CEB, load case scenarios were defined until the maximal possible height was reached, constituting the Nsd values on one hand, which were compared to the resisting values Nrd on the other hand. The Nrd values were determined for CEBs and for traditional masonry (Annex F and Annex G), assembled both in stretching course (14cm-thick walls) and in stretching and heading alternation course (29,5 and 29cm-thick walls). Table 11 summarises the results obtained for each scenario.

This table exhibits the last step of the dimensioning, namely the comparison between the soliciting actions Nsd and the bearing capacity of the structure Nrd for each case:

$$N_{sd} \leq N_{rd}$$

This equation needed to be verified for exterior walls as well as for interior walls; for thin walls (14cm) and for thick walls (29,5cm or 29cm) if thin walls were not satisfying; for each type of material (CEBs, straw-CEBs and fired bricks); and for each scenario (number of floors). Satisfying values for CEBs, straw CEBs and fired bricks were respectively tinted yellow, green and orange.

In the case of a CEB structure, one could build up to a 2-storey high building for CEBs assembled in stretching course, and up to a 6-storey high building for CEBs assembled in stretching and heading alternation course. A 7-storey high building could not be reached because the soliciting normal force of the interior wall was higher than the bearing capacity of this interior wall (320,51 MPa > 299,59 MPa).

In the case of a straw reinforced CEB structure, one could also build a 2-storey high building completely out of straw-CEBs assembled in stretching course. Moreover, building up to a 6-storey high structure was possible with straw-CEBs when they were piled up in stretching and heading alternation. As for the case of simple CEB structures, a 7-storey high building could not be reached with straw-CEBs, as the bearing capacity of the interior walls was lower than the soliciting normal forces of the exterior and interior walls (306,28 MPa > 264,58 MPa).

In the case of a traditional brick masonry, a 4-storey building could be sustained with bricks assembled exclusively in stretching course. A 5-storey high building could be built with exterior walls assembled in stretching and heading alternation, and with interior walls assembled in stretching course. After that, 7-storey high buildings and more could be reached with both exterior and interior walls assembled in stretching and heading alternation course.

It has to be noted that these results agree with data found in literature about the height of earthen buildings, being between 1 and 3 floors (Houben & Guillaud, 2006; Hall, Lindsay, & Krayenhoff, 2012), and exceptionally up to 7 levels (Baridon, Garric, & Richaud, 2016).

6. Conclusion

The fact that CEBs and straw CEBs can sustain a building of the same height, while CEBs had a higher compression strength (3,49 MPa) than reinforced CEBs (3,08 MPa) proves that the compression strength of a material is not the only property to consider to achieve structural potential. In fact, the density plays an important role in the structural dimensioning too: the decrease in dry density of the straw-reinforced CEBs (1700 kg/m³ compared to 2100 kg/m³ unreinforced CEBs) allowed to build as high as in the case of unreinforced CEBs, despite of the lower compression strength of straw-CEBs compared to CEBs. It can thus be concluded that a decrease in compression strength is not unfavourable in terms of structural potential when it goes hand in hand with a decrease in density.

Part II: LCA

Life cycle assessment is one of the many methods to evaluate environmental impacts of construction materials or systems. It consists in four detailed steps: the goal and scope definition, the life-cycle inventory creation, the impact assessment, and the results interpretation.

In this study, too many data were lacking to do a complete accurate LCA with the software *SImaPro®*. Therefore, only a targeted LCA has been performed to obtain the embodied energy of a CEB structure and has been compared to the case of fired bricks. The determination of this embodied energy was based on the results obtained in the previous Part I: Structural dimensioning, and on data available on the website *EcoConso.be*. In addition to that, the benefits of earth as a construction material were discussed through a cradle-to-cradle analysis, focusing on the transport parameter, and exposing the recycling possibilities of CEBs.

1. Embodied energy

As already told in the *State-of-the-art* section, it was found that the specific embodied energy (e_m) of raw clay bricks is of 120 kWh/m³, and 700 kWh/m³ for fired bricks. In order to evaluate the embodied energy of a structural entity, it is necessary to multiply these values with the total volume of the needed CEBs or fired bricks, like suggested by the following equation.

$$E_E = V_m . e_m$$

With $E_E = Embodied\ energy\ [kWh]$
$V_m = Volume\ of\ the\ CEB\ or\ brick\ units\ [m^3]$
$e_m = specific\ embodied\ energy\ of\ a\ material\ [kWh/m^3]$

Table 12 exposes the embodied energy results for all 5 of the previous structural cases: from a 2-storey building to a 6-storey building. As a reminder, these results only included the structural part of the building made either with CEB, with straw-CEB or with traditional masonry. Elements like foundations, timber beams, insulation, facades, roofing, finishing's, etc, are not in the scope of this study and were therefore not implemented in the calculations.

An estimation of the embodied energy of straw-CEBs could be made by combining both contributions of earth and straw, which specific embodied energy was considered equal to 40kWh/m³ ("*chanvre"* on EcoConso.be). As embodied energy is calculated on basis of the volume of each material and not on basis of their mass (units : kWh/m³), the volume of soil and the volume of straw contained in the reinforced samples needed to be known:

The density of straw was unknown at first but could be determined thanks to the mass ratio of straw in the samples (2,3%) and to the densities of unreinforced CEBs (2055 kg/m³) and reinforced CEBs (1675 kg/m³). This was done according to the following reasoning, assuming that the volumes of water and air of the samples were included both in straw volumes and in soil volumes, i.e. decomposing a hypothetical 1 m³ reinforced CEB only in terms of mass and volume of soil and straw :

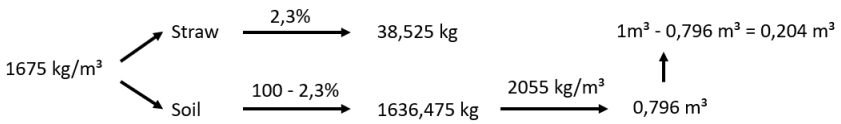

The density of straw could then be determined as follows:

$$\rho_{straw} = \frac{m_{straw}}{V_{straw}} = \frac{2{,}3\ \% * m_{straw-CEB}}{1 - V_{soil}} = \frac{38{,}525}{0{,}204} = 187\ kg/m^3$$

To evaluate the embodied energy of straw reinforced samples, the following equation revealing the volumetric quantities of straw and soil and their respective specific embodied energy could then be used:

$$E_{Straw-CEB} = 0{,}796\ .V_{straw-CEB}.e_{CEB} + 0{,}204\ .V_{straw-CEB}.e_{straw}$$

With $E_{Straw-CEB} = Embodied\ energy\ of\ straw\ reinforced\ CEBs\ [kWh]$
$V_{straw-CEB} = Volume\ of\ the\ straw\ CEBs\ [m^3]$
$e_{CEB} = specific\ embodied\ energy\ of\ pure\ CEBs\ [kWh/m^3]$
$e_{straw} = specific\ embodied\ energy\ of\ straw\ [kWh/m^3]$

		Volume [m³]	Embodied energy [kWh]	E_{brick}/E_{CEB}	$E_{brick}/E_{straw\text{-}CEB}$
2-storey building	CEB	23,52	2822	5,83	6,75
	Straw-CEB	23,52	2438		
	Fired brick	23,52	16464		
3-storey building	CEB	35,28	4233	5,90	5,83
	Straw-CEB	39,62	4108		
	Fired brick	35,28	24696		
4-storey building	CEB	60,06	7207	4,57	4,93
	Straw-CEB	64,40	6677		
	Fired brick	47,04	32928		
5-storey building	CEB	84,84	10180	4,91	5,74
	Straw-CEB	89,18	8710		
	Fired brick	71,40	49980		
6-storey building	CEB	109,62	13154	5,10	5,67
	Straw-CEB	113,96	11815		
	Fired brick	95,76	67032		

Table 12: Embodied energy

It could be noticed that for a similar structure, the embodied energy could be from 4,57 up to 5,90 times lower when CEBs are used instead of traditional masonry. The embodied energy was even lower when straw-CEBs are used: it could be from 4,93 up to 6,75 times lower when straw-CEBs were used instead of traditional masonry.

It is important to note that these values represent a main embodied energy per volume both for soil and for straw, obtained with average values on the extraction method, on the manufacture, and on the transportation. Moreover, there is no indication about the composition of the mentioned clay blocks, i.e. whether the clay blocks contain a chemical stabiliser or not, arises their environmental impact (Shukla, Tiwari, & Sodha, 2009; Fernandes, Peixoto, Mateus, & Gervasio, 2019). Therefore, the embodied energy found for each scenario had to be considered in a more generic extent. Nevertheless, these values gave a first estimation of the potential of CEBs and straw-CEBs and were in line with some other LCA studies found in literature about earthen materials used in the construction sector (Ben-Alon, Loftness, Harries, DiPietro, & Cochran Hameen, 2019; Fernandes, Peixoto, Mateus, & Gervasio, 2019; Christoforou, Kylili, Fokaides, & Ioannou, 2016).

2. Cradle-to-gate

Cradle-to-gate is an assessment of a product on a partial life cycle basis, from the extraction to the gate stage, i.e. just before the use stage. For example, Figure 80 illustrates the cradle to gate boundaries of CEBs

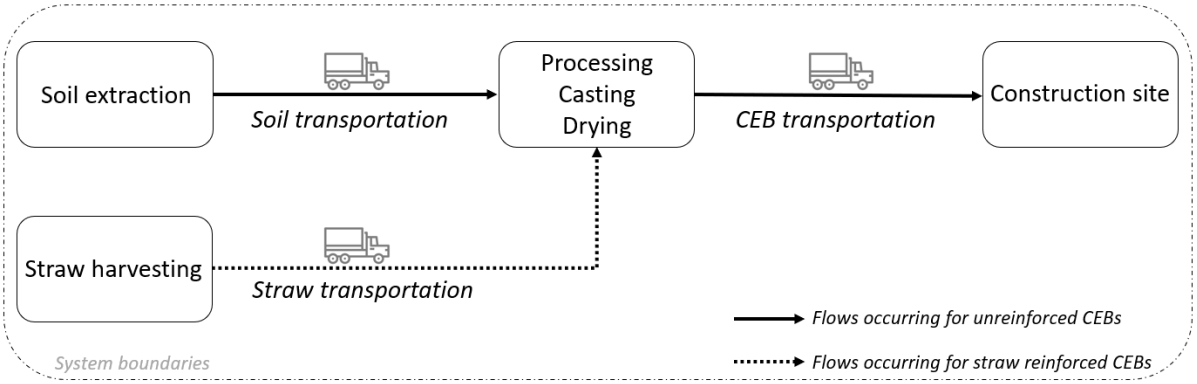

Figure 80: Cradle-to-gate boundaries for CEBs

The transportation and manufacture (in the case of chemically stabilised blocks) of CEB were reported to be the highest contribution to the environmental impact and embodied energy in the case of CEB used as a construction material (Fernandes, Peixoto, Mateus, & Gervasio, 2019). In this study, CEBs were not chemically stabilised, which places transport as first contribution. This is why a parametric analysis was made on transport. In fact, after making the choice of using a sustainable and eco-friendly material, the next target point to optimise in a cradle-to-gate situation is the transport parameter.

Three transport scenarios were assessed in terms of energy for this sensibility analysis. They depended on the locations of the excavation of the soil and on the manufacture of the CEBs (scenarios 1, 2 and 3), and whether the CEBs were reinforced or not (scenarios 4, 5 and 6). In the case of reinforced straw CEBs, as straw is widely available on the Belgian territory, the harvesting of straw and its industrial processing was considered to be in a relatively close vicinity of the manufacture location. Therefore, an average distance of 25km between the harvesting place and processing mill, and an average distance of 25km as well between the processing mill and the manufacture place of straw-CEBs were chosen, resulting in a total distance of 50km travelled by straw.

- Scenario 1: the excavation of the soil and the manufacture of the CEBs takes place in the vicinity of the construction site (no use of straw).
  → distance travelled by CEBs = 0km.
- Scenario 2: the excavation of the soil and/or the manufacture of the CEBs take place at a quarry distant of 50km from the construction site (no use of straw).
  → distance travelled by CEBs = 50km.
- Scenario 3: the excavation of the soil is at 50km from the manufacture plant of CEBs, which is at a 50km distance from the construction site (no use of straw).
  → distance travelled by CEBs = 100km.
- Scenario 4: the excavation of the soil and the manufacture of the CEBs takes place in the vicinity of the construction site while straw is transported on 50km.
  → distance travelled by straw = 50km; distance travelled by straw-CEBs = 0km.

- Scenario 5: the excavation of the soil and/or the manufacture of the CEBs take place at a quarry distant of 50km from the construction site while straw is transported on the manufacture place for 50km.
  → distance travelled by straw = 50km; distance travelled by straw-CEBs = 50km.
- Scenario 6: the excavation of the soil is at 50km from the manufacture plant of CEBs, which is at a 50km distance from the construction site while straw is transported on the manufacture place for 50km.
  → distance travelled by straw = 50km; distance travelled by straw-CEBs = 100km.

To evaluate the transport parameter energy-wisely, several assumptions had to be formulated. Firstly, it was assumed that the manufactured CEBs travelled on wooden euro-pallets and were wrapped in plastic film by range of 145 CEB per pallets (1100kg), according to the procedure proposed by *BC Materials*. The provision impact of these required pallets and plastic film were not in the scope of this work and were thus not considered for this calculation. Secondly, the vehicles used for the transport of the excavated soil and for the CEB pallets were 7-ton diesel trucks, according to Fernandes et al., 2019, consummating an average of 35,33L/100km of diesel (Statista, 2018). As the energy released by 1L of diesel is of 10,64 kWh (MesFournisseurs, 2020), the energy due to transport could be calculated according to the following formula:

$$E_{Transport} = 10{,}64(kWh/L) * \frac{35{,}33(L)}{100(km)} * \frac{V_{CEB}.\rho_{CEB}.10^{-3}.L\ (ton.km)}{7(ton)}$$

With: $L = 0\ km; 50\ km; 100\ km$

In the case of straw-CEB, transport energies for soil, straw and straw-CEBs needed to be added to each other in function of the considered scenario, according to the following formulas:

$$E_{Transport-soil} = 10{,}64(kWh/L) * \frac{35{,}33(L)}{100(km)} * \frac{0{,}796.V_{strawCEB}.\rho_{CEB}.10^{-3}.L\ (ton.km)}{7(ton)}$$

$$E_{Transport-straw} = 10{,}64(kWh/L) * \frac{35{,}33(L)}{100(km)} * \frac{0{,}204.V_{strawCEB}.\rho_{straw}.10^{-3}.L\ (ton.km)}{7(ton)}$$

$$E_{Transport-CEB} = 10{,}64(kWh/L) * \frac{35{,}33(L)}{100(km)} * \frac{V_{strawCEB}.\rho_{strawCEB}.10^{-3}.L\ (ton.km)}{7(ton)}$$

	CEB Embodied energy [kWh]	Straw-CEB Embodied energy [kWh]	Transport energy [kWh]					
			Scen. 1	Scen. 2	Scen. 3	Scen. 4	Scen. 5	Scen. 6
2-storey building	2822	2438	0	1326	2652	24	1098	2129
3-storey building	4234	4108	0	1989	3979	41	1850	3587
4-storey building	7207	6677	0	3387	6773	66	3006	5830
5-storey building	10181	8710	0	4784	9568	91	4162	8073
6-storey building	13154	11815	0	6181	12362	117	5319	10317

Table 13: Transport energy

Table 13 shows the results obtained for each scenario, which agrees with the findings of Fernandes et al., 2019 and Christoforou et al., 2016. When the energy due to transportation was compared to the mean embodied energy of a CEB structure, it reflected the weight of transport in the environmental impact of CEB.

Even if these values could not strictly be compared to one another, they contributed to the understanding of the potential of CEBs as construction material with respect to transport. This optimisation of transport couldn't be achieved for fired brick masonry. In fact, the fabrication process of fired bricks requires important infrastructures often established in a close vicinity of the extraction quarries. Such infrastructures include industrialised crushing chains, homogenisation containers, mixing and extrusion units, drying containers, large ovens, and geometry rectifications chains, which are impossible to move (Hoyet, 2013).

Therefore, one of the benefits of locally sourced materials is that the transport contribution was considerably reduced compared to non-locally sourced materials, and that this contribution could even be minimised in function of the scenario adopted for a construction project (e.g. up to a reduction factor of 2 between scenarios 2 and scenario 3). One could conclude that the excavation place and manufacturing location needed to be as close to the construction site as possible; or eventually close to one another if the proximity to the construction site couldn't be reached.

Moreover, it could be noticed that the addition of straw in CEBs was interesting when transport energies of CEB structures and straw-CEB structure were compared: up to reduction factors of 0,8 could be observed between scenarios 2 and 5 and of 0,72 between scenarios 3 and 6).

Nevertheless, it has to be noted that scenario 1 is hardly ever possible for the entirety of a project (Kapfinger & Sauer, 2015). This scenario needs to satisfy several requirements in order to be viable: the suitability of the soil, the amount of soil, the possibility to store the excavated soil in situ, the possibility to manufacture CEBs in situ, etc. When these conditions are reunited, the amount of topsoil available is often not enough for the whole project, and extra soil needs to be provided. Therefore, when scenario 1 is not strictly possible, a mix between scenarios 1 and 2 or scenarios 1 and 3 are often more representative of the reality for larger scale projects.

3. End-of-life stage

Another benefit of working with locally sourced natural materials is that the waste processing is simple and straightforward: it includes the crushing of the waste material (mix CEB-earth mortar). It has been reported that more than 90% of the waste mix could be reintroduced into a recovery/recycling system, because 10% consists of dust from the demolition procedure and of some broken parts that are left on site (Fernandes, Peixoto, Mateus, & Gervasio, 2019). As this left 10% is made out of soil without any chemical adjuvant, the return of this waste to the natural environment does not present any inconvenient in terms of environmental impact.

This recovery/recycling process induced that the waste disposal returned to the manufacturing process to be recycled in new CEBs, creating a closed loop between the end-of-life stage and the producing stage (Figure 81). This circularity of the material revealed the potential of earth to be suitable for a cradle-to-cradle scenario. Moreover, it has to be noted that using recovered materials does not alter the quality of the final product and has environmental as well as economic advantages (Hoyet, 2013).

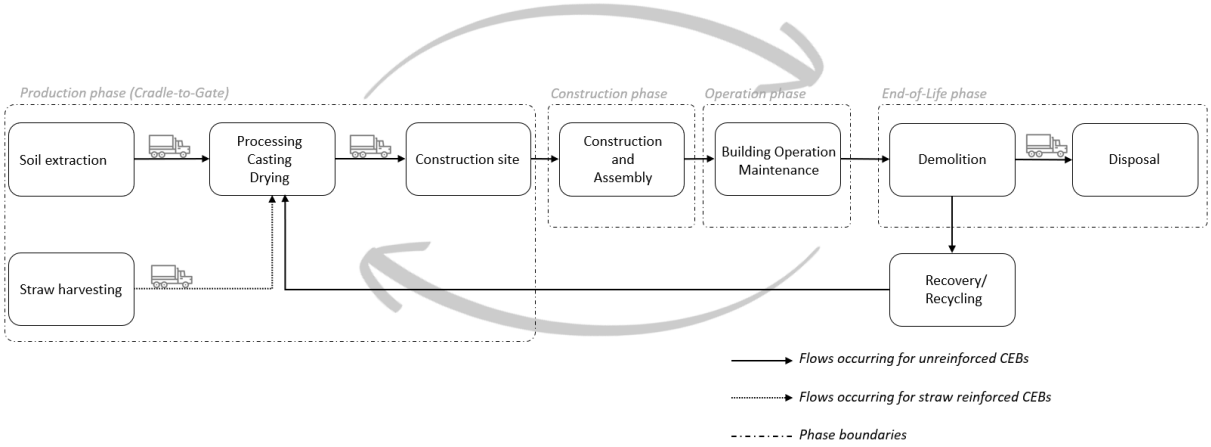

Figure 81: End of life scenario of CEBs

On the other hand, the end of life of fired brick masonry did not present the same ability to consider a recovery/recycling process. In fact, the demolition of a fired brick masonry structure results in inert waste materials which can't be recycled. In some rare cases, often for experimental sake, the reuse of facing bricks can be carried out, but this is often reserved for experimental sake, as the economical output of such practices in not particularly interesting (Hoyet, 2013).

4. Conclusion

CEB structures have a significantly lower embodied energy than traditional masonry structures: up to 5,90 times smaller for CEB structures and up to 6,75 times smaller for straw-CEB structures. These low values of embodied energy could contribute to decrease the environmental impacts of such structures. Besides that, it could be observed that the transport parameter represented an important weight in the embodied energy of CEBs. The contribution of transport could be reduced by opting for close extraction quarries and manufacture plants, when they were not possible in situ, and by opting for a straw reinforced structure, which resulted in an additional decrease of the embodied energy of the structure.

Moreover, the natural and low-processed characteristics of CEBs can assure an easy circularity of the raw material into a cradle-to-cradle scenario, implying less impacts than end-of-life scenarios of conventional materials, like fired brick masonry.

7. Conclusion

This study allowed to expose the potential of reinforced CEB constructions as well as its limitations, and encourages to continue investigating into the following points, representing the main outcomes of this study.

Type of straw

The nature of straw added in the samples played an important role in the optimisation of the straw ratio, especially in terms of absorbance. In fact, a more absorbent straw type induced a smaller amount of water distributed in the soil matrix while a less absorbent straw type induced a larger amount of water in the soil matrix. This difference in water content present in the soil before the incorporation of straw can't be neglected, especially in the case of clayey soils where water plays an important role in the cohesion between particles. Therefore, the optimal straw ratio needed to be a compromise between the dry mass of straw and its absorbance. In this study, this relation was translated into the concept of saturated straw ratio, which was a way to consider this compromise.

Importance of cure

It was found that the optimal ratio of straw found at day 0 of cure was not optimised for cured samples. In fact, it was assumed that the effects of cure would improve mechanical properties of straw reinforced samples, as it is the case for unreinforced samples. Instead, the contrary was observed in this study. Compression strength and tensile strength of reinforced CEBs happened to improve significantly during the first week of cure, i.e. when samples were still "wet", while they revealed an important decrease from this first cure week onwards. Shrinkage of the straw wisps, hence the loss of cohesion in the straw-soil matrix, was assumed to be the cause of this decrease.

Further investigations on this behaviour should determine if this is inherent for this type of straw and soil, or if it is a consequence of a too large straw ratio.

Static dynamic

The theoretical static compaction curve proposed as an alternative to the optimal Proctor compaction curve needs to be corrected and verified by future experiments. In fact, this curve, introduced by needs of a more suitable water content for statically compacted earth samples, only revealed relevance for reinforced CEBs, in the sense that straw-CEBs made with the hypothetical optimal static water content showed a higher density than straw-CEBs made with the optimal Proctor. Nevertheless, the less dense straw-CEBs showed a better compression strength than the straw-CEBs having a higher density.

Production process

An adapted fabrication procedure for straw reinforced samples is recommended to reach a good reproducibility of the tests. The lower reproducibility of the experiments performed on CEBs in the second experimental part of this study is undoubtably due the disparity of the straw distribution in the soil mixture.

Structure and LCA

Only focusing on compression strength properties of a material to predict structural performances is not a realistic decision. The duality of compression strength and density needs to be investigated:

The generally accepted strong link between density and compression strength often leads to seek for a higher density to obtain a larger compression strength, while ideally, the contrary should be sought: try to reduce the density and increase the compression strength at the same time.

The ratio *compression strength/density* must be considered to predict the structural potential of a material. In fact, in order to improve the structural abilities of CEB, in fact, there is no point in increasing the compression strength of a material if it means to equally enlarge its density. Structurally speaking, its improved bearing capacity will be deserved by its heavier weight. Moreover, a larger amount of material will be needed to support a similar structure due to its increased density, which will have a direct impact on its embodied energy.

In this study, both CEBs and straw reinforced CEBs were able to sustain up to a 6-storey high building. This means that even if the compression strength did not improve *per se* for reinforced samples, the decrease in density due to the incorporation of straw created a more lightened material, which compensated its decrease in compression strength. This resulted in an equivalent structural potential for CEBs as for straw reinforced CEBs.

References

(2008). Retrieved from Lehm ton Erde: https://www.lehmtonerde.at

(2018). Retrieved from Statista: https://fr.statista.com

(2019). Retrieved from StatBel, Belgium in figures: https://statbel.fgov.be

(2020). Retrieved from CRATerre: https://craterre.org

(2020). Retrieved from MesFournisseurs: https://www.mesfournisseurs.be

Al Rim, K., Ledhem, A., Douzane, O., Dheilly, R., & Que'neudec, M. (1999). Influence of the proportion of wood on the thermal and mechanical performances of clay-cement-wood composites. *Cement and Concrete Composites, 21*, 269-276.

Algin, H. M., & Turgut, P. (2007). Cotton and limestone powder wastes as brick material. *Construction and Building Materials*.

Aubert, J., Fabbri, A., Morel, J., & Maillard, P. (2013). An earth block with a compression strength higher than 45MPa! *Construction and Building Materials*.

Aymerich, F., Fenu, L., & Meloni, P. (2011). Effect of reinforcing wool fibres on fracture and energy absorption properties of an earthen material. *Construction and Building Materials,*.

Baridon, L., Garric, J.-P., & Richaud, G. (2016). *Les leçons de la terre. François Cointeraux.* Editions des Cendres.

Ben-Alon, L., Loftness, V., Harries, K. A., DiPietro, G., & Cochran Hameen, E. (2019). Cradle to site Life Cysle Assessment (LCA) of natural vs conventional building materials: A case study on cob earthen materials. *Building and Environment, 160*, 106-150.

Bouguerra, A., Ledhem, A., de Barquin, F., Dheilly, R. M., & Que'neudec, M. (1998). Effect of microstructure on the material and thermal properties of lightweight concrete prepared from clay, cement, and wood aggregates. *Cement and Concrete Research, 28*(8), 1179-1190.

Bui, Q. B., Morel, J., Reddy, B., & Ghayad, W. (2009). Durability of rammed earth exposed walls exposed for 20 years of natural weathering. *Buildnig and Environment, 44*, 912-919.

Cardinale, T., Arleo, G., Bernardo, F., & Feo, A. D. (2017). Thermal and mechanical characterization of panels made by cement mortar and sheep's wool fibres. *AiCARR 50th International Congress. Beyond nZEB Buildings*, (pp. 10-11). Matera, Italy.

Catalan, G., Hegyi, A., Dico, C., & Mircea, C. (2015). Determining the optimum addition of vegetable materials in adobe bricks. *Procedia Technology*.

Christoforou, E., Kylili, A., Fokaides, P. A., & Ioannou, I. (2016). Cradle to site Life Cycle Assessment (LCA) of adobe bricks. *Journal of Cleaner Production, 112*, 443-452.

Danso, H., Martinson, D. B., Ali, M., & Williams, J. B. (2015). Physical, mechanical and durability propertes of soil building blocks reinforced with natural fibres. *Construction and Building Materials*.

Data and Statistics. (2020). Retrieved from International Energy Agency: https://www.iea.org

Devos, R. (2018-2019). Course of Post-war History. Brussels: ULB.

Elizondo, M., Guerrero, L., & Mendoza, L. (2011). Environmental impact: comparison between earthen architecture and conventionnal construction. *Structural Repairs and Maintenance of Heritage Architecture XII*, 475-484.

Fernandes, J., Peixoto, M., Mateus, R., & Gervasio, H. (2019). Life cycle analysis of environmental impacts of earthen materials in the Portuguese context: Rammed earth and compressed earth blocks. *Journal of Cleaner Production, 241*, 118-286.

François, B. (2017-2018). Soil Mechanics: Course Notes. Brussels: ULB.

Gmira, A. (2013). *Etude structurale et thermodynamique d'hydrates : modèle du ciment.* Thèse de doctorat, Université d'Orléans, Matériaux.

Hakimi, A., Yamani, H., & Ouissi, H. (1996, December). Rapport: Résultats d'essais de résistance mécanique sur échantillons de terre comprimée. *Matériaux et construction, 29*, 600-608.

Hall, M. R., Lindsay, R., & Krayenhoff, M. (Eds.). (2012). *Modern earth buildings: Materials, engineering, construction and applications.* Woodhead Publishing Limited.

Hamard, E., Cazacliu, B., Razakamanantsoa, A., & Morel, J.-C. (2016). Cob, a vernacular earth construction process in the context of modern sustainable building. *Building and Environment*.

Houben, H., & Guillaud, H. (2006). *Traité de construction en terre.* (CRATerre, Ed.) Editions Parenthèses.

Hoyet, N. (2013). *Matériaux et Architecture durable.* DUNOD.

Kapfinger, O., & Sauer, M. (2015). *Martin Rauch: Refined earth construction & design with rammed earth.* Details.

Khan, A. Z. (2017-2018). Course of Bioclimatic Design. Brussels: ULB.

Khasreen, M. M., Banfill, P. F., & Menzies, G. F. (2009). Life-Cycle Assessment and the Environmental Impact of Building: A Review. *Sustainability, 1*, 674-701.

Laborel-Préneron, A., Aubert, J., Magniont, C., Tribout, C., & Bertron, A. (2016). Plant aggregates and fibres in earth construction materials: A review. *Construction and Building Materials*.

Laurent, J.-P. (1986). *Contribution à la caractérisation thermique des milieux poreux granulaires: optimisation d'outils de mesure "in situ" des paramètres thermiques. Application à l'étude des propriétés thermiques du matériaux terre.* Thèse de doctorat, INP Grenoble, Mécanique.

L'énergie grise des matériaux de construction. (2016). Retrieved from EcoConso.be: https://www.ecoconso.be

Mansour, M. B., Jelidi, A., Cherif, A. S., & Jabrallah, S. B. (2015). Optimizing thermal and mechanical performances of compressed earth blocks (CEB). *Construction and Building Materials*.

Matriche, R. (2020). Pathologies, rénovation et réhabilitation des structures. Brussels: ULB.

Mesbah, A., Morel, J., & Olivier, M. (1999, November). Comportement des sols fins argileux pendant un essai de compactage statique: détermination des paramètres pertinents. *Matériaux et Constructions, 32*, 687*694.

Miccoli, L., Müller, U., & Fontana, P. (2014). Mechanical behaviour of earthen materials: A comparison between earth block masonry, rammed earth and cob. *Construction and Building Materials*.

Millogo, Y., Aubert, J.-E., Hamard, E., & Morel, J.-C. (2015). How properties of Kenaf fibres from Burkina Faso contribute to the reinforcement of earth blocks. *Materials, 8*, 2332-2345.

Morel, J., Mesbah, A., Oggero, M., & Walker, P. (2000). Building houses with local materials: means to drastically reduce the environmental impact of construction. *Building and Environment*.

Morel, J., Pkla, A., & Walker, P. (2007). Compressive strength testing of compressed earth blocks. *Contruction and Building Materials, 21*, 303-309.

National Institute of Building. (2020). *Innovative Solutions for the Built Environment*. Retrieved from Whole Building Design Guide: https://www.wbdg.org

Olivier, M., & Mesbah, A. (1986). Le matériau terre: Essai de compactage statique pour la fabrication de briques de terre compressées. *Bull. Liaison Labo. P. et Ch., 146*, 37-43.

Olivier, M., Mesbah, A., Gharbi, E., & Morel, J. (1997, November). RILEM TC 164-EBM: Mechanics of earth as a building material. Test method for strength tests on blocks of compressed earth. *Materials and Structures, 30*, 515-517.

Pacheco-Torgal, F., & Jalali, S. (2011). Earth constructions : Lessons from the past for future eco-efficient constructions. *Construction and Building Materials*.

Parisi, F., Asprone, D., Fenu, L., & Prota, A. (2015). Experimental characterization of Italian composite adobe bricks reinforced with straw fibers. *Composite Structures*, 300-307.

Pkla, A. (2002). *Caractérisation en compression simple des blocs de terre comprimées (BTC): application aux maçonneries "BTC-mortier de terre".* Thèse de Doctorat, Université de Lyon.

Robert, A. (2013). *Non-stabilized rammed earth constructions: Material characteristics and Application to Urban Co-Housing in Brussels.* Master thesis, ULB, Brussels.

Sharma, V., Marwaha, B. M., & Vinayak, H. K. (2016). Enhancing durability of adobe by natural reinforcement for propagating sustainable mud housing. *International Journal of Sustainable Built Environment* , 141-155.

Shukla, A., Tiwari, G., & Sodha, M. (2009). Embodied energy analysis of adobe house. *Renewable Energy, 34*, 755-761.

Silveira, D., Varum, H., & Costa, A. (2013). Influence of the testing procedures in the mechanical characterization of adobe bricks. *Construction and Building Materials*, 719-728.

Standards New Zealand. (1998). *New Zealand Standard 4298: "Materials and workmanship for earth buildings".*

Taylor, P., & Luther, M. (2004). Evaluating rammed earth walls: a case study. *Solar Energy, 76*, 79-84.

Venkatarama Reddy, B., & Jagadish, K. (1995). Influence of soil composition on strength and durability of soil-cement blocks. *Indian Concr. J., 69*(9).

Vyncke, J., Kupers, L., & Denies, N. (2017). Earth as Building Material: an overview of RILEM activities and recent innovation in Geotechnics. *CSTC*.

Walker, P. (2004). Strength and erosion characteristics of earth blocks and earth block masonry. *J.Mater. Civil Eng., 16*(5), 497-506.

Annexes

Annex A

Details on the three main earth constructions methods

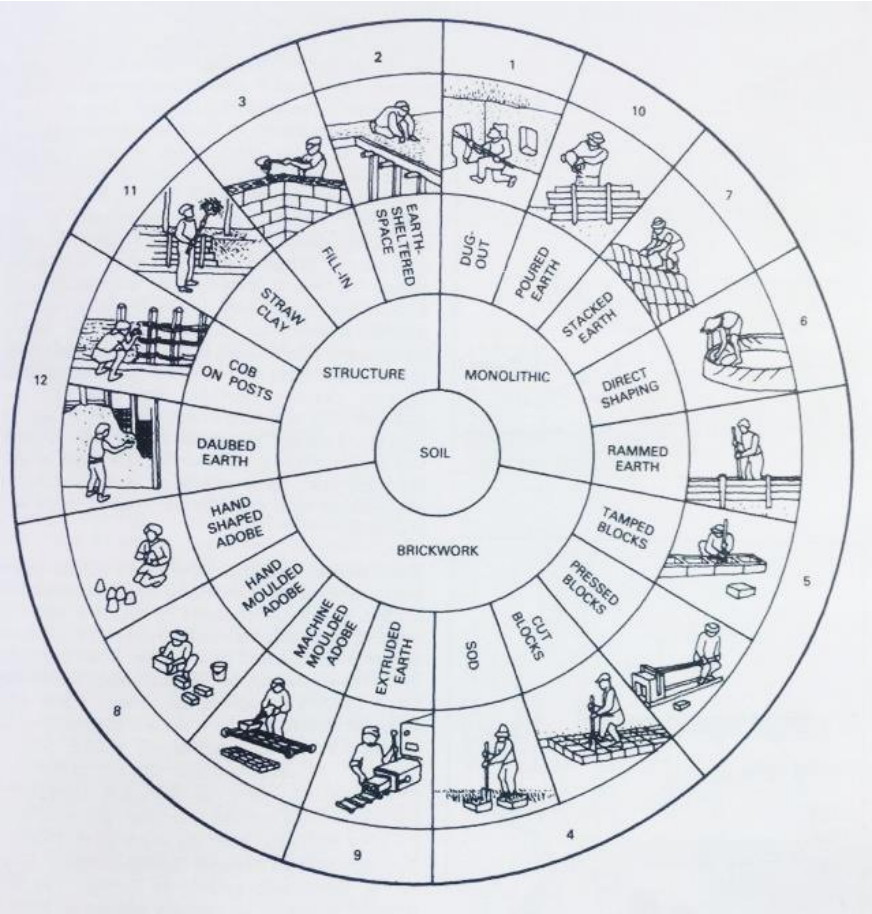

Figure 82: Earth construction methods (Houben & Guillaud, 2006)

Monolithic constructions

In monolithic constructions, earth is directly implemented in situ to proceed to the construction. Creating such monolithic structures can be performed by means of five different methods which are the following:

- digging volumes directly out of the layers of the earth's crust, which results in troglodytic housings,
- manually shaping plastic earth like for pottery, which ends up in creating thinner earth walls,
- piling up balls of earth one onto another to obtain thick walls,
- pouring liquid soil into a formwork like for concrete,
- compressing earth layers by layers into a formwork, which is the technique of rammed earth walls, or PISE (pneumatically impacted stabilised earth).

Brickwork constructions

This method is done in two distinct steps. It consists first in the fabrication of small earthen units that are often sun-dried. After that, the units are assembled like in masonry constructions, to create vaults, walls, etc. The main techniques are the following:

- Adobe: adobe is a method that consists in moulding earth to make earthen bricks. The moulding process can be realised by hand, to obtain either hand shaped or hand moulded adobe; or can be realised in a more industrial way, which results in machine moulded adobe.
- Cut blocks: earthen blocks are directly cut in the upper layer of the ground surface ("sod") or in a prepared layer of earth mixture.
- Compressed earth blocks: within a mould, an earth mixture is compressed with a manual or automated press to obtain compressed earth blocks, also known as CEB.
- Extruded earth: a plastic soil mixture is extruded thanks to a machine, which creates building elements containing hollow alveoli.

Mixed structure constructions

The structuring elements of a construction can also be made of a mix of two different materials that complement each other. The most common choices are to combine earth with wooden frameworks, with fibres, or to use the earth mixture as a filling of any hollow materials, like hollow bricks. Four distinct categories can be identified for such constructions:

- Earth-sheltered spaces: a soil mixture is inserted between the elements of a roof structure and is then entirely covering the top structure. This technique is mainly used to insulate underground constructions but is also be used to protect roofs alone, especially when grass begins to grow on top this soil layer (like in northern countries).
- Fill-in: an ungraded soil mixture is poured or compressed in hollow elements, considered as formworks, that are stacked on one another.
- Straw-clay: a mixture of liquid clayey soil and straw is created (fibrous slurry) and is used to fill-in wooden frames. This method can also be adapted to prefabricate small straw-clay bricks, drying rapidly, and pile them up like masonry elements, but still into a main structural framework.
- Daubed earth: a clayey soil mixture is combined with fibres in order to fill-in a structural support. When applied onto a fibrous weaving, this technique, called "daub" (FR: *torchis*) is essentially used as a covering because it is only applied in quite thin layers. On the other hand, when the clay-straw mixture needs to fill the spaces between vertical and horizontal structural poles, it is applied according to the cob technique (FR: *bauge*), meaning that small balls of mixture are stacked on each other between the poles.

Annex B

Systems tried for the application of the mortar layer

Figure 83: First application system

Figure 84: Third optimised application system

Figure 85: Third application system

Annex C

Experimental results samples E, EP, C, CP

Samples E

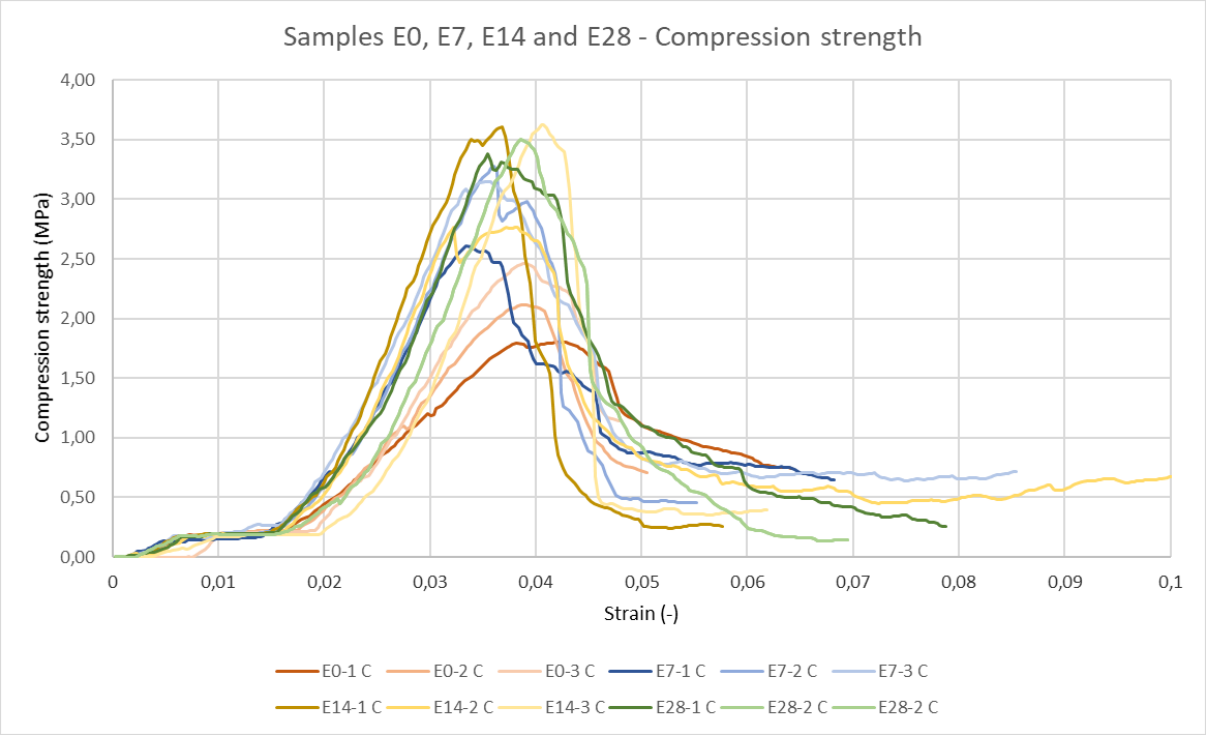

	Force Max (kg)	W (%)	ρ_{dry} (kg/m³)	Compr stress (MPa)	E-pseudo (GPa)	Flexural force [kg]	Tensile strength [MPa]
E0-1	608,07	5,96	2008	1,804	30,74	7,15	0,282
E0-2	711,69	7,13	2144	2,117	53,29	8,99	0,402
E0-3	825,92	5,74	2014	2,462	72,29	7,85	0,310
E0	**715,23**	**6.28**	**2055**	**2,128**	**52,11**	**7,99**	**0,331**
E7-1	877,84	2,85	/	2,611	84,33	37,15	1,430
E7-2	1100,76	2,71	/	3,277	99,28	62,54	2,410
E7-3	1066,84	2,80	/	3,150	95,42	75,69	2,872
E7	**1015,15**	**2.79**	**/**	**3,013**	**93,01**	**58,46**	**2,237**
E14-1	1220,99	2,19	/	3,609	117,44	62,77	2,397
E14-2	928,84	2,14	/	2,767	89,91	51,69	1,970
E14-3	1219,38	2,23	/	3,626	106,89	57,46	2,336
E14	**1123,07**	**2.19**	**/**	**3,334**	**104,74**	**57,31**	**2,234**
E28-1	1108,61	2,35	/	3,378	116,77	70,85	2,677
E28-2	1153,84	2,67	/	3,505	110,05	59,31	2,268
E28-3	1166,53	2,56	/	3,577	112,45	68,54	2,790
E28	**1142,99**	**2.53**	**/**	**3,486**	**113,09**	**66,23**	**2,579**

Table 14: Results samples E

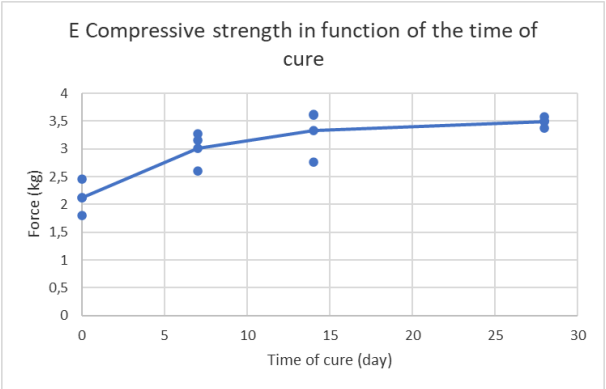
E Compressive strength in function of the time of cure
Force (kg)
Time of cure (day)

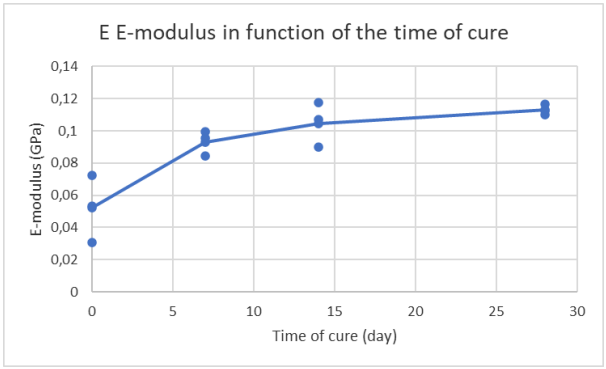
E E-modulus in function of the time of cure
E-modulus (GPa)
Time of cure (day)

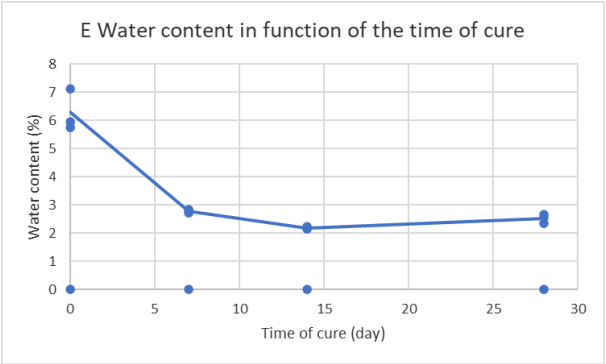
E Water content in function of the time of cure
Water content (%)
Time of cure (day)

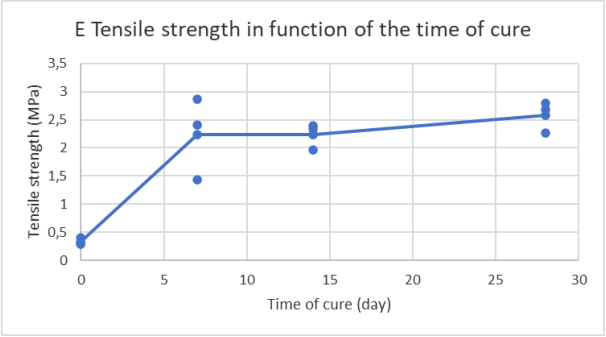
E Tensile strength in function of the time of cure
Tensile strength (MPa)
Time of cure (day)

Samples EP

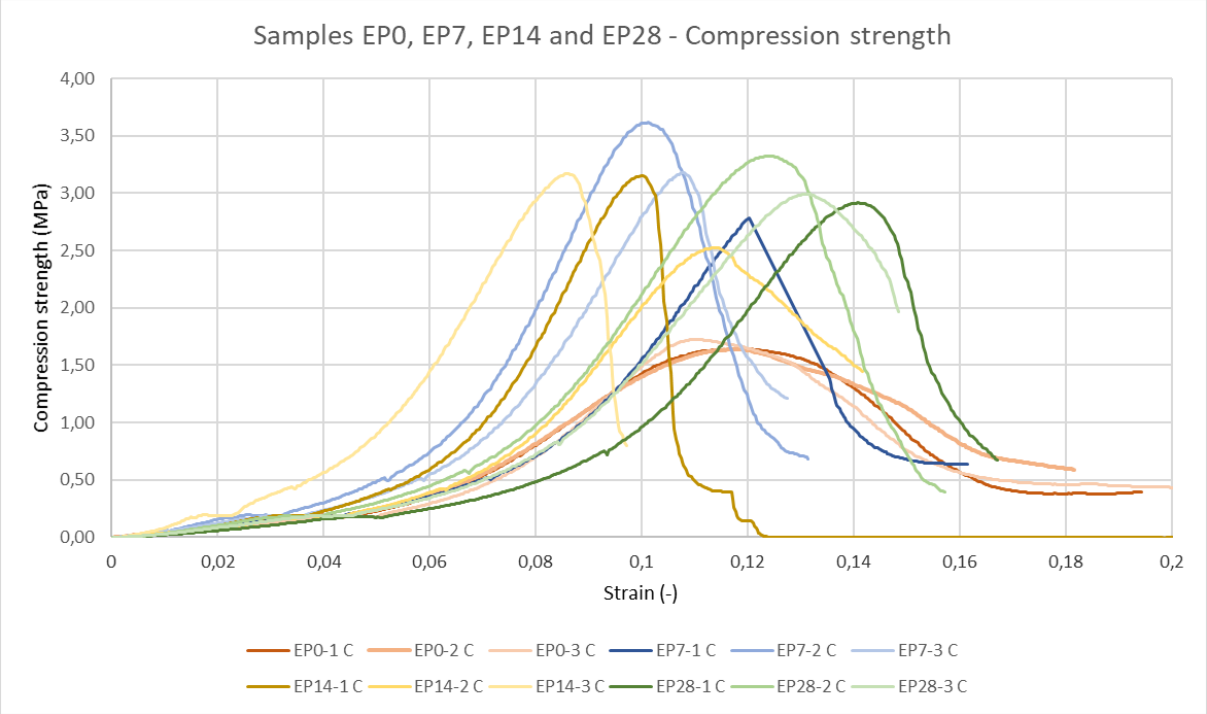

	Force Max (kg)	W (%)	ρ_{dry} (kg/m³)	Compr stress (MPa)	E-pseudo (GPa)	Flexural force	Flexural strength
EP0-1	614,99	5,64	1686,38584	1,642322221	0,019308697	19,38449707	1,670344699
EP0-2	612,46	6,52	1704,65238	1,636210592	0,014947951	24,23062134	2,115690716
EP0-3	637,84	5,46	1633,60272	1,724711038	0,020215601	25,38446045	2,13028885
EP0	**621,89**	**5,87**	**1674,88032**	**1,66774795**	**0,018157416**	**22,99985962**	**1,972108088**
EP7-1	1043,53	3,14	/	2,783548585	0,030041244	37,15361938	3,086917047
EP7-2	1316,53	3,16	/	3,616239779	0,046571136	62,53807983	5,333594802
EP7-3	1169,30	3,23	/	3,176616243	0,036814344	75,6918457	6,380964774
EP7	**1176,45**	**3,18**	**/**	**3,192134869**	**0,037808908**	**58,46118164**	**4,933825541**
EP14-1	1168,37	2,53	/	3,152661002	0,041967108	24,46138916	1,910635594
EP14-2	920,76	3,36	/	2,522271297	0,027503602	15,46144409	1,249468723
EP14-3	1151,30	3,20	/	3,169882876	0,039231732	25,61522827	1,951021684
EP14	**1080,14**	**3,03**	**/**	**2,948271725**	**0,036234147**	**21,84602051**	**1,703708667**
EP28-1	1121,07	2,44	/	2,91568313	0,028252411	20,769104	1,752295999
EP28-2	1246,38	2,62	/	3,324922868	0,03260047	20,99987183	1,744659678
EP28-3	1119,22	3,45	/	2,993136877	0,027400497	21,69217529	1,847294494
EP28	**1162,22**	**2,84**	**/**	**3,077914292**	**0,029417793**	**21,15371704**	**1,781416724**

Table 15: Results samples EP

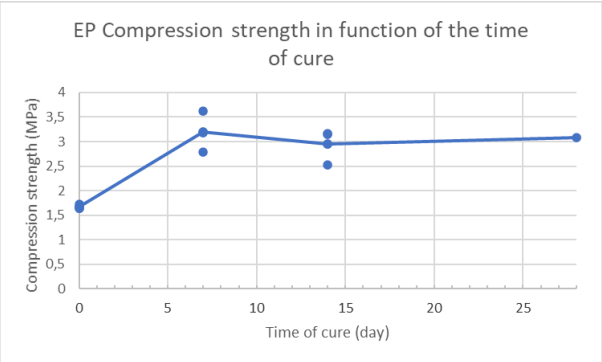
EP Compression strength in function of the time of cure
Compression strength (MPa)
4
3,5
3
2,5
2
1,5
1
0,5
0
0
5
10
15
20
25
Time of cure (day)

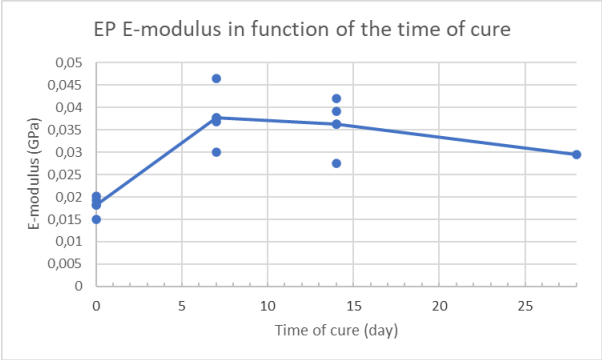
EP E-modulus in function of the time of cure
E-modulus (GPa)
0,05
0,045
0,04
0,035
0,03
0,025
0,02
0,015
0,01
0,005
0
0
5
10
15
20
25
Time of cure (day)

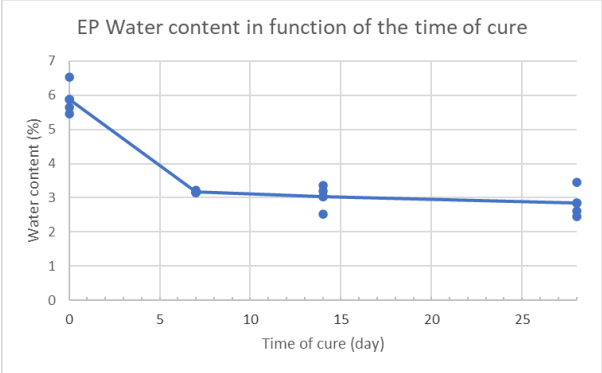
EP Water content in function of the time of cure
Water content (%)
7
6
5
4
3
2
1
0
0
5
10
15
20
25
Time of cure (day)

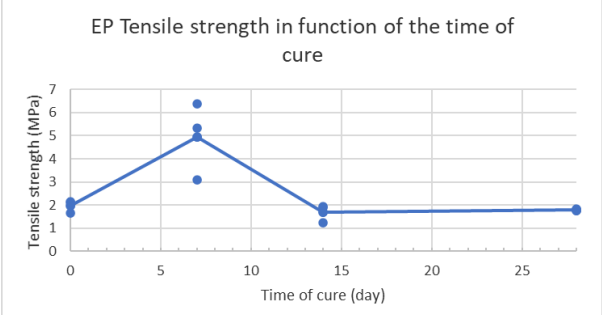
EP Tensile strength in function of the time of cure
Tensile strength (MPa)
7
6
5
4
3
2
1
0
0
5
10
15
20
25
Time of cure (day)

Samples C

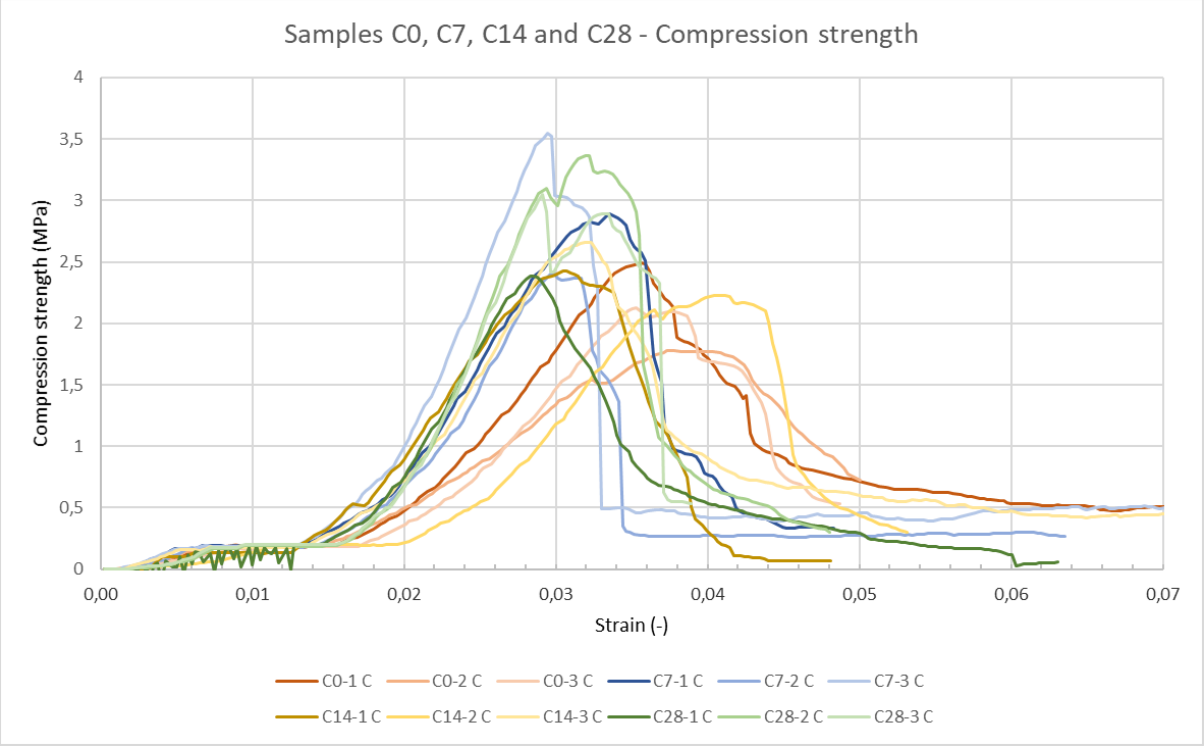

	Force Max (kg)	W (%)	ρ_{dry} (kg/m³)	Compr stress (MPa)	E-pseudo (GPa)	Flexural force	Flexural strength
C0-1	836,30	4,80	1997,561224	2,494960602	0,077138435	17,30758667	0,637282307
C0-2	596,07	5,31	1934,177417	1,780042556	0,045814012	14,5383728	0,51864627
C0-3	709,84	5,41	1963,378124	2,127988985	0,072575185	16,84605103	0,620879197
C0	**714,07**	**5,17**	**1948,777771**	**2,134330714**	**0,065175877**	**16,23067017**	**0,592269258**
C7-1	968,76	2,80	/	2,893262107	0,101888523	51,69199219	1,92148315
C7-2	804,23	2,89	/	2,406594489	0,105768038	26,99983521	0,942764325
C7-3	1181,76	2,82	/	3,544281767	0,138289279	43,38435059	1,557986635
C7	**984,92**	**2,84**	**/**	**2,948046121**	**0,11531528**	**40,69205933**	**1,474078037**
C14-1	812,07	2,61	/	2,427844532	0,084038772	/	/
C14-2	753,92	2,35	/	2,228234746	0,074566453	40,61513672	1,525209616
C14-3	890,30	2,50	/	2,661526064	0,048677528	41,07667236	1,415859771
C14	**818,76**	**2,49**	**/**	**2,439201781**	**0,069094251**	**40,84590454**	**1,470534694**
C28-1	795,23	1,99	/	2,385469267	0,110861664	31,61519165	1,098568063
C28-2	1128,69	1,24	/	3,366761677	0,150626481	38,76899414	1,40435888
C28-3	1015,38	1,60	/	3,047056477	0,143124072	48,23047485	1,78891167
C28	**979,77**	**1,61**	**/**	**2,933095807**	**0,134870739**	**39,53822021**	**1,430612871**

Table 16: Results samples C

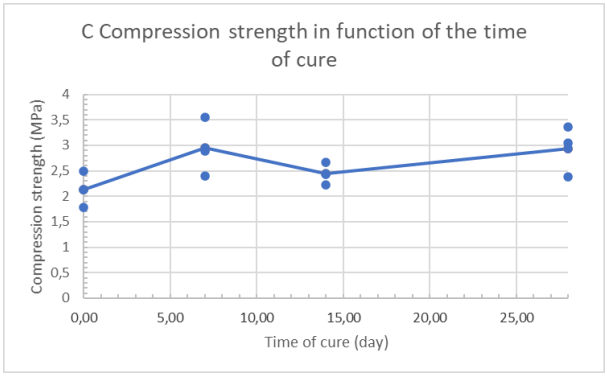
C Compression strength in function of the time of cure
Compression strength (MPa)
4
3,5
3
2,5
2
1,5
1
0,5
0
0,00
5,00
10,00
15,00
20,00
25,00
Time of cure (day)

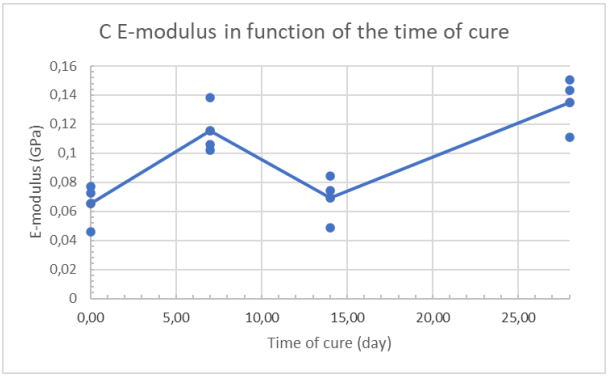
C E-modulus in function of the time of cure
E-modulus (GPa)
0,16
0,14
0,12
0,1
0,08
0,06
0,04
0,02
0
0,00
5,00
10,00
15,00
20,00
25,00
Time of cure (day)

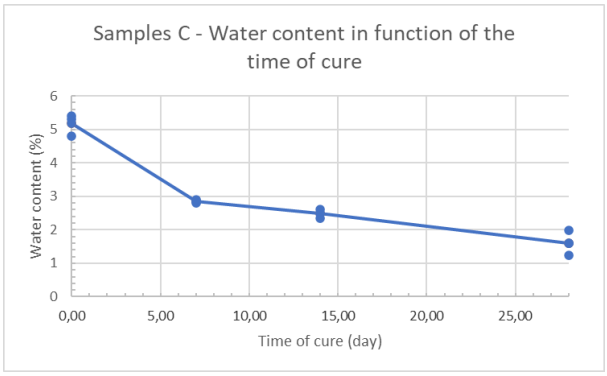
Samples C - Water content in function of the time of cure
Water content (%)
6
5
4
3
2
1
0
0,00
5,00
10,00
15,00
20,00
25,00
Time of cure (day)

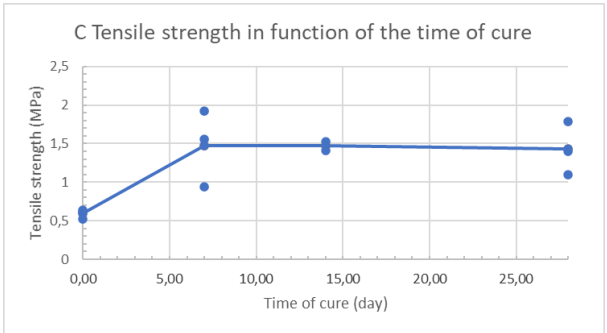
C Tensile strength in function of the time of cure
Tensile strength (MPa)
2,5
2
1,5
1
0,5
0
0,00
5,00
10,00
15,00
20,00
25,00
Time of cure (day)

Samples CP

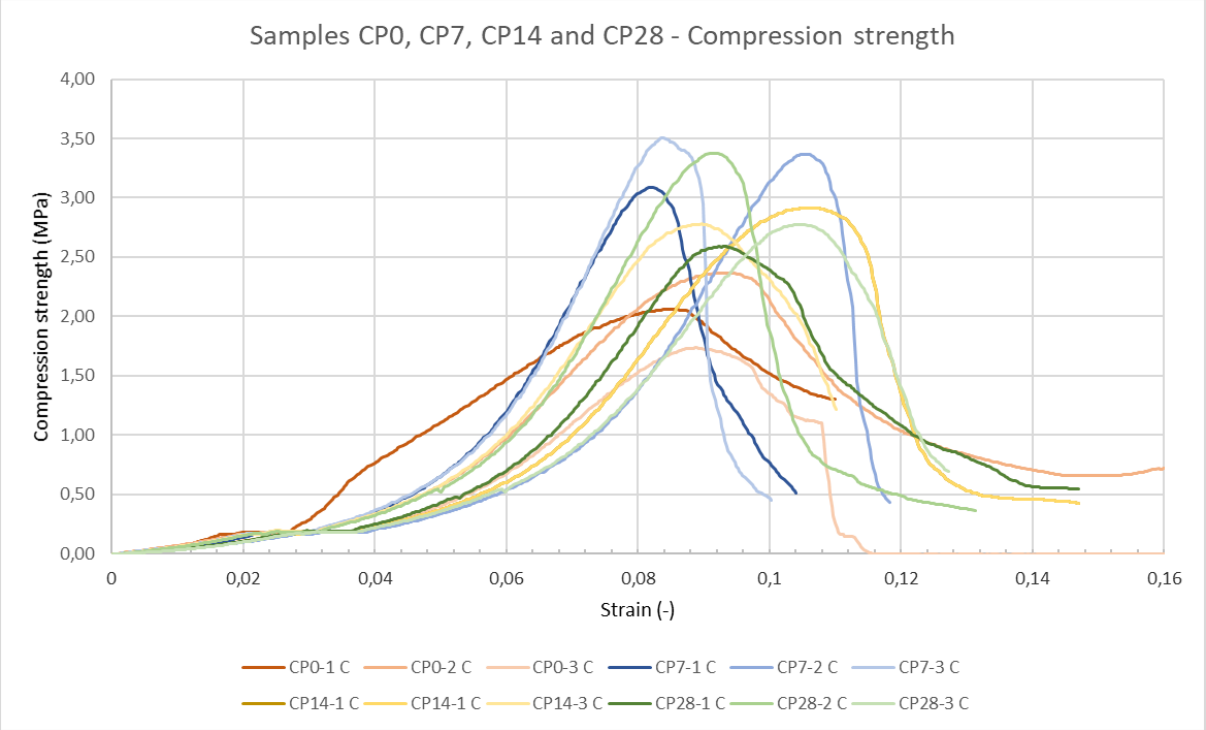

	Force Max (kg)	W (%)	ρ_{dry} (kg/m³)	Compr stress (MPa)	E-pseudo (GPa)	Flexural force	Flexural strength
CP0-1	760,15	6,30	1674,87845	2,058487058	0,017827613	7,846105957	0,700607856
CP0-2	855,69	5,95	1785,26622	2,364754273	0,028363176	12,69223022	1,183224068
CP0-3	625,84	4,65	1675,70654	1,734729384	0,021947239	9,692248535	0,79257363
CP0	**747,23**	**5,63**	**1711,9504**	**2,052656905**	**0,022712676**	**10,07686157**	**0,892135185**
CP7-1	1112,53	2,82	/	3,088031986	0,04895185	17,30758667	1,460842235
CP7-2	1256,07	3,20	/	3,368563012	0,044675617	30,92288818	2,460364665
CP7-3	1269,22	2,82	/	3,507532521	0,053391557	23,53831787	1,826964021
CP7	**1212,61**	**2,95**	**/**	**3,32137584**	**0,049006341**	**23,92293091**	**1,916056974**
CP14-1	1083,69	2,83	/	2,910988426	0,035191475	19,38449707	1,571620266
CP14-2	1184,76	2,80	/	3,153357312	0,032374526	21,92294312	1,728597372
C14-3	1006,38	2,58	/	2,779085099	0,022673414	20,769104	1,732340786
CP14	**1091,61**	**2,74**	**/**	**2,947810279**	**0,030079805**	**20,6921814**	**1,677519475**
CP28-1	934,15	2,65	/	2,586464773	0,037101128	27,92290649	2,494475284
CP28-2	1226,53	2,74	/	3,372998798	0,046043762	25,84599609	2,091538345
CP28-3	1019,53	2,53	/	2,776520525	0,033685163	24,69215698	2,042237667
CP28	**1060,07**	**2,64**	**/**	**2,911994699**	**0,038943351**	**26,15368652**	**2,209417099**

Table 17: Results samples CP

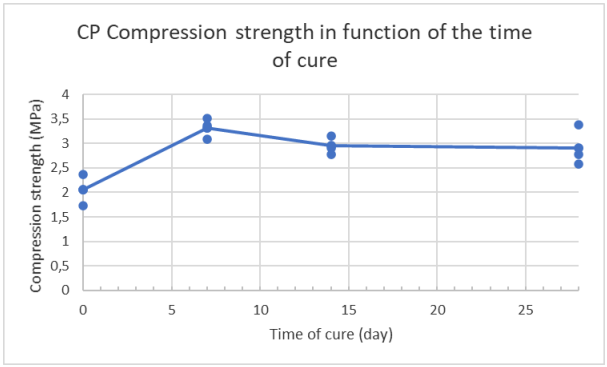
CP Compression strength in function of the time of cure
Compression strength (MPa)
4
3,5
3
2,5
2
1,5
1
0,5
0
0
5
10
15
20
25
Time of cure (day)

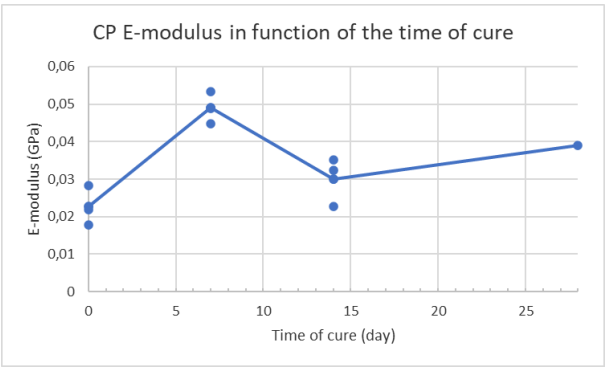
CP E-modulus in function of the time of cure
E-modulus (GPa)
0,06
0,05
0,04
0,03
0,02
0,01
0
0
5
10
15
20
25
Time of cure (day)

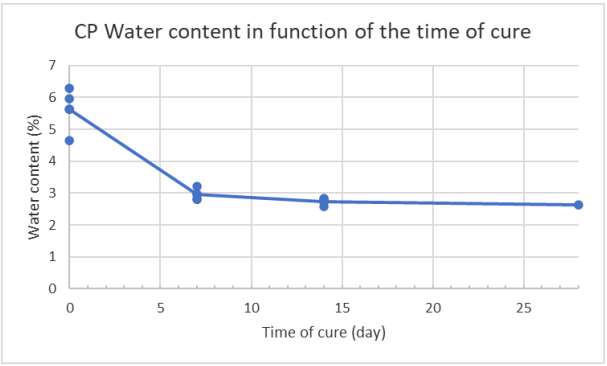
CP Water content in function of the time of cure
Water content (%)
7
6
5
4
3
2
1
0
0
5
10
15
20
25
Time of cure (day)

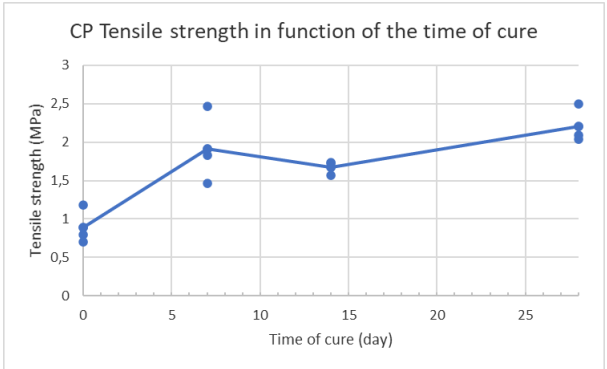
CP Tensile strength in function of the time of cure
Tensile strength (MPa)
3
2,5
2
1,5
1
0,5
0
0
5
10
15
20
25
Time of cure (day)

Annex D

Structural dimensioning (EC6)

- **Characteristic values**

Characteristic compression strength of a brick f_{bk}

The characteristic compression strength of a brick f_{bk} is determined according to the NBN EN 772-1. Then, according to the NBN EN 1996-1-1 ANB, the mean equivalent compression strength $f_{bm,\,eq}$ can be found with the following equation:

$$f_{bk,eq} = 1{,}18\, f_{bk}$$

Normalised compression strength fb

The normalised compression strength fb can be deducted from the mean equivalent compression strength $f_{bm,\,eq}$. To do so, the equivalent compression strength is transformed into a strength relative to the conditioning coefficient δc (air drying conditioning) and to the form factor δ, according to the NBN EN 1996-1-1 ANB §3.6.1.2.).

$$f_b = \delta.\delta_c.f_{bk,eq}$$

Type d'élément de maçonnerie	δ_c
Terre cuite	1
Silico-calcaire	0,8
Béton de granulats	1,2
Béton cellulaire	1

Table a – δc values

Hauteur	Plus petite dimension horizontale (en mm)				
	50	100	140/150	190/200	≥250
50	0,85	0,75	0,70	-	-
65	0,95	0,85	0,75	0,70	0,65
100	1,15	1,00	0,90	0,80	0,75
150	1,30	1,20	1,10	1,00	0,95
200	1,45	1,35	1,25	1,15	1,10
≥ 250	1,55	1,45	1,35	1,25	1,15

Table b – δ values

Characteristic compression strength of masonry f_k

The characteristic compression strength of masonry fk can be determined according to the following equation:

$$f_k = K.f_b^{0,65}.f_m^{0,25}$$

Where:

- If the width of the masonry is equal to the width of the masonry elements, meaning that there are no vertical longitudinal joints in the wall section:
  - For group 1 masonry: K = 0,60
  - For group 2a masonry: K = 0,55
  - For group 2b masonry: K = 0,50

- For group 3 masonry: K = 0,40

- If there are vertical longitudinal joints in the wall section:
  - For group 1 masonry: K = 0,50
  - For group 2a masonry: K = 0,45
  - For group 2b masonry: K = 0,40

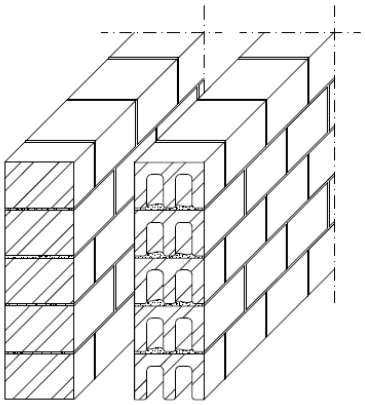

Walls without vertical longitudinal joints

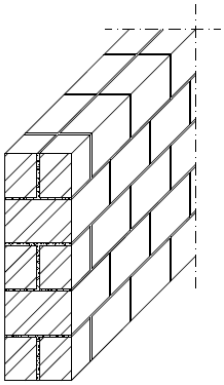

Walls with vertical longitudinal joints

The group categorisation is performed according to the article 3.1.1. of the EC6, namely for masonry:

- Group 1: less than 25% hollow spaces
- Group 2a: 25-45% hollow spaces
- Group 2b: 45-55% hollow spaces (common case)
- Group 3: up to 70% hollow spaces

Characteristic compression strength of masonry parallel to the laying bed fkh

When masonry is subject to flexion, compression stresses parallel to the laying bed will appear. The characteristic compression strength of masonry parallel to the laying bed fkh needs to be controlled according to the following:

$$f_{kh} \geq \frac{\gamma_M . M_{sd}}{c . b . d^2}$$

Where: $f_{kh} = 0{,}3 . f_k$
γ_M = security factor of masonry
M_{sd} = bending moment
$c = 0{,}30$ for groups 2a,2b and 3
$c = 0{,}40$ for group 1
b = thickness of the wall
d = useful height

Characteristic shear strength of masonry fvk

The characteristic shear strength of masonry fvk is determined as being the smallest value between the following ones:

$$f_{vk} = f_{vk0} + 0{,}4 . \sigma_d$$

$$or \qquad f_{vk} = 0{,}065 . f_b$$

Where: σ_d = permanent vertical compression stress

f_{vk0} is based on the following table:

Type de maçonnerie	f_m M 10 à M 20	f_m M 5 à M 10
Brique groupe 1	0,3	0,2
Brique groupe 2a	0,3	0,2
Brique groupe 2b	0,2	0,15
Brique groupe 3	0,2	0,15

The characteristic shear strength of masonry fvk is nevertheless limited to the following values:

Type de maçonnerie	f_m M 10 à M 20	f_m M 5 à M 10
groupe 1	1,7	1,5
groupe 2 et 3	1,4	1,2

For group 2 masonries, fvk also needs to be limited to the characteristic compression strength of masonry parallel to the laying bed fkh.

This characteristic shear strength of masonry fvk then needs to be controlled according to the following:

$$f_{vk} \geq \frac{\gamma_M . V_{sd}}{b.d}$$

Where: γ_M = security factor of masonry

V_{sd} = shear stress

b = thickness of the wall

d = useful height

a. Dimensioning structural masonry elements

The maximal stress authorised is calculated according to the Eurocode 6 and the Belgian DAN, separately for each wall, with the corresponding reduction factor Φ depending on the geometry, the slenderness, the limit conditions and the load eccentricity.

- **Slenderness**

$$S = \frac{h_{ef}}{t_{ef}}$$

Where: Hef = effective height of the wall

Tef = effective thickness of the wall (t = tef except in the case of a double wall)

The effective height of the wall is determined as follows:

$$h_{ef} = \rho_n . h$$

- Wall supported on top and bottom:

In this case, the reduction factor ρn = ρ2

Where: ρ2 = 0,75 for an embedded wall

ρ2 = 1,00 in any other case

- Wall supported on both horizontal sides and on one vertical side.

In this case, the reduction factor ρn = ρ3

In which case:

- If h ≤ 3,5 L:

$$\rho_3 = \frac{\rho_2}{1 + \left(\frac{\rho_2 . h}{3L}\right)^2} > 0{,}3$$

- If h > 3,5 L:

$$\rho_3 = \frac{1{,}5L}{h}$$

Where: h= height of the wall

L = distance between vertical walls

- Wall blocked on both horizontal sides and both vertical sides.

In this case, the reduction factor ρn = ρ4

In which case:

- If h ≤ L:

$$\rho_4 = \frac{\rho_2}{1 + \left(\frac{\rho_2 . h}{L}\right)^2} > 0{,}3$$

- If h > L:

$$\rho_4 = \frac{0{,}5L}{h}$$

Where: h= height of the wall

L = distance between vertical walls

- **Eccentricity**
  - On top or bottom of the wall

$$e_i = \frac{M_i}{N_i} + e_{hi} + e_a \geq 0{,}005 . t$$

Where:

Mi = bending moment on top or bottom of the wall due to the eccentricity of the vertical loads;

Ni = vertical load on the considered section;

Ehi = eccentricity induced by horizontal loads, such as wind;

Ea = fortuitous eccentricity = hef / 450.

  - In the middle of the wall

$$e_m = \frac{M_m}{N_m} + e_{hm} + e_a \geq 0{,}005.t$$

Two cases can occur which will imply the following eccentricity values for Mm/Nm values, namely if angular displacements are or aren't possible on top and bottom of the consered wall.

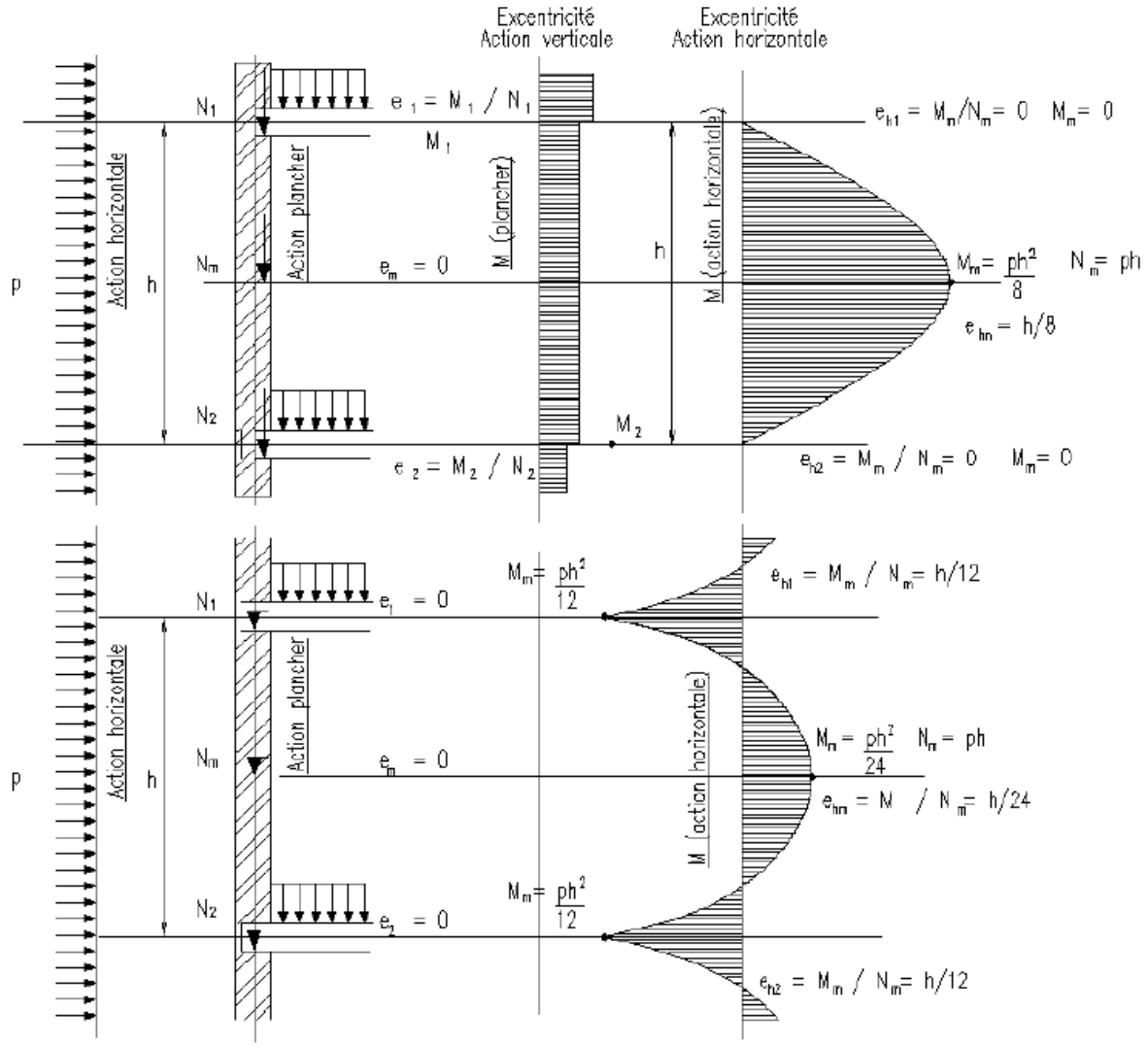

- **Control of the compression strength**

- Control of the section on top and bottom of the wall

The reduction factor Φi can be introduced as such:

$$\Phi_i = 1 - 2.\frac{e_i}{t_{eff}}$$

The value of the weighted ULS loads Nsd needs to be smaller than the design resisting value of the wall, such as:

$$N_{Sd} \leq \frac{\Phi_i.t_{eff}.f_k}{\gamma_M}$$

- Control of the section in the middle of the wall

The reduction factor Φm can be determined with the graph here-below, giving Φm in function of the slenderness and the relative eccentricity emk.

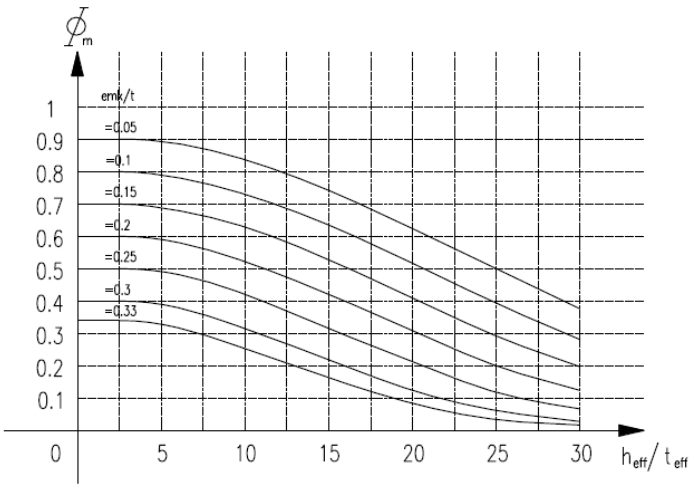

The value of the weighted ULS loads Nsd needs to be smaller than the design resisting value of the wall, such as:

$$N_{Sd} \leq \frac{\Phi_m . t_{eff} . f_k}{\gamma_M}$$

N.B. the value of γM is determined as follows:

Valeur de γ_M	Contrôle à l'usine (matériaux de construction)	Contrôle au chantier (matériaux de construction et exécution)
Catégorie normale	**3,50**	**3,00**
Autre catégorie	**3,00**	**2,50**

Annex D

Determination of the ELU loads

1. 2-storey high building

1.1. CEB, 14cm thick wall

Roof: 1,5.1,35 + 1,0.1,5 = 3,525 kN/m²
Floor: 1,5.1,35 + 2,0.1,5 = 5,025 kN/m²
Wall (14cm CEB): 0,14.21.2,8.1,35 = 11,113 kN/m
Wall (14cm straw-CEB): 0,14.17.2,8.1,35 = 8,996 kN/m

Exterior wall

Nsd = 3,525 kN/m².2,5m + 2.5,025 kN/m².2,5m + 2.11,113 = 56,164 kN/m

Straw-CEB: Nsd = 3,525 kN/m².2,5m + 2.5,025 kN/m².2,5m + 2.8,996 = 51,291 kN/m

Interior wall

Nsd = 3,525 kN/m².5m + 2.5,025 kN/m².5m + 2.11,113 = 64,976 kN/m

Straw-CEB: Nsd = 3,525 kN/m².5m + 2.5,025 kN/m².5m + 2.8,996 = 77,054 kN/m

1.2. CEB, 29,5cm thick wall

Roof: 1,5.1,35 + 1,0.1,5 = 3,525 kN/m²
Floor: 1,5.1,35 + 2,0.1,5 = 5,025 kN/m²
Wall (29,5cm CEB): 0,295.21.2,8.1,35 = 23,417 kN/m
Wall (29,5cm straw-CEB): 0,295.17.2,8.1,35 = 18,957 kN/m

Exterior wall

Nsd = 3,525 kN/m².2,5m + 2.5,025 kN/m².2,5m + 11,113 + 23,417 = 68,467 kN/m

Straw-CEB: Nsd = 3,525 kN/m².2,5m + 2.5,025 kN/m².2,5m + 8,996 + 18,957 = 61,890 kN/m

Interior wall

Nsd = 3,525 kN/m².5m + 2.5,025 kN/m².5m + 11,113 + 23,417 = 102,405 kN/m

Straw-CEB: Nsd = 3,525 kN/m².5m + 2.5,025 kN/m².5m + 2.18,957 = 95,828 kN/m

1.3. Brick, 14cm thick wall

Roof: 1,5.1,35 + 1,0.1,5 = 3,525 kN/m²
Floor: 1,5.1,35 + 2,0.1,5 = 5,025 kN/m²
Wall (14cm brick): 0,14.18.2,8.1,35 = 9,526 kN/m

Exterior wall

Nsd = 3,525 kN/m².2,5m + 2.5,025 kN/m².2,5m + 2.9,526 = 52,989 kN/m

Interior wall

Nsd = 3,525 kN/m².5m + 2.5,025 kN/m².5m + 2.9,526 = 86,927 kN/m

1.4. Brick, 29cm thick wall

Roof: 1,5.1,35 + 1,0.1,5 = 3,525 kN/m²
Floor: 1,5.1,35 + 2,0.1,5 = 5,025 kN/m²

Wall (29cm CEB): 0,29.18.2,8.1,35 = 19,732 kN/m

Exterior wall

Nsd = 3,525 kN/m².2,5m + 2.5,025 kN/m².2,5m + 9,526 + 19,732 = 63,195 kN/m

Interior wall

Nsd = 3,525 kN/m².5m + 2.5,025 kN/m².5m + 9,526 + 19,732 = 97,133 kN/m

2. 3-storey building

2.1. CEB, 14cm thick wall

Roof: 1,5.1,35 + 1,0.1,5 = 3,525 kN/m²
Floor: 1,5.1,35 + 2,0.1,5 = 5,025 kN/m²
Wall (14cm CEB): 0,14.21.2,8.1,35 = 11,113 kN/m
Wall (14cm straw-CEB): 0,14.17.2,8.1,35 = 8,996 kN/m

Exterior wall

Nsd = 3,525 kN/m².2,5m + 3.5,025 kN/m².2,5m + 3.11,113 = 68,726 kN/m

Straw-CEB: Nsd = 3,525 kN/m².2,5m + 3.5,025 kN/m².2,5m + 3.8,996 = 73,488 kN/m

Interior wall

Nsd = 3,525 kN/m².5m + 3.5,025 kN/m².5m + 3.11,113 = 126,339 kN/m

Straw-CEB: Nsd = 3,525 kN/m².5m + 3.5,025 kN/m².5m + 3.8,996 = 119,988 kN/m

2.2. CEB, 29,5cm thick wall

Roof: 1,5.1,35 + 1,0.1,5 = 3,525 kN/m²
Floor: 1,5.1,35 + 2,0.1,5 = 5,025 kN/m²
Wall (29,5cm CEB): 0,295.21.2,8.1,35 = 23,417 kN/m
Wall (29,5cm straw-CEB): 0,295.17.2,8.1,35 = 18,957 kN/m

Exterior wall

Nsd = 3,525 kN/m².2,5m + 3.5,025 kN/m².2,5m + 2.11,113 + 23,417 = 92,143 kN/m

Straw-CEB: Nsd = 3,525 kN/m².2,5m + 3.5,025 kN/m².2,5m + 2.8,996 + 18,957 = 83,449 kN/m

Interior wall

Nsd = 3,525 kN/m².5m + 3.5,025 kN/m².5m + 2.11,113 + 23,417 = 138,643 kN/m

Straw-CEB: Nsd = 3,525 kN/m².5m + 3.5,025 kN/m².5m + 2.8,996 + 18,957 = 104,82 kN/m

2.3. Brick, 14cm thick wall

Roof: 1,5.1,35 + 1,0.1,5 = 3,525 kN/m²
Floor: 1,5.1,35 + 2,0.1,5 = 5,025 kN/m²
Wall (14cm CEB): 0,14.18.2,8.1,35 = 9,526 kN/m

Exterior wall

Nsd = 3,525 kN/m².2,5m + 3.5,025 kN/m².2,5m + 3.9,526 = 75,078 kN/m

Interior wall

Nsd = 3,525 kN/m².5m + 3.5,025 kN/m².5m + 3.9,526 = 121,578 kN/m

2.4. Brick, 29cm thick wall

Roof: 1,5.1,35 + 1,0.1,5 = 3,525 kN/m²
Floor: 1,5.1,35 + 2,0.1,5 = 5,025 kN/m²
Wall (29cm CEB): 0,29.18.2,8.1,35 = 19,732 kN/m

Exterior wall

Nsd = 3,525 kN/m².2,5m + 3.5,025 kN/m².2,5m + 2.9,526 + 19,732 = 93,13 kN/m

Interior wall

Nsd = 3,525 kN/m².5m + 3.5,025 kN/m².5m + 2.9,526 + 19,732 = 131,784 kN/m

3. 4-storey building

3.1. CEB, 14cm thick wall

Roof: 1,5.1,35 + 1,0.1,5 = 3,525 kN/m²
Floor: 1,5.1,35 + 2,0.1,5 = 5,025 kN/m²
Wall (14cm CEB): 0,14.21.2,8.1,35 = 11,113 kN/m
Wall (14cm straw-CEB): 0,14.17.2,8.1,35 = 8,996 kN/m

Exterior wall

Nsd = 3,525 kN/m².2,5m + 4.5,025 kN/m².2,5m + 4.11,113 = 103,51 kN/m

Straw-CEB: Nsd = 3,525 kN/m².2,5m + 4.5,025 kN/m².2,5m + 4.8,996 = 95,0465 kN/m

Interior wall

Nsd = 3,525 kN/m².5m + 4.5,025 kN/m².5m + 4.11,113 = 162,577 kN/m

Straw-CEB: Nsd = 3,525 kN/m².5m + 4.5,025 kN/m².5m + 4.8,996 = 154,109 kN/m

3.2. CEB, 29,5cm thick wall

Roof: 1,5.1,35 + 1,0.1,5 = 3,525 kN/m²
Floor: 1,5.1,35 + 2,0.1,5 = 5,025 kN/m²
Wall (29,5cm CEB): 0,295.21.2,8.1,35 = 23,417 kN/m
Wall (29,5cm straw-CEB): 0,295.17.2,8.1,35 = 18,957 kN/m

Exterior wall

Nsd = 3,525 kN/m².2,5m + 4.5,025 kN/m².2,5m + 3.11,113 + 23,417 = 115,818 kN/m

Straw-CEB: Nsd = 3,525 kN/m².2,5m + 4.5,025 kN/m².2,5m + 3.8,996 + 18,957 = 105,007 kN/m

Interior wall

Nsd = 3,525 kN/m².5m + 4.5,025 kN/m².5m + 3.11,113 + 23,417 = 174,881 kN/m

Straw-CEB: Nsd = 3,525 kN/m².5m + 4.5,025 kN/m².5m + 2.8,996 + 2.18,957 = 174,031 kN/m

3.3. Brick, 14cm thick wall

Roof: 1,5.1,35 + 1,0.1,5 = 3,525 kN/m²
Floor: 1,5.1,35 + 2,0.1,5 = 5,025 kN/m²
Wall (14cm CEB): 0,14.18.2,8.1,35 = 9,526 kN/m

Exterior wall

Nsd = 3,525 kN/m².2,5m + 4.5,025 kN/m².2,5m + 4.9,526 = 97,166 kN/m

Interior wall

Nsd = 3,525 kN/m².5m + 4.5,025 kN/m².5m + 4.9,526 = 156,229 kN/m

3.4. Brick, 29cm thick wall

Roof: 1,5.1,35 + 1,0.1,5 = 3,525 kN/m²
Floor: 1,5.1,35 + 2,0.1,5 = 5,025 kN/m²
Wall (29cm CEB): 0,29.18.2,8.1,35 = 19,732 kN/m

Exterior wall

Nsd = 3,525 kN/m².2,5m + 4.5,025 kN/m².2,5m + 3.9,526 + 19,732 = 107,372 kN/m

Interior wall

Nsd = 3,525 kN/m².5m + 4.5,025 kN/m².5m + 3.9,526 + 19,732 = 166,435 kN/m

4. 5-storey building

4.1. CEB, 14cm thick wall

Roof: 1,5.1,35 + 1,0.1,5 = 3,525 kN/m²
Floor: 1,5.1,35 + 2,0.1,5 = 5,025 kN/m²
Wall (14cm CEB): 0,14.21.2,8.1,35 = 11,113 kN/m
Wall (14cm straw-CEB): 0,14.17.2,8.1,35 = 8,996 kN/m

Exterior wall

Nsd = 3,525 kN/m².2,5m + 5.5,025 kN/m².2,5m + 5.11,113 = 127,19 kN/m

Straw-CEB: Nsd = 3,525 kN/m².2,5m + 5.5,025 kN/m².2,5m + 5.8,996 = 116,605 kN/m

Interior wall

Nsd = 3,525 kN/m².5m + 5.5,025 kN/m².5m + 5.11,113 = 198,815 kN/m

Straw-CEB: Nsd = 3,525 kN/m².5m + 5.5,025 kN/m².5m + 5.8,996 = 188,230 kN/m

4.2. CEB, 29,5cm thick wall

[insert plan, elevation and 3D]

Roof: 1,5.1,35 + 1,0.1,5 = 3,525 kN/m²
Floor: 1,5.1,35 + 2,0.1,5 = 5,025 kN/m²
Wall (29,5cm CEB): 0,295.21.2,8.1,35 = 23,417 kN/m
Wall (29,5cm straw-CEB): 0,295.17.2,8.1,35 = 18,957 kN/m

Exterior wall

Nsd = 3,525 kN/m².2,5m + 5.5,025 kN/m².2,5m + 3.11,113 + 2.23,417 = 151,849 kN/m
Straw-CEB: Nsd = 3,525 kN/m².2,5m + 5.5,025 kN/m².2,5m + 3.8,996 + 2.18,957 = 136,527 kN/m

Interior wall

Nsd = 3,525 kN/m².5m + 5.5,025 kN/m².5m + 3.11,113 + 2.23,417 = 223,423 kN/m

Straw-CEB: Nsd = 3,525 kN/m².5m + 5.5,025 kN/m².5m + 2.8,996 + 3.18,957 = 218,113 kN/m

4.3. Brick, 14cm thick wall

Roof: 1,5.1,35 + 1,0.1,5 = 3,525 kN/m²
Floor: 1,5.1,35 + 2,0.1,5 = 5,025 kN/m²
Wall (14cm CEB): 0,14.18.2,8.1,35 = 9,526 kN/m

Exterior wall

Nsd = 3,525 kN/m².2,5m + 5.5,025 kN/m².2,5m + 5.9,526 = 119,255 kN/m

Interior wall

Nsd = 3,525 kN/m².5m + 5.5,025 kN/m².5m + 5.9,526 = 190,880 kN/m

4.4. Brick, 29cm thick wall

Roof: 1,5.1,35 + 1,0.1,5 = 3,525 kN/m²
Floor: 1,5.1,35 + 2,0.1,5 = 5,025 kN/m²
Wall (29cm CEB): 0,29.18.2,8.1,35 = 19,732 kN/m

Exterior wall

Nsd = 3,525 kN/m².2,5m + 5.5,025 kN/m².2,5m + 4.9,526 + 19,732 = 129,461 kN/m

Interior wall

Nsd = 3,525 kN/m².5m + 5.5,025 kN/m².5m + 4.9,526 + 19,732 = 201,086 kN/m

5. 6-storey building

5.1. CEB, 14cm thick wall

Roof: 1,5.1,35 + 1,0.1,5 = 3,525 kN/m²
Floor: 1,5.1,35 + 2,0.1,5 = 5,025 kN/m²
Wall (14cm CEB): 0,14.21.2,8.1,35 = 11,113 kN/m
Wall (14cm straw-CEB): 0,14.17.2,8.1,35 = 8,996 kN/m

Exterior wall

Nsd = 3,525 kN/m².2,5m + 6.5,025 kN/m².2,5m + 6.11,113 = 150,865 kN/m

Straw-CEB: Nsd = 3,525 kN/m².2,5m + 6.5,025 kN/m².2,5m + 6.8,996 = 138,163 kN/m

Interior wall

Nsd = 3,525 kN/m².5m + 6.5,025 kN/m².5m + 6.11,113 = 235,053 kN/m

Straw-CEB: Nsd = 3,525 kN/m².5m + 6.5,025 kN/m².5m + 6.8,996 = 222,351 kN/m

5.2. CEB, 29,5cm thick wall

Roof: 1,5.1,35 + 1,0.1,5 = 3,525 kN/m²
Floor: 1,5.1,35 + 2,0.1,5 = 5,025 kN/m²
Wall (29,5cm CEB): 0,295.21.2,8.1,35 = 23,417 kN/m
Wall (29,5cm straw-CEB): 0,295.17.2,8.1,35 = 18,957 kN/m

Exterior wall

Nsd = 3,525 kN/m².2,5m + 6.5,025 kN/m².2,5m + 3.11,113 + 3.23,417 = 187,777 kN/m

Straw-CEB: Nsd = 3,525 kN/m².2,5m + 6.5,025 kN/m².2,5m + 3.8,996 + 3.18,957 = 168,046 kN/m

Interior wall

Nsd = 3,525 kN/m².5m + 6.5,025 kN/m².5m + 3.11,113 + 3.23,417 = 271,965 kN/m

Straw-CEB: Nsd = 3,525 kN/m².5m + 6.5,025 kN/m².5m + 2.8,996 + 4.18,957 = 262,195 kN/m

5.3. Brick, 14cm thick wall

Roof: 1,5.1,35 + 1,0.1,5 = 3,525 kN/m²
Floor: 1,5.1,35 + 2,0.1,5 = 5,025 kN/m²
Wall (14cm CEB): 0,14.18.2,8.1,35 = 9,526 kN/m

Exterior wall

Nsd = 3,525 kN/m².2,5m + 6.5,025 kN/m².2,5m + 6.9,526 = 141,343 kN/m

Interior wall

Nsd = 3,525 kN/m².5m + 6.5,025 kN/m².5m + 6.9,526 = 200,409 kN/m

5.4. Brick, 29cm thick wall

Roof: 1,5.1,35 + 1,0.1,5 = 3,525 kN/m²
Floor: 1,5.1,35 + 2,0.1,5 = 5,025 kN/m²
Wall (29cm CEB): 0,29.18.2,8.1,35 = 19,732 kN/m

Exterior wall

Nsd = 3,525 kN/m².2,5m + 6.5,025 kN/m².2,5m + 4.9,526 + 2.19,732 = 161,755 kN/m

Interior wall

Nsd = 3,525 kN/m².5m + 6.5,025 kN/m².5m + 4.9,526 + 2.19,732 = 245,943 kN/m

6. 7-storey building

6.1. CEB, 14cm thick wall

Roof: 1,5.1,35 + 1,0.1,5 = 3,525 kN/m²
Floor: 1,5.1,35 + 2,0.1,5 = 5,025 kN/m²
Wall (14cm CEB): 0,14.21.2,8.1,35 = 11,113 kN/m
Wall (14cm straw-CEB): 0,14.17.2,8.1,35 = 8,996 kN/m

Exterior wall

Nsd = 3,525 kN/m².2,5m + 7.5,025 kN/m².2,5m + 7.11,113 = 174,541 kN/m

Straw-CEB: Nsd = 3,525 kN/m².2,5m + 7.5,025 kN/m².2,5m + 7.8,996 = 159,722 kN/m

Interior wall

Nsd = 3,525 kN/m².5m + 7.5,025 kN/m².5m + 7.11,113 = 271,291 kN/m

Straw-CEB: Nsd = 3,525 kN/m².5m + 7.5,025 kN/m².5m + 7.8,996 = 256,472 kN/m

6.2. CEB, 29,5cm thick wall

Roof: 1,5.1,35 + 1,0.1,5 = 3,525 kN/m²
Floor: 1,5.1,35 + 2,0.1,5 = 5,025 kN/m²
Wall (29,5cm CEB): 0,295.21.2,8.1,35 = 23,417 kN/m
Wall (29,5cm straw-CEB): 0,295.17.2,8.1,35 = 18,957 kN/m

Exterior wall

Nsd = 3,525 kN/m².2,5m + 7.5,025 kN/m².2,5m + 3.11,113 + 4.23,417 = 236,061 kN/m

Straw-CEB: Nsd = 3,525 kN/m².2,5m + 7.5,025 kN/m².2,5m + 3.8,996 + 4.18,957 = 219,488 kN/m

Interior wall

Nsd = 3,525 kN/m².5m + 7.5,025 kN/m².5m + 3.11,113 + 4.23,417 = 320,51 kN/m

Straw-CEB: Nsd = 3,525 kN/m².5m + 7.5,025 kN/m².5m + 2.8,996 + 5.18,957 = 306,277 kN/m

6.3. Brick, 14cm thick wall

Roof: 1,5.1,35 + 1,0.1,5 = 3,525 kN/m²
Floor: 1,5.1,35 + 2,0.1,5 = 5,025 kN/m²
Wall (14cm CEB): 0,14.18.2,8.1,35 = 9,526 kN/m

Exterior wall

Nsd = 3,525 kN/m².2,5m + 7.5,025 kN/m².2,5m + 7.9,526 = 163,43 kN/m

Interior wall

Nsd = 3,525 kN/m².5m + 7.5,025 kN/m².5m + 7.9,526 = 260,182 kN/m

6.4. Brick, 29cm thick wall

Roof: 1,5.1,35 + 1,0.1,5 = 3,525 kN/m²
Floor: 1,5.1,35 + 2,0.1,5 = 5,025 kN/m²
Wall (29cm CEB): 0,29.18.2,8.1,35 = 19,732 kN/m

Exterior wall

Nsd = 3,525 kN/m².2,5m + 7.5,025 kN/m².2,5m + 4.9,526 + 3.19,732 = 204,256 kN/m

Interior wall

Nsd = 3,525 kN/m².5m + 7.5,025 kN/m².5m + 4.9,526 + 3.19,732 = 290,80 kN/m

Annex F

Bearing capacity CEB wall, calculation notes

1. Bearing capacity of a 14cm-thick CEB wall

1.1. Dimensioning of an exterior structural masonry element

Slenderness

$$S = \frac{h_{ef}}{t_{ef}} = \frac{2{,}60}{0{,}14} = 18{,}57 < 27$$

Where: $h_{ef} = \rho_n . h = 0{,}93 \,.\, 2{,}80m = 2{,}60m$

With: $\rho_n = \rho_4 = \frac{\rho_2}{1+\left(\frac{\rho_2 . h}{L}\right)^2} = \frac{1}{1+\left(\frac{1\,.\,2{,}80}{10}\right)^2} = 0{,}93 > 0{,}3$

$\rho_2 = 1$

Eccentricity

- On top or bottom of the wall

$$e_i = \frac{M_i}{N_i} + e_{hi} + e_a = 23{,}33 + 0 + 5{,}78 = 29{,}11mm \qquad \geq 0{,}005 . t = 7mm$$

With: $e_a = \frac{h_{ef}}{450} = \frac{2{,}60}{450} = 5{,}78mm$

$\frac{M_i}{N_i} = \frac{h}{12} = 23{,}33mm$

$e_{hi} = 0mm$

- In the middle of the wall

$$e_m = \frac{M_m}{N_m} + e_{hm} + e_a = 11{,}67 + 5 + 5{,}78 = 22{,}45mm \qquad \geq 0{,}005 . t = 7mm$$

With: $e_a = \frac{h_{ef}}{450} = \frac{2{,}60}{450} = 5{,}78mm$

$\frac{M_m}{N_m} = \frac{h}{24} = 11{,}67mm$

$e_{hm} = 5mm$

Control of the compression strength

On top or bottom of the wall

$$\Phi_i = 1 - 2 . \frac{e_i}{t_{eff}} = 1 - 2 . \frac{29{,}11}{140} = 0{,}58$$

In the middle of the wall

$$\Phi_m = 0{,}44$$

With: $\frac{e_{mk}}{t} = \frac{22{,}45}{140} = 0{,}16$

$\frac{h_{ef}}{t_{ef}} = \frac{260}{14} = 18{,}57$

The control of the dimensioning is done with the smallest value between Φi and Φm.

$$N_{Sd} \leq \frac{\Phi_m . t_{eff} . f_k}{\gamma_M} = \frac{0{,}44 \,.\, 0{,}14 \,.\, 3{,}49 . 10^3}{2{,}5} = 85{,}99\ kN$$

For a straw reinforced CEB:

$$N_{Sd} \leq \frac{\Phi_m . t_{eff} . f_k}{\gamma_M} = \frac{0{,}44 \,.\, 0{,}14 \,.\, 3{,}08 . 10^3}{2{,}5} = 75{,}89\ kN$$

1.2. Dimensioning of an interior structural masonry element

Slenderness

$$S = \frac{h_{ef}}{t_{ef}} = \frac{2{,}60}{0{,}14} = 18{,}57 < 27$$

Where: $h_{ef} = \rho_n . h = 0{,}93 \,.\, 2{,}80 = 2{,}60m$

With: $\rho_n = \rho_4 = \frac{\rho_2}{1+\left(\frac{\rho_2 . h}{L}\right)^2} = \frac{1}{1+\left(\frac{1 \,.\, 2{,}80}{10}\right)^2} = 0{,}93 > 0{,}3$

$\rho_2 = 1$

Eccentricity

- On top or bottom of the wall

$$e_i = e_m = \frac{M_i}{N_i} + e_{hi} + e_a = 0 + 0 + 4{,}73 = 5{,}78mm \qquad \not\geq 0{,}005 . t = 7mm$$

$$\rightarrow e_i = 7mm$$

With: $e_a = \frac{h_{ef}}{450} = \frac{2{,}60}{450} = 5{,}78mm$

$\frac{M_i}{N_i} = \frac{M_m}{N_m} = 0mm$ (interior wall)

$e_{hi} = e_{hm} = 0mm$ (interior wall)

Control of the compression strength

On top or bottom of the wall

$$\Phi_i = 1 - 2 . \frac{e_i}{t_{eff}} = 1 - 2 . \frac{7}{140} = 0{,}9$$

In the middle of the wall

$$\Phi_m = 0{,}67$$

With: $\frac{e_{mk}}{t} = \frac{7}{140} = 0{,}05$

$\frac{h_{ef}}{t_{ef}} = \frac{260}{14} = 18{,}57$

The control of the dimensioning is done with the smallest value between Φi and Φm.

$$N_{Sd} \leq \frac{\Phi_m . t_{eff} . f_k}{\gamma_M} = \frac{0{,}67 \,.\, 0{,}14 \,.\, 3{,}49 . 10^3}{2{,}5} = 130{,}94\ kN/m^2$$

For a straw reinforced CEB:

$$N_{Sd} \leq \frac{\Phi_m . t_{eff} . f_k}{\gamma_M} = \frac{0{,}67 \,.\, 0{,}14 \,.\, 3{,}08 . 10^3}{2{,}5} = 115{,}56 \; kN/m^2$$

2. Bearing capacity of 29,5cm-thick CEB wall

2.1. Dimensioning of an exterior structural masonry element

Compression strength fk

As this type of wall presents vertical longitudinal joints, a certain devaluation factor needs to be applied the same way as it is done for traditional masonry with the factor K. It can be noticed that the K factor ratio between both scenarios (see Annex) is more severe for masonry belonging to group 2b than for masonry belonging to group 1:

Group1: 0,50/0,60 = 0,83

Group 2a: 0,45/0,55 = 0,82

Group 2b: 0,40/0,50 = 0,80

As no information was found on this particular issue, a K' factor of 0,80 will be applied on the design compression strength of CEB in order to stay on the safe side. The following equation can thus be applied:

$$f_k = K' . f'_k = 0{,}80 \,.\, 3{,}49 = 2{,}79 \; N/mm^2$$

With: $K' = 0{,}4$ (group 2b; with vertical longitudinal joints)

$f'_k = 3{,}49 \; N/mm^2$

For a straw reinforced CEB, the following value is obtained:

$$f_k = K' . f'_k = 0{,}80 \,.\, 3{,}08 = 2{,}46 \; N/mm^2$$

With: $K' = 0{,}4$ (group 2b; with vertical longitudinal joints)

$f'_k = 3{,}08 \; N/mm^2$

Slenderness

$$S = \frac{h_{ef}}{t_{ef}} = \frac{2{,}60}{0{,}295} = 8{,}81 < 27$$

Where: $h_{ef} = \rho_n . h = 2{,}60$ m

With: $\rho_n = \rho_4 = \frac{\rho_2}{1+\left(\frac{\rho_2 . h}{L}\right)^2} = \frac{1}{1+\left(\frac{1 \,.\, 2{,}80}{10}\right)^2} = 0{,}93 > 0{,}3$

$\rho_2 = 1$

Eccentricity

- On top or bottom of the wall

$$e_i = \frac{M_i}{N_i} + e_{hi} + e_a = 23{,}33 + 0 + 5{,}78 = 29{,}11mm \qquad \geq 0{,}005.t = 7mm$$

With: $e_a = \frac{h_{ef}}{450} = \frac{2{,}60}{450} = 5{,}78mm$

$\frac{M_i}{N_i} = \frac{h}{12} = 23{,}33mm$

$e_{hi} = 0mm$

- In the middle of the wall

$$e_m = \frac{M_m}{N_m} + e_{hm} + e_a = 11{,}67 + 5 \ + 5{,}78 = 22{,}45mm \qquad \geq 0{,}005.t = 7mm$$

With: $e_a = \frac{h_{ef}}{450} = \frac{2{,}60}{450} = 5{,}78mm$

$\frac{M_m}{N_m} = \frac{h}{24} = 11{,}67m$

$e_{hm} = 5mm$

Control of the compression strength

On top or bottom of the wall

$$\Phi_i = \ 1 - 2.\frac{e_i}{t_{eff}} = 1 - 2.\frac{29{,}11}{295} = 0{,}80$$

In the middle of the wall

$$\Phi_m = \ 0{,}77$$

With: $\frac{e_{mk}}{t} = \frac{22{,}45}{295} = 0{,}08$

$\frac{h_{ef}}{t_{ef}} = \frac{260}{29{,}5} = 8{,}81$

The control of the dimensioning is done with the smallest value between Φi and Φm.

$$N_{Sd} \leq \frac{\Phi_m.t_{eff}.f_k}{\gamma_M} = \frac{0{,}77.0{,}295\ .2{,}79.10^3}{2{,}5} = 213{,}99\ kN$$

For a straw reinforced CEB:

$$N_{Sd} \leq \frac{\Phi_m.t_{eff}.f_k}{\gamma_M} = \frac{0{,}77\ .0{,}295\ .2{,}46.10^3}{2{,}5} = 188{,}68\ kN$$

2.2. Dimensioning of an interior structural masonry element

Compression strength fk

$$f_k = \ K'.f'_k = 0{,}80\ .3{,}49 = 2{,}79\ N/mm^2$$

With: $K' = 0{,}8$ (with vertical longitudinal joints)

$f'_k = \ 3{,}49\ N/mm^2$

Slenderness

$$S = \frac{h_{ef}}{t_{ef}} = \frac{2{,}60}{0{,}295} = 8{,}81 < 27$$

Where: $h_{ef} = \rho_n . h = 0{,}93 \,.\, 2{,}80m = 2{,}60m$

With: $\rho_n = \rho_4 = \frac{\rho_2}{1+\left(\frac{\rho_2 . h}{L}\right)^2} = \frac{1}{1+\left(\frac{1\,.\,2{,}80}{10}\right)^2} = 0{,}93 > 0{,}3$

$\rho_2 = 1$

Eccentricity

- On top or bottom of the wall

$$e_i = e_m = \frac{M_i}{N_i} + e_{hi} + e_a = 0 + 0 + 5{,}78 = 5{,}78mm \qquad \not\geq 0{,}005 . t = 7mm$$

$$\rightarrow e_i = 7mm$$

With: $e_a = \frac{h_{ef}}{450} = \frac{2{,}60}{450} = 5{,}78mm$

$\frac{M_i}{N_i} = \frac{M_m}{N_m} = 0mm$ (interior wall)

$e_{hi} = e_{hm} = 0mm$ (interior wall)

Control of the compression strength

On top or bottom of the wall

$$\Phi_i = 1 - 2.\frac{e_i}{t_{eff}} = 1 - 2.\frac{7}{295} = 0{,}95$$

In the middle of the wall

$$\Phi_m = 0{,}91$$

With: $\frac{e_{mk}}{t} = \frac{7}{295} = 0{,}02$

$\frac{h_{ef}}{t_{ef}} = \frac{260}{29{,}5} = 8{,}81$

The control of the dimensioning is done with the largest value between Φi and Φm.

$$N_{Sd} \leq \frac{\Phi_m . t_{eff} . f_k}{\gamma_M} = \frac{0{,}91 \,.\, 0{,}295 \,.\, 2{,}79 . 10^3}{2{,}5} = 299{,}59\ kN/m^2$$

For a straw reinforced CEB:

$$N_{Sd} \leq \frac{\Phi_m . t_{eff} . f_k}{\gamma_M} = \frac{0{,}91 \,.\, 0{,}295 \,.\, 2{,}46 . 10^3}{2{,}5} = 264{,}58\ kN/m^2$$

Annex G

Bearing capacity masonry wall, calculation notes

1. Bearing capacity of a 14cm-thick brick wall

1.1. Dimensioning of an exterior structural masonry element

Compression strength fk

$$f_{bk} = 10\ N/mm^2$$

$$f_{bk,eq} = 1{,}18\ f_{bk} = 1{,}18 \,.\, 10 = 11{,}8\ N/mm^2$$

$$f_b = \delta . \delta_c . f_{bk,eq} = 1 \,.\, 1{,}25 \,.\, 11{,}8 = 14{,}75\ N/mm^2$$

With: $\delta = 1$ (fired brick)

$\delta_c = 1{,}25$

$$f_k = K . f_b^{0,65} . f_m^{0,25} = 0{,}50 . 14{,}75^{0,65} . 8^{0,25} = 4{,}84\ N/mm^2$$

With: $K = 0{,}5$ (group 2b)

$f_m = 8\ N/mm^2$

Slenderness

$$S = \frac{h_{ef}}{t_{ef}} = \frac{2{,}60}{0{,}14} = 18{,}57 < 27$$

Where: $h_{ef} = \rho_n . h = 0{,}93 \,.\, 2{,}80m = 2{,}60m$

With: $\rho_n = \rho_4 = \frac{\rho_2}{1+\left(\frac{\rho_2 . h}{L}\right)^2} = \frac{1}{1+\left(\frac{1 \,.\, 2{,}80}{10}\right)^2} = 0{,}93 > 0{,}3$

$\rho_2 = 1$

Eccentricity

- On top or bottom of the wall

$$e_i = \frac{M_i}{N_i} + e_{hi} + e_a = 23{,}33 + 0 + 5{,}78 = 29{,}11mm \qquad \geq 0{,}005 . t = 7mm$$

With: $e_a = \frac{h_{ef}}{450} = \frac{2{,}60}{450} = 5{,}78mm$

$\frac{M_i}{N_i} = \frac{h}{12} = 23{,}33mm$

$e_{hi} = 0mm$

- In the middle of the wall

$$e_m = \frac{M_m}{N_m} + e_{hm} + e_a = 11{,}67 + 5 \ + 5{,}78 = 22{,}45mm \qquad \geq 0{,}005 . t = 7mm$$

With: $e_a = \frac{h_{ef}}{450} = \frac{2{,}60}{450} = 5{,}78mm$

$\frac{M_m}{N_m} = \frac{h}{24} = 11{,}67mm$

$e_{hm} = 5mm$

Control of the compression strength

On top or bottom of the wall

$$\Phi_i = 1 - 2.\frac{e_i}{t_{eff}} = 1 - 2.\frac{29{,}11}{140} = 0{,}58$$

In the middle of the wall

$$\Phi_m = 0{,}42$$

With: $\frac{e_{mk}}{t} = \frac{22{,}45}{140} = 0{,}16$

$\frac{h_{ef}}{t_{ef}} = \frac{260}{14} = 18{,}57$

The control of the dimensioning is done with the smallest value between Φi and Φm.

$$N_{Sd} \leq \frac{\Phi_i . t_{eff} . f_k}{\gamma_M} = \frac{0{,}42 \,.\, 0{,}14 \,.\, 4{,}84 . 10^3}{2{,}5} = 113{,}84\ kN$$

1.2. Dimensioning of an interior structural masonry element

Compression strength fk

$$f_{bk} = 10\ N/mm^2$$

$$f_{bk,eq} = 1{,}18\, f_{bk} = 1{,}18 \,.\, 10 = 11{,}8\ N/mm^2$$

$$f_b = \delta . \delta_c . f_{bk,eq} = 1 \,.\, 1{,}25 \,.\, 11{,}8 = 14{,}75\ N/mm^2$$

With: $\delta = 1$ (fired brick)

$\delta_c = 1{,}25$

$$f_k = K . f_b^{0{,}65} . f_m^{0{,}25} = 0{,}50 . 14{,}75^{0{,}65} . 8^{0{,}25} = 4{,}84\ N/mm^2$$

With: $K = 0{,}5$ (group 2b)

$f_m = 8\ N/mm^2$

Slenderness

$$S = \frac{h_{ef}}{t_{ef}} = \frac{2{,}60}{0{,}14} = 18{,}57 < 27$$

Where: $h_{ef} = \rho_n . h = 0{,}93 \,.\, 2{,}80m = 2{,}60m$

With: $\rho_n = \rho_4 = \frac{\rho_2}{1+\left(\frac{\rho_2 . h}{L}\right)^2} = \frac{1}{1+\left(\frac{1 \,.\, 2{,}80}{10}\right)^2} = 0{,}93 > 0{,}3$

$\rho_2 = 1$

Eccentricity

- On top or bottom of the wall

$$e_i = e_m = \frac{M_i}{N_i} + e_{hi} + e_a = 0 + 0 + 5{,}78 = 5{,}78mm \qquad \not\geq 0{,}005.t = 7mm$$

$$\rightarrow e_i = 7mm$$

With: $e_a = \frac{h_{ef}}{450} = \frac{2{,}60}{450} = 5{,}78mm$

$\frac{M_i}{N_i} = \frac{M_m}{N_m} = 0mm$ (interior wall)

$e_{hi} = e_{hm} = 0mm$ (interior wall)

Control of the compression strength

On top or bottom of the wall

$$\Phi_i = 1 - 2.\frac{e_i}{t_{eff}} = 1 - 2.\frac{7}{140} = 0{,}9$$

In the middle of the wall

$$\Phi_m = 0{,}67$$

With: $\frac{e_{mk}}{t} = \frac{7}{140} = 0{,}05$

$\frac{h_{ef}}{t_{ef}} = \frac{260}{14} = 18{,}57$

The control of the dimensioning is done with the smallest value between Φi and Φm.

$$N_{Sd} \leq \frac{\Phi_m.t_{eff}.f_k}{\gamma_M} = \frac{0{,}67\ .0{,}14\ .4{,}84.10^3}{2{,}5} = 181{,}60\ kN/m^2$$

2. Bearing capacity of a 29cm-thick brick wall

2.1. Dimensioning of an exterior structural masonry element

Compression strength fk

$$f_{bk} = 10\ N/mm^2$$

$$f_{bk,eq} = 1{,}18\ f_{bk} = 1{,}18\ .\ 10 = 11{,}8\ N/mm^2$$

$$f_b = \delta.\delta_c.f_{bk,eq} = 1\ .\ 1{,}25\ .\ 11{,}8 = 14{,}75\ N/mm^2$$

With: $\delta = 1$ (fired brick)

$\delta_c = 1{,}25$

$$f_k = K.f_b^{0,65}.f_m^{0,25} = 0{,}40.\ 14{,}75^{0,65}.\ 8^{0,25} = 3{,}87\ N/mm^2$$

With: $K = 0{,}4$ (group 2b; with vertical longitudinal joints)

$f_m = 8\ N/mm^2$

Slenderness

$$S = \frac{h_{ef}}{t_{ef}} = \frac{2{,}60}{0{,}29} = 8{,}97 < 27$$

Where: $h_{ef} = \rho_n.h = 0{,}93\ .\ 2{,}80m = 2{,}80m$

With: $\rho_n = \rho_4 = \frac{\rho_2}{1+\left(\frac{\rho_2.h}{L}\right)^2} = \frac{1}{1+\left(\frac{1\ .2{,}80}{10}\right)^2} = 0{,}93 > 0{,}3$

$\rho_2 = 1$

Eccentricity

- On top or bottom of the wall

$$e_i = \frac{M_i}{N_i} + e_{hi} + e_a = 23{,}33 + 0 + 5{,}78 = 29{,}11mm \qquad \geq 0{,}005.t = 7mm$$

With: $e_a = \frac{h_{ef}}{450} = \frac{2{,}60}{450} = 5{,}78mm$

$\frac{M_i}{N_i} = \frac{h}{12} = 23{,}33mm$

$e_{hi} = 0mm$

- In the middle of the wall

$$e_m = \frac{M_m}{N_m} + e_{hm} + e_a = 11{,}67 + 5\ + 5{,}78 = 22{,}45mm \qquad \geq 0{,}005.t = 7mm$$

With: $e_a = \frac{h_{ef}}{450} = \frac{2{,}60}{450} = 5{,}78mm$

$\frac{M_m}{N_m} = \frac{h}{24} = 11{,}67mm$

$e_{hm} = 5mm$

Control of the compression strength

On top or bottom of the wall

$$\Phi_i = 1 - 2.\frac{e_i}{t_{eff}} = 1 - 2.\frac{29{,}11}{290} = 0{,}80$$

In the middle of the wall

$$\Phi_m = 0{,}76$$

With: $\frac{e_{mk}}{t} = \frac{22{,}45}{290} = 0{,}08$

$\frac{h_{ef}}{t_{ef}} = \frac{260}{29} = 8{,}97$

The control of the dimensioning is done with the smallest value between Φi and Φm.

$$N_{Sd} \leq \frac{\Phi_m . t_{eff} . f_k}{\gamma_M} = \frac{0{,}76 \,.\, 0{,}29 \,.\, 3{,}87 . 10^3}{2{,}5} = 341{,}18kN$$

2.2. Dimensioning of an interior structural masonry element

Compression strength fk

$$f_{bk} = 10\ N/mm^2$$

$$f_{bk,eq} = 1{,}18\ f_{bk} = 1{,}18 \,.\, 10 = 11{,}8\ N/mm^2$$

$$f_b = \delta . \delta_c . f_{bk,eq} = 1 \,.\, 1{,}25 \,.\, 11{,}8 = 14{,}75\ N/mm^2$$

With: $\delta = 1$ (fired brick)

$\delta_c = 1{,}25$

$$f_k = K . f_b^{0{,}65} . f_m^{0{,}25} = 0{,}40 . 14{,}75^{0{,}65} . 8^{0{,}25} = 3{,}87\ N/mm^2$$

With: $K = 0{,}4$ (group 2b; with vertical longitudinal joints)

$f_m = 8\ N/mm^2$

Slenderness

$$S = \frac{h_{ef}}{t_{ef}} = \frac{2{,}60}{0{,}29} = 8{,}97 < 27$$

Where: $h_{ef} = \rho_n . h = 0{,}93 \,.\, 2{,}80m = 2{,}60m$

With: $\rho_n = \rho_4 = \frac{\rho_2}{1+\left(\frac{\rho_2 . h}{L}\right)^2} = \frac{1}{1+\left(\frac{1\,.\,2{,}80}{10}\right)^2} = 0{,}93 > 0{,}3$

$\rho_2 = 1$

Eccentricity

- On top or bottom of the wall

$$e_i = e_m = \frac{M_i}{N_i} + e_{hi} + e_a = 0 + 0 + 5{,}78 = 5{,}78mm \qquad \not\geq 0{,}005 . t = 7mm$$

$$\rightarrow e_i = 7mm$$

With: $e_a = \frac{h_{ef}}{450} = \frac{2{,}60}{450} = 5{,}78mm$

$\frac{M_i}{N_i} = \frac{M_m}{N_m} = 0mm$ (interior wall)

$e_{hi} = e_{hm} = 0mm$ (interior wall)

Control of the compression strength

On top or bottom of the wall

$$\Phi_i = 1 - 2.\frac{e_i}{t_{eff}} = 1 - 2.\frac{7}{290} = 0{,}95$$

In the middle of the wall

$$\Phi_m = 0{,}90$$

With: $\frac{e_{mk}}{t} = \frac{7}{290} = 0{,}02$

$\frac{h_{ef}}{t_{ef}} = \frac{260}{29} = 8{,}97$

The control of the dimensioning is done with the largest value between Φi and Φm.

$$N_{Sd} \leq \frac{\Phi_m . t_{eff} . f_k}{\gamma_M} = \frac{0{,}90 \,.\, 0{,}29 \,.\, 3{,}87 . 10^3}{2{,}5} = 404{,}03\ kN/m^2$$